
Oregon State
UNIVERSITY
College of Forestry
Swiss Needle Cast Cooperative
Annual Report
2014

Staff

Dave Shaw – Director and Associate Professor of Forest Health

Gabriela Ritóková – Faculty Research Assistant

Members of the Swiss Needle Cast Cooperative

Bureau of Land Management

Oregon department of Forestry

Starker Forests

Stimson Lumber

USDA Forest Service

Weyerhaeuser Company

Edited by Dave Shaw and Gabriela Ritóková

Cover photo by Sandra Arbogast

TABLE OF CONTENTS

SNCC Background and Organization

A major challenge to intensive management of Douglas-fir in Oregon and Washington is the current Swiss needle cast (SNC) epidemic. Efforts to understand the epidemiology, symptoms, and growth losses from SNC have highlighted gaps in our knowledge of basic Douglas-fir physiology, growth, and silviculture. The original mission of the Swiss Needle Cast Cooperative (SNCC), formed in 1997, was broadened in 2004 to include research aiming to ensure that Douglas-fir remains a productive component of the Coast Range forests. The SNCC is located in the Department of Forest Engineering, Resources and Management within the College of Forestry at Oregon State University. The Membership is comprised of private, state, and federal organizations. Private membership dues are set at a fixed rate. An annual report, project reports, and newsletters are distributed to members each year. Our objective is to carry out projects in cooperation with members on their land holdings.

SNCC Mission

To conduct research on enhancing Douglas-fir productivity and forest health in the presence of Swiss needle cast and other diseases in coastal forests of Oregon and Washington.

SNCC Objectives

(1) Understand the epidemiology of Swiss needle cast and the basic biology of the causal fungus, *Phaeocryptopus gaeumannii*.

(2) Design silvicultural treatments and regimes to maximize Douglas-fir productivity and ameliorate disease problems in the Coast Range of Oregon and Washington.

(3) Understand the growth, structure, and morphology of Douglas-fir trees and stands as a foundation for enhancing productivity and detecting and combating various diseases of Douglas-fir in the Coast Range of Oregon and Washington.

Department of Forest Engineering, Resources and Management
Oregon State University, 280 Peavy Hall, Corvallis, Oregon 97331-8615
Tel: 541-737-4952 | **Fax:** 541-737-4316 | **Email**: fermdept@oregonstate.edu

January 19, 2015

To: Swiss Needle Cast Cooperative Membership

From: David Shaw, Director and Gabriela Ritokova, Faculty Research Assistant, Swiss Needle Cast Cooperative, College of Forestry, Oregon State University

Re: Introduction to the Annual Report for 2014

Swiss needle cast is continuing to intensify along the coast strip, move marginally east, and develop around the Mary's Peak area. In addition, reports are emerging along the foothills of the western Cascades (east of Sweet Horne and north) of plantations with moderate symptoms. ODF and SNCC visited some of these sites and confirmed the presence of SNC. In 2015 we plan to include aerial survey of the Cascade foothills north of Springfield to the Columbia if visible symptoms warrant, and our annual 2015 Spring Field Trip is planned for the area in collaboration with OSU Forestry Extension and Oregon Small Woodland Owners Association.

2014 was another record year for the USFS-ODF Cooperative Aerial Survey at 586,249 acres of visible symptoms seen from the air. Therefore, it is clear the disease is not abating, and could be intensifying and emerging in a broader area of the Douglas-fir - Region. Washington State will again survey the western portion of the state in 2015. What exactly is happening with SNC? The climate record during the previous three years would imply some abatement of SNC because of cooler temperatures, yet it continues to intensify. Rainfall has not changed significantly during the same period, though some analysis indicates less fog has been occurring along the coast.

The SNC Research and Monitoring plot network is designed to provide the framework and regional assessment to let us make some conclusions, develop hypotheses, and overlay additional studies. We are about mid-way through the 3-year cycle to install plots from California to Washington State and inland 35 miles in 10-25 year old plantations. We are collecting data on soil and foliar nutrients, foliage retention, disease severity, and tree growth in collaboration with CIPS (Center for Intensive Plantation Silviculture). Our scale of inference for modeling disease severity and predicting disease occurrence and severity will be vastly improved. We are also collaborating with Jeff Stone and Patrick Bennett of the OSU Botany and Plant Pathology department, to investigate the molecular genetics ecology of the disease, as they pursue study of two biotypes of the fungus which causes SNC.

The plot network is allowing us to leverage other studies and write grant proposals that use a regional network of existing plots to do experiments. Currently, we are working on an emerging hypothesis regarding dew as a major factor in disease epidemiology with an integrated

research group at the College. With luck this group will secure funds external to the SNC budget.

Perhaps the most significant new development in SNC research is a new collaboration with the USFS PNW Research Station, Connie Harrington and Brad St. Clair. Within an already-installed reciprocal planting (common garden) study of west- side Douglas-fir, we will be investigating the genetics of Douglas-fir host- disease interactions by assessing disease incidence and severity. Nicholas Wilhelmi is a Masters' student who will work on the project, with field work scheduled for Spring 2015. This project will allow a direct test of the idea that local seed source is always better.

On a positive note, USFS FHP California and ODF cooperative aerial survey again surveyed N. Coastal California and detected no significant SNC symptoms, particularly interesting given the disease pressure predicted by the Zhao climate model for that region. Luckily, Connie Harrington and Brad St. Clair included N. California in the common garden study, and we will have insight into whether there is a tree genetics component involved.

The SNCC continues to focus on this important disease that is not abating. It is critical that we advance our understanding at this time as we have a solid foundation to move ahead.

Sincerely,

David Shaw Gabriela Ritokova

2014 Swiss Needle Cast Aerial Survey

Alan Kanaskie and Danny Norlander, Oregon Department of Forestry

Survey procedures:

The observation plane flew at 1,500 to 2,000 feet above the terrain, following north-south lines separated by 2 miles. Observers looked for areas of Douglas-fir forest with obvious yellow to yellow-brown foliage, a symptom of Swiss needle cast. Patches of forest with these symptoms (patches are referred to as polygons) were sketched onto computer touch-screens displaying topographic maps or ortho-photos and the position of the aircraft. Each polygon was classified for degree of discoloration as either "S" (severe) or "M" (moderate). Polygons classified as "S" had very sparse crowns and brownish foliage, while those classified as "M" were predominantly yellow to yellow-brown foliage with slightly denser crowns than those classified as "S". The survey area extended from the Columbia River in Oregon south to the middle of Humboldt County, California, and from the coastline eastward until obvious symptoms were no longer visible. We did not survey the Cascade Range in 2014, but Swiss needle cast does occur at damaging levels in some areas.

In Curry County we ground-checked a random sample of 14 polygons. Each polygon was given a plantation-level score for discoloration (1 to 4; 1 = normal green, 4 = severe yellowing) and SNC disease severity (1 to 6; 1 = healthy, 6 = severe SNC damage). A 250 foot transect was established in a representative part of each stand and 10 trees were evaluated for mid-crown foliage retention.

Results:

The survey was flown on April 29, 30, and May 1, 7, 12, 13, 14. Weather conditions and symptom development both were excellent during the survey period. The survey covered a total of 4,543,908 acres; 3,765,590 in Oregon and 778,318 in California (figure 1).

For Oregon, the 2014 survey results show an increase in the area of forest with symptoms of Swiss needle cast compared to the previous 3 years and reached an all-time high for the fourth year in a row. We mapped 586,249 acres of Douglas-fir forest with obvious symptoms of Swiss needle cast (figure 2). As has been the case for the past several years, the easternmost area with obvious SNC symptoms was approximately 28 miles inland from the coast in the Highway 20 corridor, but most of the area with symptoms occurred within 18 miles of the coast. Figures 3 and 4 show the trend in damage from 1996 through 2014. This year's increase in SNC likely is due in part to prolonged wet weather in spring of 2013 which was very conducive to infection, and the near perfect conditions for symptom development and detection in 2014.

Usually the survey stops in northern Curry County because few symptoms have been observed south of there. In 2014, we extended the survey south through Curry County into Del Norte County and the northern half of Humboldt County in California. In Curry County we mapped 96 polygons representing 7,362 acres with symptoms. In California we mapped only 3 polygons (94 acres total): two just south of the Oregon border and one in northern Humboldt County.

The Humboldt County polygon was ground-checked and the yellowing was not due to Swiss needle cast (Zach Heath, USFS, personal communication). The two Del Norte County polygons were not ground-checked, but photographs taken from the survey plane suggested a rather weak SNC signature.

Swiss needle cast was present at all 14 of the Curry County ground-check polygons. Mean foliage retention ranged from 2.0 to 4.2 annual compliments with a mean of 2.7. Stand color ratings were either 2 or 3, with a mean of 2.4. Mean stand SNC rating was 2.6, ranging from 2 to 3. It is unlikely that SNC was the cause of discoloration in the two stands with the highest foliage retention (3.7 and 4.2).

The Swiss needle cast aerial survey provides a conservative estimate of damage because observers can map only those areas where disease symptoms have developed enough to be visible from the air. We know Swiss needle cast occurs throughout the survey area, but discoloration often is not severe enough to enable aerial detection. The total area of forest affected by Swiss needle cast is far greater than indicated by the aerial survey. The aerial survey does, however, provide a reasonable depiction of the extent of moderate and severe damage, and coarsely documents trends in damage over time.

Acknowledgements:

The survey was conducted by the Oregon Department of Forestry Forest Health and Air Operations sections, and was funded by the Oregon State University Swiss Needle Cast Cooperative, the USDA Forest Service Forest Health Monitoring Program, and the Oregon Department of Forestry. Steve Larsen (ODF) piloted the plane. Danny Norlander (ODF) is the survey coordinator. The aerial observers were Bob Schroeter (USFS Region 6 FHP), Rob Flowers (ODF) and Bob Noyes (USFS).

Additional Notes:

We appreciate any information regarding the accuracy or usefulness of the maps. If you have a chance to look at some of the mapped areas on the ground, please let us know what you observe. Please call Alan Kanaskie (503-945-7397) or Danny Norlander (503-945-7395) if you have questions, suggestions, or comments.

The GIS data and a .pdf file can be accessed via the ODF web page at:

http://www.oregon.gov/ODF/privateforests/fhMaps.shtml

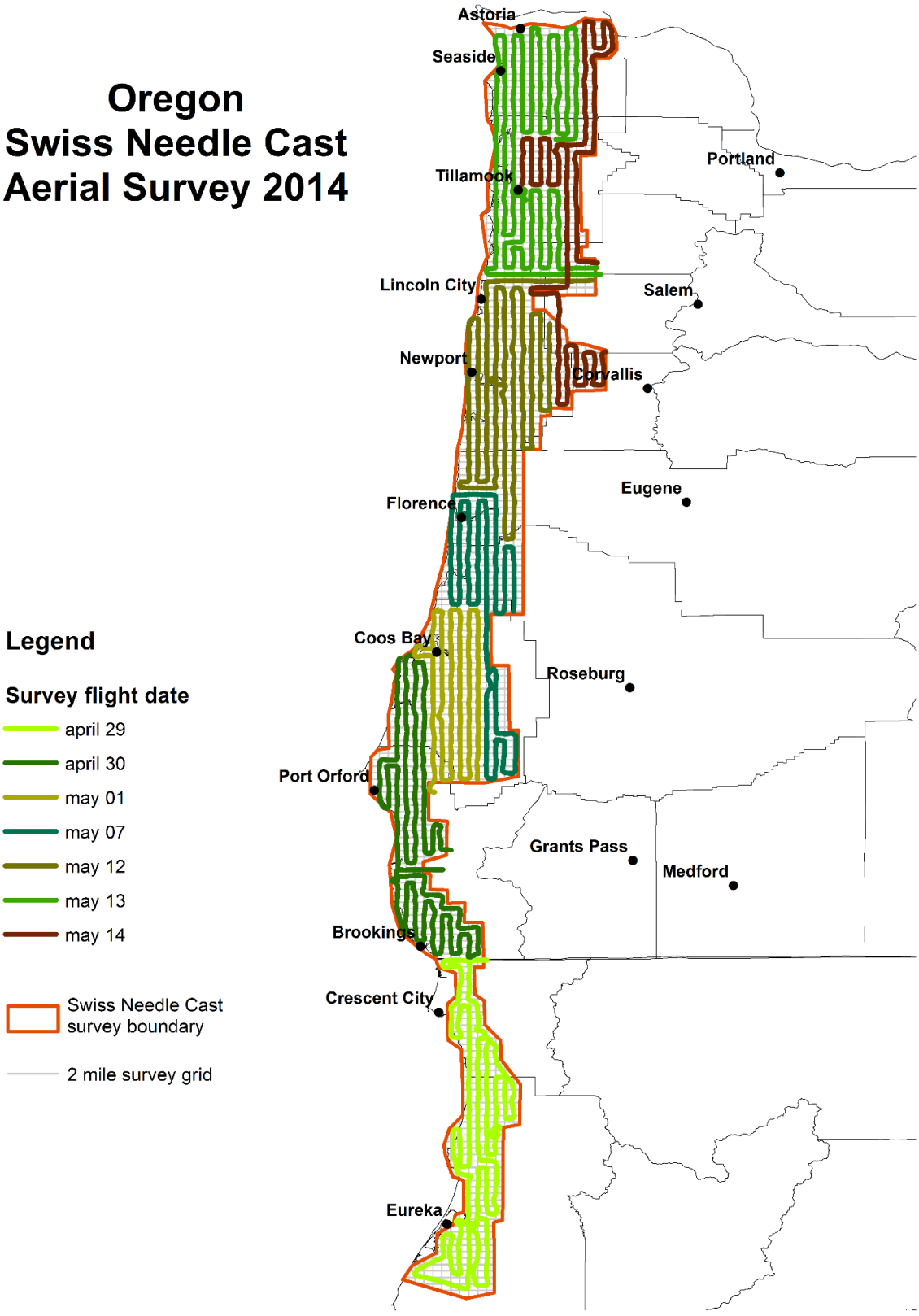

Figure 1. Area surveyed for Swiss needle cast symptoms, 2014.

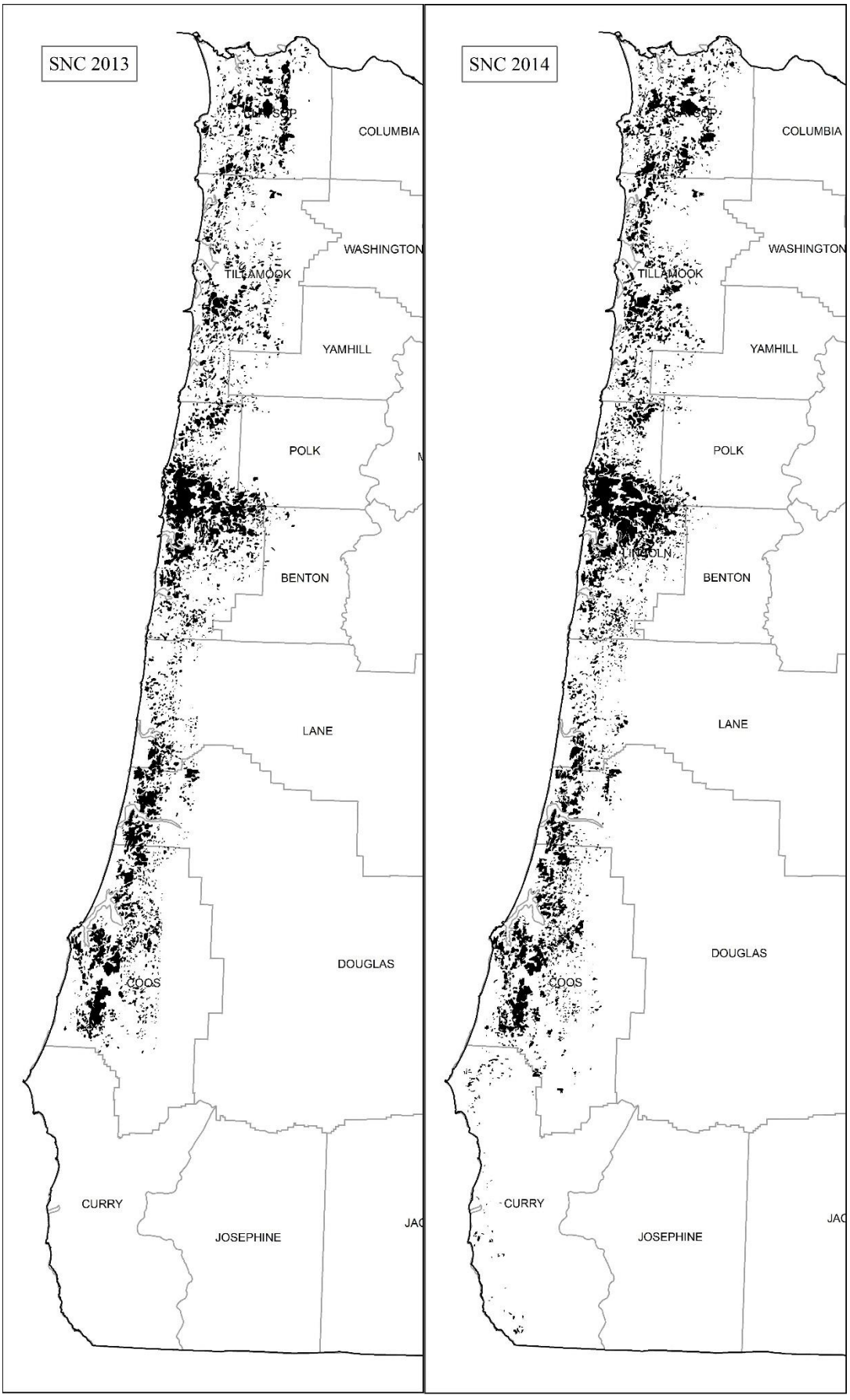
SNC 2013
COLUMBIA
WASHINGTON
TILLAMOOK
YAMHILL
POLK
BENTON
LANE
DOUGLAS
COOS
CURRY
JOSEPHINE
SNC 2014
COLUMBIA
WASHINGTON
TILLAMOOK
YAMHILL
POLK
BENTON
LANE
DOUGLAS
COOS
CURRY
JOSEPHINE

Figure 2. Areas of Douglas-fir forest with symptoms of Swiss Needle Cast detected in the 2013 and 2014 aerial surveys.

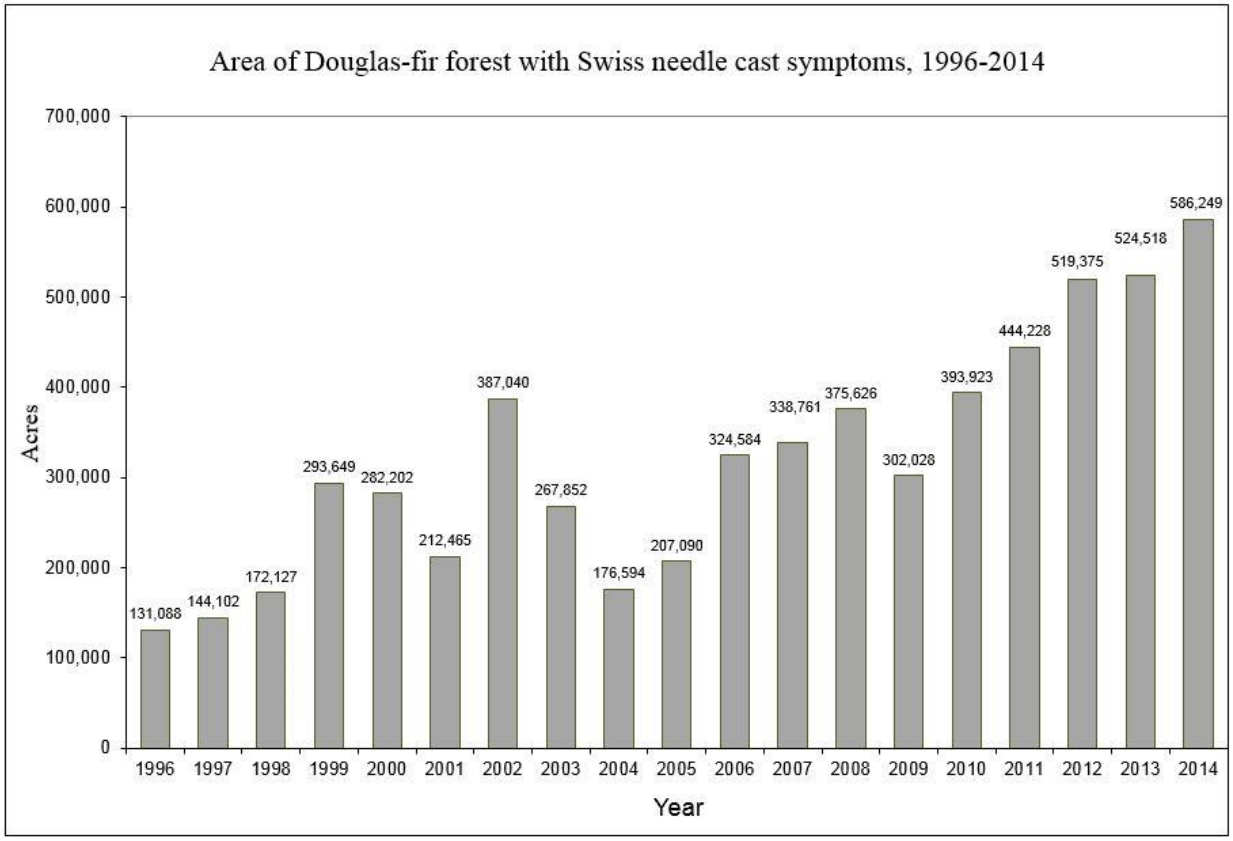

Figure 3. Area of Douglas-fir forest in western Oregon with symptoms of Swiss needle cast detected during aerial surveys conducted in April-June, 1996-2014 (2008 area estimated from partial survey consisting of 3 sample blocks).

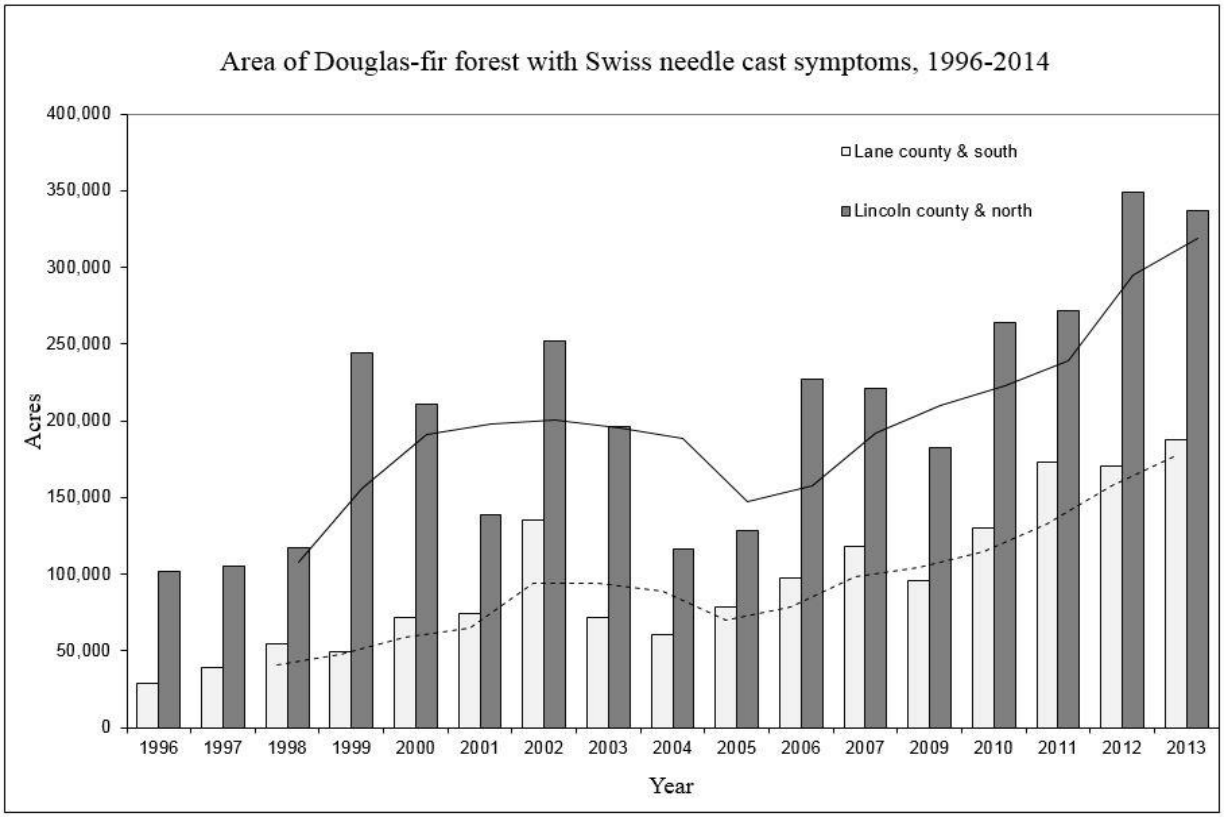

Figure 4. Area of Douglas-fir forest in western Oregon with symptoms of Swiss needle cast detected during aerial surveys conducted in April-June, 1996-2014; north and south halves of survey area (2008 area estimated from partial survey consisting of 3 sample blocks).

2014 Conditions in brief – Aerial survey in California

Zachary Heath, Aerial Survey Program Manager, USDA Forest Service, Forest Health Protection

Background

Swiss Needle Cast (SNC), caused by the fungus *Phaeocryptopus gaeumannii*, is a foliar disease affecting Douglas-fir causing premature needle drop. In severe cases, trees look very sparse and chlorotic with a transparent yellow to brown hue. The Swiss Needle Cast Cooperative, comprised of various academic, industrial and government participants have flown special aerial surveys to detect the extent and severity of this disease for many years especially along the Oregon coast. Surveys are timed at just prior to tree budbreak in spring when the symptoms of this disease are most apparent. The first survey for SNC was conducted in California in 2013, in response to ground reports of the disease in the Arcata area. To date, SNC is not known to cause extensive damage in California but does have economic impact in Oregon. This flight was done as an extension of Region 6's SNC survey in Oregon and Washington.

Objective

Detect and map the extent and severity of SNC along the northwest coast of California.

Methodology

Stands of plantation Douglas-fir were mapped visually by surveyors using digital aerial sketch-mapping systems flying in a light fixed-wing aircraft approximately 1,000 feet above ground level. The surveyors recorded areas of discolored Douglas-fir having the signature of SNC. Attempts will be made to verify the presence of the disease.

Details

Coastal areas of Del Norte and Humboldt Counties were surveyed, mostly covering private lands but including potions of the Redwood State and National Parks. (Figure 1)

Very few areas were observed to have symptoms similar to severe SNC. Most of the discoloration was observed near the Oregon state line (Figure 2), and an additional area that looked like SNC was mapped a few miles away, just north of the state line, as well in a subsequent flight.

Surveyors noted damage to eucalyptus, possibly from cold damage or insect activity. A ground visit in Sonoma County, about 200 miles south of the survey area, found widespread leaf feeding by insects in eucalyptus at that location. (Figure 3)

The surveyors also noted widespread, low intensity tree mortality and damage throughout the survey area from black bears and, to a lesser extent, Port-Orford-Cedar root disease.

Figure 1. Flown area and mapped tree mortality and damage.

Figure 2. Discolored Douglas-fir in Del Norte County, with red line delineating area of discoloration. Photo Bob Schroeter.

Figure 3. Eucalyptus leaf damage in Sonoma County. Photo credit Bill Ciesla.

Direct questions pertaining to this report to Zack Heath
(email:zheath@fs.fed.us phone: 530-759-1751).
Report Date May 16, 2014.

Economic impact of Swiss needle cast in Oregon forests

Alan Kanaskie, Forest pathologist, Oregon Department of Forestry.
Brandon Kaetzel, Forest Economist, Oregon Department of Forestry.
Andrew Herstrom, Resource Analyst (retired), Oregon Department of Forestry.

Findings

Douglas-fir volume growth loss due to Swiss needle cast in the Oregon Coast Range exceeds 190 million board-feet per year in 10 to 70 year-old stands. The log value of this reduced growth is $78 million per year at current log prices. The economic impact to Oregon's economy is equivalent to more than 2,100 jobs, representing $117 million in labor income, $10 million in income tax, and $700,000 in harvest tax, for a total of $128 million per year.

Methods

We defined the analysis area as the Coast Range forest with visible damage from Swiss needle cast based on cumulative annual aerial surveys from 1996-2013 (Figure 1). In this 2.9 million acre area we are certain that SNC impacts the growth of Douglas-fir (the survey detects moderate and severe damage from SNC).

We overlaid the Swiss Needle Cast Cooperative (SNCC) and ODF permanent plot networks, which include three types of plots: 1) growth impact; 2) pre-commercial thinning, and; 3) commercial thinning. These plots provide the basis for growth impact estimates and fall mostly within the area defined by the north half of the analysis area. The age classes represented by the plots are 10-70 yrs. We assumed growth impacts in the south half of the analysis area are similar to those in the north half.

We estimated the amount of Douglas-fir in the analysis area by age class (10-30, 31-70, and >70 yrs) using Gradient Nearest Neighbor (GNN) data from the Landscape Ecology, Modeling, Mapping, and Analysis project (LEMMA: OSU, USFS PNW Station). We selected all cells in the analysis area in which Douglas-fir was the dominant tree species, and calculated the area, Douglas-fir volume, and total volume.

The GNN data do not include an estimate of periodic annual volume increment (PAI). PAI varies widely among stands due to age, site index, and other factors. Mean PAI in 50-70 year-old stands ranges from 7 to 28 m^3/ha/yr (100 to 400 ft^3/ac/yr) (Burns and Honkala, 1990). Data from the SNCC growth impact and thinning plots indicate a mean PAI of approximately 15.5 m^3/ha/yr (222 ft^3/ac/yr) for Douglas-fir plantations age 10 to 30 and 30 to 60 years old (Maguire et al, 2011; Mainwaring et al, 2005). USFS FIA data for the analysis area indicates an average Douglas-fir PAI of 17.8 m^3/ha/yr (254 ft^3/ac/yr) and 11.7 m^3/ha/yr (166 ft^3/ac/yr) for 10-30 and 31-70 yr-old stands, respectively (Dave Azuma, personal communication). We chose 15 m^3/ha/yr

(214 ft^3/ac/yr) as the average PAI for all Douglas-fir stands in the analysis area, which very likely underestimates the true PAI (Marshall and Curtis, 2001).

Older stands (>70 yrs) suffer damage from Swiss needle cast, but the majority of these are not available for harvest, so these were excluded from the analysis of economic impact. However, the disease substantially impacts the ecology of these stands in terms of stand structure and tree longevity. We also excluded very young stands (<10 yrs) from the analysis.

We chose 20 percent as the mean annual volume growth reduction due to Swiss needle cast in the analysis area. This is a conservative estimate based on SNCC studies (Maguire et al, 2011; Maguire et al, 2002).

Many of the GNN data cells with Douglas-fir as the dominant species also contain other tree species. To avoid over-estimating volume based on mean PAI, we adjusted the volume growth estimate by the ratio of Douglas-fir volume to total volume.

Job losses associated with timber volume reduction were calculated with IMPLAN (Impact Analysis for Planning). Value of Douglas-fir logs was based on current saw log pond values of $653/MBF and $715/MBF for the north and south analysis areas, respectively, and utility log values of $100/MBF and $125/MBF, north and south, respectively. We assigned utility log values to all volume estimates for 10-30 yr-old trees. IMPLAN is accepted and used by the Oregon State Economist and the DAS Employment Division.

References

Azuma, David. Research Forester. USDA Forest Service, Forest Inventory and Analysis, Portland, OR. Personal communication.

Burns, Russell M., and Barbara H. Honkala, tech. coords. 1990. Silvics of North America: 1. Conifers; 2. Hardwoods. Agriculture Handbook 654. U.S. Department of Agriculture, Forest Service, Washington, DC. vol.2, 877 p.

Kimberley, MO, Hood IA, Knowles RL. 2011. Impact of Swiss needle cast on growth of Douglas-fir. Phytopathology. 101:583-593.

Maguire, DA, Kanaskie A, Voelker W, Johnson R, Johnson G. 2002. Growth of young Douglas-fir plantations across a gradient in Swiss needle cast severity. Western Journal of Applied Forestry. 17:86-95.

Maguire, DA, Mainwaring DB, Kanaskie A. 2011. Ten-year growth and mortality in young Douglas-fir stands experiencing a range in Swiss needle cast severity. Can. J. For. Res.. 41: 2064-2076.

Mainwaring, DB, Maguire DA, Kanaskie A, Brandt J. 2005. Growth responses to commercial thinning in Douglas-fir stands with varying intensity of Swiss needle cast. Canadian Journal of Forest Research. 35:2394-2402.

Marshall, David D.; Curtis, Robert O. 2001. Levels-of-growing-stock cooperative study in Douglas-fir: report no.15-Hoskins: 1963–1998. Res. Pap. PNW-RP-537. Portland, OR: U.S. Department of Agriculture, Forest Service, Pacific Northwest Research Station.80 p.

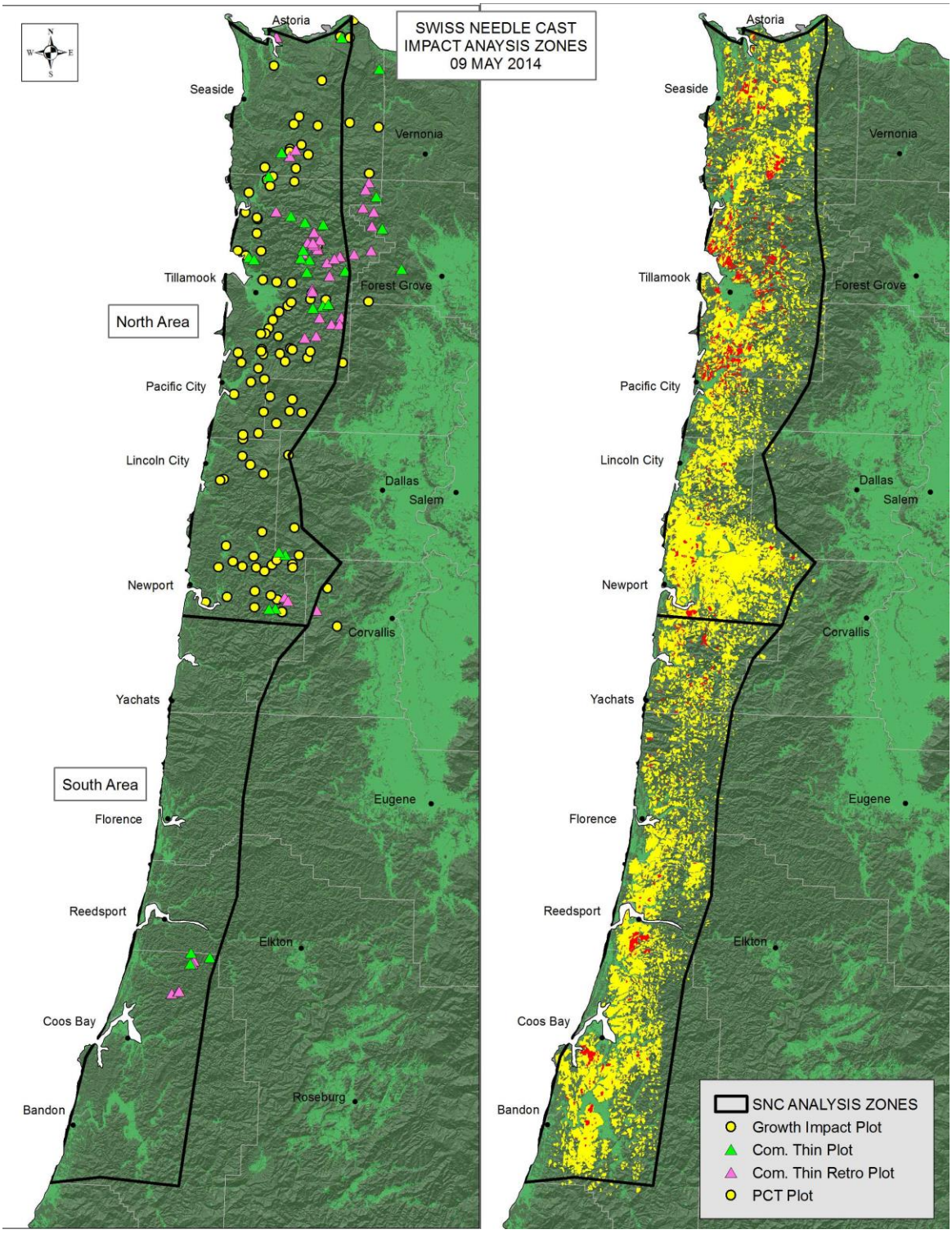

Figure 1. Swiss needle cast analysis zones represent an area in which SNC has reached damaging levels based on aerial detection surveys and plots. Map on right shows cumulative aerial survey map of moderate (yellow) and severe (red) SNC damage.

Table 1. Calculation of value of annual growth loss due to Swiss needle cast in the Oregon Coast Range.

ZONE	AGE	AREA (AC)	DF VOLUME (FT^3)	ANNUAL GROWTH (AREA*PAI) ft^3/yr	VOL LOSS (20%) FT^3/YR	VOL LOSS (20%) BF/YR (CF x 5)	RATIO DF VOL TO TOTAL VOL	ADJUSTED VOLUME LOSS (BF/YR)	JOB LOSS (# of jobs)	Pond value of log volume lost
NORTH	1-9	872	1,064,419							
NORTH	10-30	365,340	2,163,771,546	78,318,010	15,663,602	78,318,010	0.64	49,753,706	552	$4,975,371
NORTH	31-70	366,031	8,262,290,171	78,465,992	15,693,198	78,465,992	0.61	47,990,943	533	$31,338,086
NORTH	>70	242,337	16,360,695,847	51,949,748	10,389,950	51,949,748	0.65	33,855,293		
ALL		974,579	26,787,821,983					131,599,941	1,085	36,313,456
SOUTH	1-9	12	14,663							
SOUTH	10-30	243,158	1,619,893,218	52,125,763	10,425,153	52,125,763	0.79	41,293,020	458	$5,161,628
SOUTH	31-70	311,412	7,642,446,234	66,757,465	13,351,493	66,757,465	0.77	51,417,967	571	$36,763,847
SOUTH	>70	334,165	22,485,920,697	71,634,921	14,326,984	71,634,921	0.79	56,839,599		
ALL		888,747	31,748,274,812					149,550,587	1,029	41,925,474
NORTH-SOUTH TOTAL		1,863,327	58,536,096,794							
							TOTAL, 10-30 yr	91,046,726	1,011	$10,136,998
North analysis area (acres, gross)			1,604,350				TOTAL, 31-70 yr	99,408,911	1,103	$68,101,933
South analysis area (acres, gross)			1,288,679				TOTAL >70 yr			
TOTAL			2,893,029							
							GRAND TOTAL	190,455,637	2,114	$78,238,931
							Economic value of job loss			
								Labor Income	$117,306,959	
								Income Tax	$10,557,527	
								Harvest tax	$701,639	
								TOTAL	$128,566,125	

Board-foot volume = cubic volume x 5. Value of log volume lost does not account for logging costs.

SNCC Research and Monitoring Plot Network

Gabriela Ritóková, Dave Shaw, Doug Maguire, Doug Mainwaring, John Browning, Mark Gourley, Greg Filip, Alan Kanaskie

Introduction

Among the long term objectives of the SNCC is a constant monitoring of disease conditions. While this can be accomplished qualitatively with the results of the annual aerial survey, quantitative assessment of the tree growth loss resulting from Swiss needle cast requires periodic measurements. This has been accomplished up until now with the Growth Impact Study (GIS) plot network (Maguire et al. 2011).

During the final remeasurement of the GIS plots (2008), it was decided that their utility had become limited. The original sample of 10-30 year old GIS stands is now 25-45, which is considered outside the age range of those stands for which information is especially valuable. Furthermore, ground observation of foliage retention, the original methodology for determining disease severity, has become difficult to impossible as a result of crown recession and canopy closure. In addition, these plots were distributed only between Newport and Astoria, thereby providing inference only to the northern Oregon Coast Range.

In order to address these limitations, the decision was made to install a new monitoring plot network, which is foreseen to provide disease condition and growth loss information for at least 10 years. These plots have been installed in 10-20 year stands, thereby addressing the shortcomings of the aged GIS network. In addition, these plots will be distributed as far south as the California border, and as far north as southern Washington.

These plots will not only provide periodic information about disease severity, growth loss and its geographic distribution, but will also offer sites to be used for other SNC research, be it epidemiological, climatological, or other forms. Timeline is attached to the end of this report.

Methods

Criteria for selection

Candidate stands should not be treated by fertilization or disturbed (thinned, cleared) for ten years. The selected one-fifth acre plots with a 0.5 chain buffer (0.58 ac) should have not been pre-commercially thinned or fertilized in the past 5 years. The targeted basal area composition is 80% Douglas-fir, targeted age between 10 and 30-years old of Douglas-fir. Ideally dense understory should be avoided and density aimed to 300-400 trees per acre.
At each plot, a 1/5 acre plot has been laid out, and all trees tagged. Field methods have followed Kanaskie and Maguire, March 30, 2002 Field Specifications and Manual for Rating Swiss Needle Cast in Douglas-fir. The following is adapted from that document but specific to the 1/5 acre plot and needle retention will be estimated in years.

Sampling matrix

We identified four zones based on distance from coast (in miles): 0-5, 5-15, 15-25, and 25-35. Each of these zones was equally divided (north-south), following township lines as closely as possible. Each block spans approximately 58 miles north-south. This resulted in 20 sampling blocks. In addition to the 20 cell matrix in coastal Oregon, 4 sampling blocks were established in SW Washington. Attached Google Earth image shows these blocks (Fig.1.)

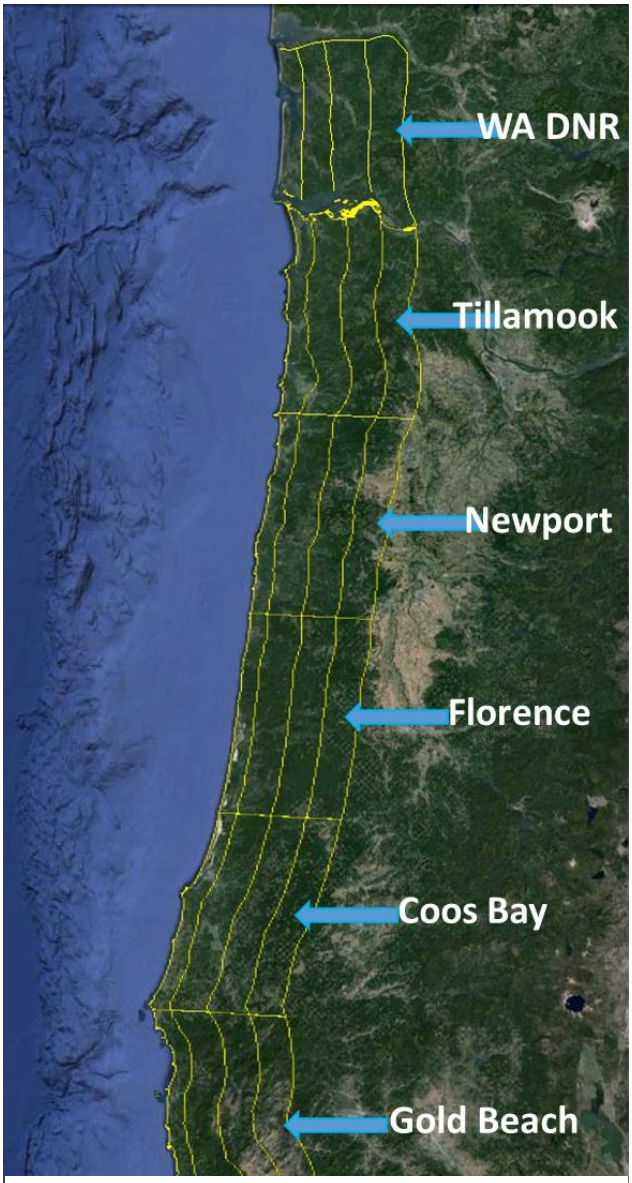

Figure 1. Research plot network matrix.

Sites

In addition to the 30 plots established in 2013, in 2014, 39 sites were selected, installed and measured. All of 2014 sites are located in Oregon on land owned by Weyerhaeuser, Menasha Forest Products Corporation, Oregon Department of Forestry, Hampton Affiliates or Hancock Forest management Inc., bringing the overall number of sites to 69. Plots within the stands were chosen subjectively.

Measurements

Following the establishment and marking of plot boundaries, all trees were given a unique numbered tag. Following the conclusion of the 2014 growing season, all trees were measured for dbh and species was recorded. A forty tree height sample was collected, such that it included the 10 largest trees by dbh, the four smallest by dbh, and the final 26 were ranged across the diameter distribution. In the spring, the 10 largest trees will be assessed for foliage retention, and needles will be sampled for pseudothecial occlusion, and foliar nutrition. In addition, soil samples were collected for Jeff Hatten's soil study.

Summary statistics

Table 1: Data from the 36 plots for which data has been entered

	Douglas-fir				Other Species	
Plot	Trees per plot	Av. Dbh (cm)	Av. Ht (m)	Av. CR	Trees per plot	Av. Dbh (cm)
CB01	96	16.5	11.08	0.68	51	8.7
CB02	119	17.1	13.50	0.63	29	8.0
CB151	99	18.3	16.61	0.57		
CB152	105	17.3	15.47	0.71		
CB251	82	16.9	14.63	0.81	5	13.7
CB252	96	18.0	17.51	0.68	1	6.0
CB51	121	15.2	13.47	0.71	17	7.3
CB52	113	12.4	9.86	0.86	1	5.8
CB53	79	16.5	11.67	0.87		
CB54	53	24.7	19.92	0.63		
F02	79	17.1	13.19	0.62	96	10.2
F251	74	14.3	11.07	0.91	15	5.4
F51	70	23.9	19.22	0.60		
G01	138	16.2	12.58	0.66	1	6.9
N01	60	17.8	14.23	0.70	34	15.1
N02	87	20.8	13.93	0.59	14	9.8
N03	54	18.6	15.07	0.65	121	9.3
N04	64	19.8	15.73	0.61	116	7.3
N05	64	23.6	20.21	0.52		
N153	58	24.6	18.69	0.62	20	8.9
N154	56	24.9	16.90	0.68	1	7.5
N155	92	17.8	15.29	0.72		
N252	76	20.0	17.28	0.69	4	12.0
N253	68	19.5	17.99	0.72	10	8.0
N255	117	15.9	14.09	0.67	34	6.7
N51	65	18.9	14.74	0.74	5	8.5
N52	64	25.4	18.28	0.62		
N53	54	26.4	18.89	0.60	1	5.9
N54	71	18.9	12.01	0.77	11	9.4
N55	93	17.9	14.21	0.68	39	7.6
T154	51	28.1	19.60	0.60	22	9.3
T155	111	17.2	15.74	0.72	9	8.6
T254	51	24.7	19.41	0.65		
T256	55	24.8	18.55	0.64	8	16.7
T257	135	13.1	13.22	0.75	1	10.4
T52	33	31.8	24.28	0.55	6	11.9

Figure 1: Height-diameter relationships for the 36 plots for which data has been entered

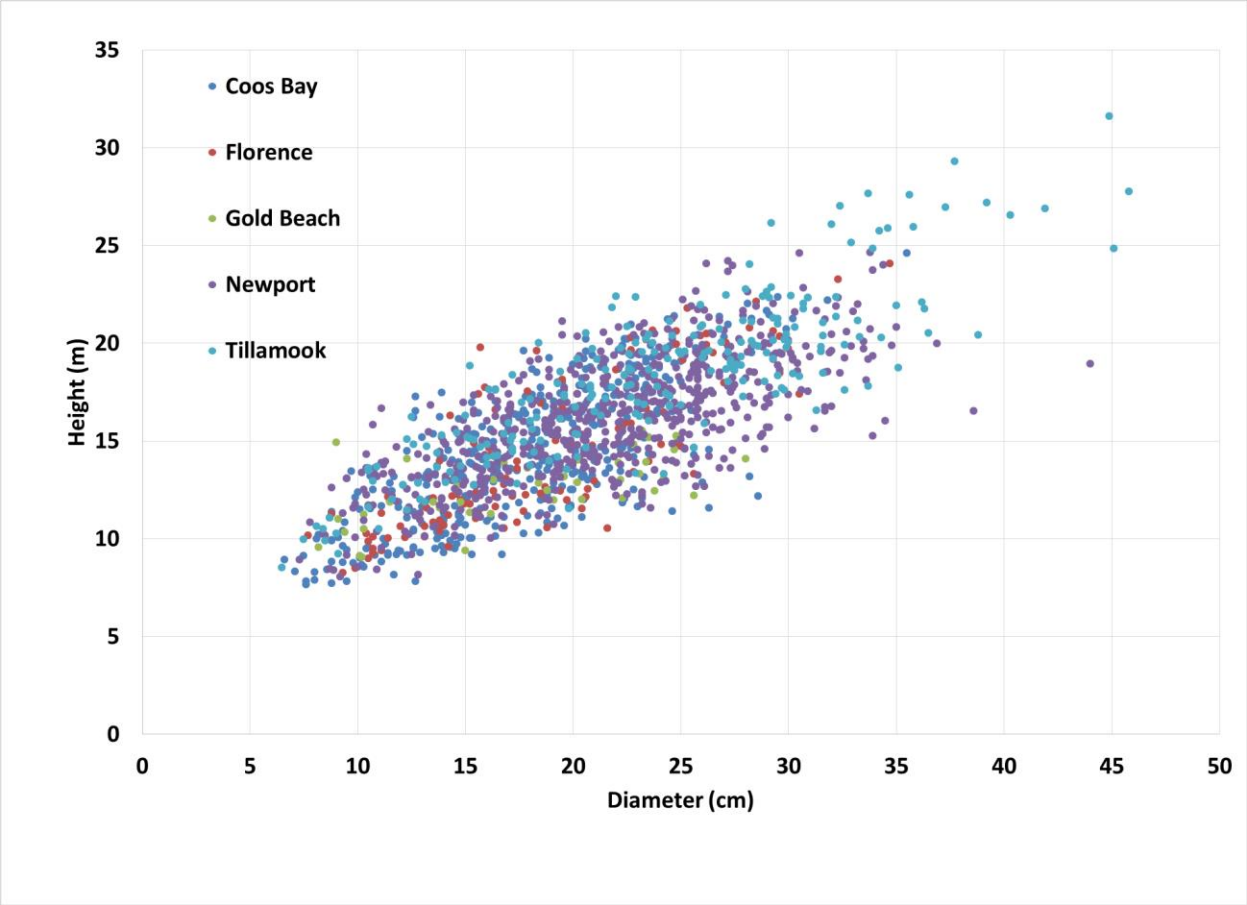

TIMELINE: Research and Monitoring Plot Network Chronology

2013 Fall, Begin Plot Establishment Tree Measurements.

2014 Spring Begin Collect Branches (FR, Disease Severity). Fall, Plot Establishment Tree Measurements

2015 Spring Collect Branches (FR, Disease Severity). Fall, Complete Plot Establishment Tree Measurements (120 plots)

2016 Spring Complete Collect Branches (FR, Disease Severity).

2017

2018 Re-measure 2013

2019 Collect Branches (FR, Disease Severity) Re-measure 2014

2020 Collect Branches (FR, Disease Severity) Complete 5 yr Re-measure 2015

2021 Complete 5 yr Collect Branches (FR, Disease Severity)

2022

2023 Re-measure 2013

2024 Collect Branches (FR, Disease Severity) Re-measure 2014

2025 Collect Branches (FR, Disease Severity) Complete 10 yr Re-measure 2015

2026 Complete 10 yr Final Collect Branches (FR, Disease Severity)

Mapping Vegetation Decline from Swiss Needle Cast using LiDAR and satellite remote sensing

Thomas Hilker, College of Forestry, Oregon State University

Introduction

Increased outbreaks of native diseases, associated with a warmer climate, have been recorded in the forests of the Pacific Northwest Region over the last two decades. These outbreaks are sufficiently severe to cause changes in the economics and management of native forests. Recent changes in regional climate appear to promote outbreaks of many native diseases and insects (Bentz et al., 2010; Woods et al., 2005), causing widespread decrease in forest health and loss in biodiversity. For instance, Swiss needle cast (SNC), a disease caused by fungal pathogen *Phaeocryptopus gaeumannii* is intensifying along the coast of Washington and Oregon affecting 586,000 acres of Douglas-fir forest (Kanaskie 2014), and causing significant economic loss (Kimberley et.al. 2011).

Current state of the art mapping includes visual interpretation from helicopter or aircraft, which is costly and not sufficiently accurate, because a) weather conditions may not permit enough flight hours to cover the entire coast range, and b) smaller areas may be overlooked, or their extent may not fully be assessed. In addition to spatial extend, ecological and economic impact is difficult to assess. Growth loss for instance, can currently only be assessed from field plots, which, while accurate, are spatially discrete, time consuming and costly.

Objective

The objective of this work is to assess impact on growth limitation of Swiss Needle Cast on Coastal Douglas-fir (*Pseudotsuga menziesii*) plantations using remote sensing techniques, specifically airborne Light Detection and Ranging (LiDAR) and satellite observations from the Landsat series of satellites.

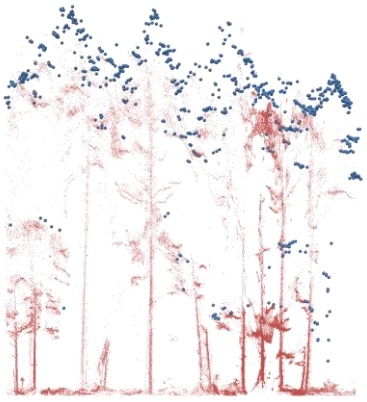

Figure 1 *Vegetation structure observed from airborne (blue) and terrestrial (red) LiDAR systems*

Methods and preliminary findings

LiDAR is a remote sensing technique that directly measures the three-dimensional distribution of canopy components as well as sub-canopy topography, thereby providing highly accurate and detailed estimates of vegetation height, cover, crown shape, density and other aspects of canopy structure (Næsset & Økland, 2002). LiDAR has been used extensively to measure tree height and canopy structure. Unlike passive remote sensing, LiDAR measures the three dimensional structure of forests directly (Hilker et al., 2012; Lim, Treitz, Wulder, St-Onge, & Flood, 2003). Height estimates from LiDAR data are typically of similar or better accuracy than corresponding field based estimates (Næsset & Økland, 2002) and studies have demonstrated that the LiDAR measurement error for individual trees is less than 1.0 m (Persson, Holmgreen, and Söderman 2014) and less than 0.5 m for plot based estimates of maximum and mean canopy height with full canopy closure (Magnussen & Boudewyn, 1998; Næsset & Økland, 2002; Næsset, 1997). The ability of LiDAR to provide high resolution canopy and sub canopy topography along with the ca-

pacity to accurately measure leaf area index (LAI), vegetation height, and above ground biomass (Lefsky, Cohen, Parker, & Harding, 2002) will allow accurate comparisons of Coastal forests with and without SNC infestation. For the state of Oregon most of the Coast Range has been flown by aerial LiDAR surveys and the Oregon Department of Geology and Mineral Industries (DOGAMI) has been involved in the collection high-resolution data since 2003. This dataset will be available at no cost to this proposal through an agreement between DOGAMI and Oregon State University.

Stand growth may be estimated from LiDAR derived stand height, if the age of the forest is known. The Landsat series of satellite data provides the longest existing satellite record of terrestrial vegetation, starting in 1972, and maturing with the Landsat MSS and TM instruments since 1984. Landsat's spatial resolution of 30 m, and extent of 185 x 185 km per scene has proven utility for monitoring vegetation change at regional scales (Wulder et al., 2008, Hansen et al., 2008) and numerous forest change algorithms have been developed, validated, and applied (Zhu and Woodcock, 2012) (e.g. Collins & Woodcock, 1996; Healey et al., 2005; Kennedy et al., 2007; Masek et al., 2008). This study uses disturbance estimates from Landsat to derive stand age for managed forests of 30 years of age or less. One of the most common techniques to determine stand replacing disturbances is the disturbance index (DI) of Healey et al (2005). This method transforms spectral observations into a tasseled Cap data space and is then calculated using the three Tasseled Cap indices (brightness, greenness and wetness) from Landsat TM/ETM+ data (Crist, and Kauth 1986; Healey et al. 2005; Masek et al. 2008). The disturbance is quantified as the normalized spectral distance of any given pixel from a nominal "mature forest" class (Healey et al., 2005; Hilker et al., 2009). Figure 2 shows a Landsat based estimate of disturbances in costal Washington and Oregon since 1984 and the overlap between Landsat observed date of disturbance and available height estimates from LiDAR. The color of the disturbed areas corresponds to the month of disturbance, running as continuous number from Jan. 1984 through Dec. 2012.

Future work/Next steps

To date, estimates of vegetation growth have been obtained across the state of Oregon using all available LiDAR data. Observations are compiled at 30 spatial resolution to match estimates of Landsat. In addition, estimates of disturbance have been finalized across the coast range since 1984. Next steps of this work include validation of remotely sensed growth estimates with existing field observations and the incorporation of field plots to assess differences in vegetation growth from SNC-infected and non-infected Douglas-fir plantations.

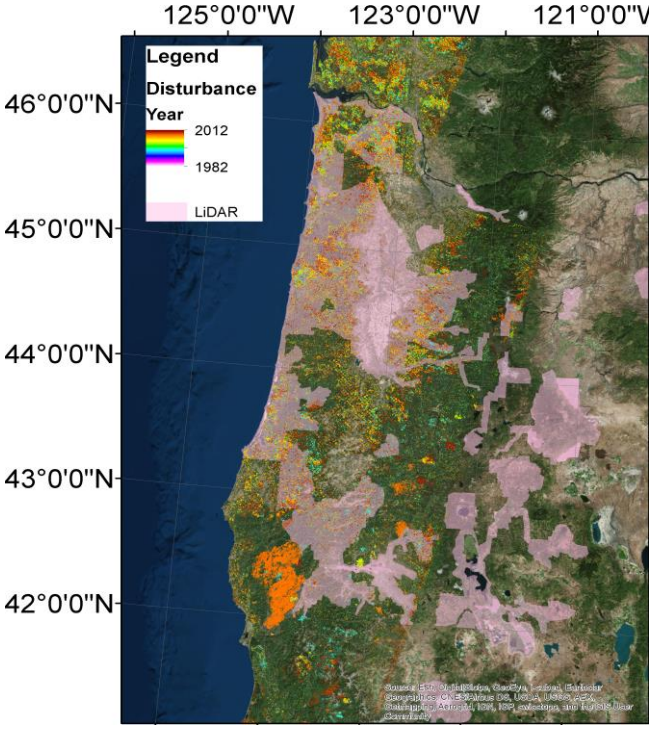

Figure 2: Potential estimates of vegetation growth along Oregon's coast range resulting the combination of Landsat based estimates of disturbance and height estimates from airborne LiDAR

References

Crist, E. P. and Kauth, R. J. (1986). The Tasseled Cap de-mystified [transformations of MSS and TM data]. *Photogrammetric Engineering and Remote Sensing*, *52*, 81–86.

Healey, S., Cohen, W., Zhiqiang, Y., & Krankina, O. (2005). Comparison of Tasseled Cap-based Landsat data structures for use in forest disturbance detection. *Remote Sensing of Environment*, *97*(3), 301–310. doi:10.1016/j.rse.2005.05.009

Hilker, T., Coops, N. C., Newnham, G. J., Leeuwen, M. Van, Wulder, M. A., Stewart, J., & Culvenor, D. S. (2012). Comparison of Terrestrial and Airborne LiDAR in Describing Stand Structure of a. *Journal of Forestry*, (March), 97–104.

Hilker, T., Wulder, M. A., Coops, N. C., Linke, J., McDermid, G., Masek, J. G., White, J. C. (2009). A new data fusion model for high spatial- and temporal-resolution mapping of forest disturbance based on Landsat and MODIS. *Remote Sensing of Environment*, *113*(8), 1613–1627. doi:10.1016/j.rse.2009.03.007

Lefsky, M. A., Cohen, W. B., Parker, G. G., & Harding, D. J. (2002). Lidar Remote Sensing for Ecosystem Studies. *BioScience*, *52*(1), 19. doi:10.1641/0006-3568(2002)052[0019:LRSFES]2.0.CO;2

Lim, K., Treitz, P., Wulder, M., St-Onge, B., & Flood, M. (2003). LiDAR remote sensing of forest structure. *Progress in Physical Geography*, *27*(1), 88–106. doi:10.1191/0309133303pp360ra

Magnussen, S., & Boudewyn, P. (1998). Derivations of stand heights from airborne laser scanner data with canopy-based quantile estimators. *Canadian Journal of Forest Research*, *28*(7), 1016–1031. doi:10.1139/cjfr-28-7-1016

Masek, J. G., Huang, C., Wolfe, R., Cohen, W., Hall, F., Kutler, J., & Nelson, P. (2008). North American forest disturbance mapped from a decadal Landsat record. *Remote Sensing of Environment*, *112*(6), 2914–2926. doi:10.1016/j.rse.2008.02.010

Næsset, E. (1997). Determination of mean tree height of forest stands using airborne laser scanner data. *Journal of Photogrammetry and Remote Sensing*, *52*(2), 49–56. doi:10.1016/S0924-2716(97)83000-6

Næsset, E., & Økland, T. (2002). Estimating tree height and tree crown properties using airborne scanning laser in a boreal nature reserve. *Remote Sensing of Environment*, *79*(1), 105–115. doi:10.1016/S0034-4257(01)00243-7

Persson, A., Holmgren, J., & Söderman, U. (n.d.). Detecting and measuring individual trees using an airborne laser scanner. *Photogrammetric Engineering and Remote Sensing*, *68*(9), 925–932.

Response of Swiss needle cast-infected Douglas-fir to pre-commercial thinning in northwestern Oregon

Doug Mainwaring, Doug Maguire, Alan Kanaskie, Gabriela Ritokova

Introduction

Reduction of stand density is commonly used in stands where low vigor limits individual tree growth or makes trees susceptible to pests (Mitchell et al. 1983). The potential benefits of thinning SNC-infected stands in northwestern Oregon had been debated vis-a-vis field observations suggesting that thinning was exacerbating symptoms by increasing air flow and tree sway within stands, thereby leading to greater foliar losses.

Because density reduction enables crowns to expand and elongate, the rationale behind thinning was an expected increase in crown length, canopy depth, and subsequent foliage area per tree, with corresponding improvement in individual tree growth and increased likelihood that trees would reach merchantable size. Furthermore, because trees show differential levels of SNC disease tolerance (Johnson 2002), thinning from below would presumably remove genotypes that were performing most poorly in the presence of SNC. All of these factors would suggest that thinning SNC impacted stands would improve their growth, as has been shown in previous analyses of post-PCT growth. An additional question is whether thinning influences disease severity, as represented by pseudothecial abundance.

Foliage retention results from this study were published in a previous SNCC annual report (2013). Therefore, this report provides updated results from the last measurement, as well as an analysis of pseudothecial occlusion from data collected in 2009.

Methods

The study sites were distributed within the Coast Range of northwestern Oregon across a gradient of Swiss needle cast (SNC) severity and exhibited initial conditions representative of young candidate stands for PCT (Table 1).

Treatments

In the late winter/early spring of 1998, 23 sets of plots were established in 5-16 yr old stands. One of the plots at each site was randomly chosen for pre-commercial thinning, generally to 500 trees per hectare (TPH), while the other was left unthinned (~1000 TPH). Because stand densities were already low on two installations, the thinned plots at these sites were prescribed to a lower target residual density of 250 TPH. Five additional 250 TPH plots were established as a third plot at five of the 21 sites that already included a plot thinned to 500 TPH. On all 21 installations that included a plot thinned to 500 TPH, both the control plots and 500-TPH plots were square and covered 0.08-ha. On the remaining two installations containing a single thinned plot with 250 residual TPH, both the control and thinned plots were twice as large, or 0.16 ha in size. On the five installations that included a third plot thinned to 250 TPH, the 250-TPH plot was also increased to 0.16 ha. All thinnings were implemented before the growing season in 1998, and were based on spacing, so stems were removed proportionally across the diameter distribution.

On each measurement plot, all trees were measured for dbh prior to thinning. At least 40 residual Douglas-fir trees, distributed across the dbh distribution, were measured for total height (nearest 0.01 m) and height to lowest live branch (nearest 0.01 m). After two, four, six, ten, and fifteen growing seasons (1998-99, 2000-01, 2002-03, 2004-07, and 2008-2012 growth periods), all trees were remeasured for dbh, and all trees from the original height subsample were remeasured for total height and height to crown base. Missing total heights and heights to crown

base for Douglas-fir trees were estimated as a function of dbh by fitting regression models specific to each plot and growth period. Cubic volume of each Douglas-fir was estimated with equations previously developed for second-growth Douglas-fir (Bruce and DeMars 1974).

In April and May of each of the first seven years of the study (1998-2004), ten dominant or codominant trees in each plot were assessed for SNC symptoms. From the ground, foliage retention was assessed for each third of the live crown (upper, middle, lower) by visually estimating the average number of years (nearest 0.1 yrs) of foliage retained. Tree-level foliage retention was calculated as the average of all crown-thirds. Estimates were made on the same trees each year.

In the spring of 2009, the largest four-year old lateral of the southernmost five year old branch was collected from 10 trees per plot for assessment of foliage retention. A random sample of one and two year old needles were collected from the four-year old lateral and assessed for pseudothecial abundance. At three locations on ten needles per age per tree, the number of visible pseudothecial out of 100 stomates was counted.

Statistical Analysis

The effect of thinning on foliage retention was analyzed for the crown as a whole, as well as for individual crown-thirds, recognizing the randomized block design of the experiment and repeated measures on individual plots. Comparisons were made among the control, 500 TPH and 250 TPH treatments. Treatment effects were considered significant at $\alpha=0.05$ and marginally significant at $\alpha=0.10$.

Treatment effects on net periodic annual stem volume increment of all Douglas-fir TPH, the largest 500 Douglas-fir TPH, and the largest 250 Douglas-fir TPH were tested with the following full statistical model:

$$[1]\quad \ln(\Delta V_C) = \beta_0 + \beta_1 \cdot \ln(FR_0) + \beta_2 \cdot \ln(BA_{DF}) + \beta_3 \cdot \ln(BA_{ODF}) + \beta_4 \cdot \ln(BA_{OS}) + \beta_5 \cdot I_{250} + \beta_6 \cdot I_{500} + \beta_7 \cdot \ln(FR_0) \cdot I_{250} + \beta_8 \cdot \ln(FR_0) \cdot I_{500} + \beta_9 \cdot \ln(SI) + \delta_2 + \varepsilon_2$$

where ΔV_C = Periodic net annual volume increment of Douglas-fir component *C*, where *C=ALL* for all Douglas-fir trees ha^{-1}; *500* for the largest 500 trees ha^{-1}; and *250* for the largest 250 trees ha^{-1} (m^{3}ha^{-1})

BA_{DF} = Initial Douglas-fir basal area (m^{2}ha^{-1})

BA_{ODF} = Initial basal area of Douglas-fir not included in component *C*

BA_{OS} = Initial basal area of other species (m^{2}ha^{-1})

SI = Bruce's 50 yr SI (based on 2004 height-age pairs) (Bruce 1981)

δ_2 = Random block effect with $\delta_2 \sim N(0, \sigma_\delta^2)$

ε_2 = Residual error

and all other variables are defined above

The residual errors were again expected to be correlated among observations within a plot, so four alternative variance-covariance structures were considered for ε_2 (PROC MIXED in SAS version 9.2): unstructured, Toeplitz, AR(1), and heterogeneous compound symmetry (Littell et al. 2006). Application of this model to only the largest 250 and 500 Douglas-fir per ha across all treatments was done to test if results would differ when limiting the comparisons to similar stand components.

In order to assess differences among growth periods in thinning effects and their interaction with foliage retention, a reduced model [1] (no covariance among observations) was also applied separately to each growth period.

Treatment differences in the proportion of pseudothecia-occluded stomates (total count per needle/300) was tested using ANCOVA, using initial foliage retention as a covariate.

Results

Growth

Periodic annual increment was positively correlated with initial foliage retention. For a given level of initial Douglas-fir basal area, periodic annual increment was significantly greater on plots thinned to 500 TPH than on control plots, with the thinning response greater at lower levels of initial foliage retention (Fig. 1, Table 2). For healthy stands with foliage retention of 4.0 yrs, thinning to 500 TPH was implied to increase PAI by 4.9%, for a given level of initial basal area in Douglas-fir and in other species. For stands with a foliage retention of 1.1 yrs, this increase was implied to be 58.5% (Fig. 1). There were no significant differences between the response of control plots and those thinned to 250 TPH.

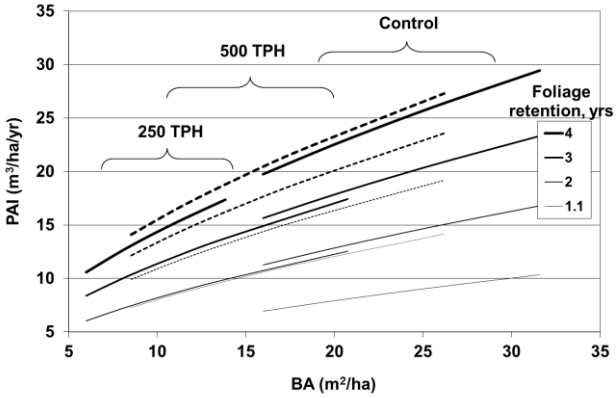

Figure 1 Estimated volume PAI for a given initial Douglas-fir basal area on the control, 500 TPH, and 250 TPH thinning treatments (equation [1]). Additional Douglas-fir basal area and basal area of other species were set to their mean values within each treatment.

When the analysis was limited to the largest 500 TPH, net PAI of the largest 500 TPH in the 500 TPH thinning exceeded that of the control plot regardless of foliage retention (Fig. 2, Table 2). The largest 500 TPH in stands with a foliage retention of 1.1 yrs were implied to produce 81.9% more volume for a given level of initial basal area, while those in stands with a foliage retention of 4.0 yrs produced only 17.8% more volume (Fig. 2).

When the analysis was limited to the largest 250 TPH, net PAI of the largest 250 TPH in the 500

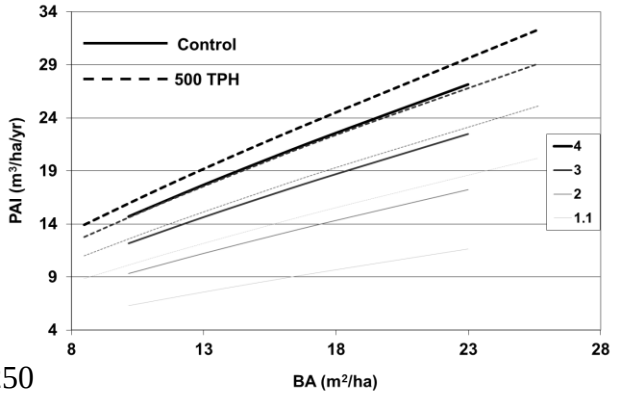

Figure 2 Estimated volume PAI for the largest 500 TPH on the control and 500 TPH thinning treatments (equation [1]). Additional Douglas-fir basal area and basal area of other species were set to their mean values within each treatment.

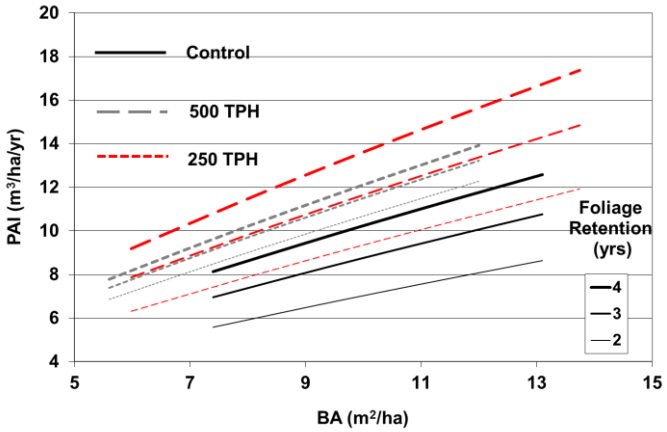

Figure 3 Estimated volume PAI for the largest 250 TPH on control, 500 TPH, and 250 TPH thinning treatments ((equation [1]). Additional Douglas-fir basal area and basal area of other species were set to their mean values within each treatment.

TPH thinning exceeded that of the same component within the control plot regardless of foliage retention (Fig. 3, Table 2). There were no significant differences between the response of the 250 largest TPH on the control plots and the same stand component on plots thinned to 250 TPH.

When growth periods were analyzed separately, no response to thinning was apparent in the first two years following treatment at either level of thinning. In subsequent periods, the thinning response in plots with maximal foliage retention and thinned to 500 TPH was significant and positive, ranging from 13% in the second growth period (3-4 years after thinning) to 20% in the fourth growth period (7-10 years after thinning). During the same periods, response to thinning to 500 TPH in the most severely infected stands (1.1 yrs foliage retention) ranged from 90 to 123%.

Pseudothecial occlusion

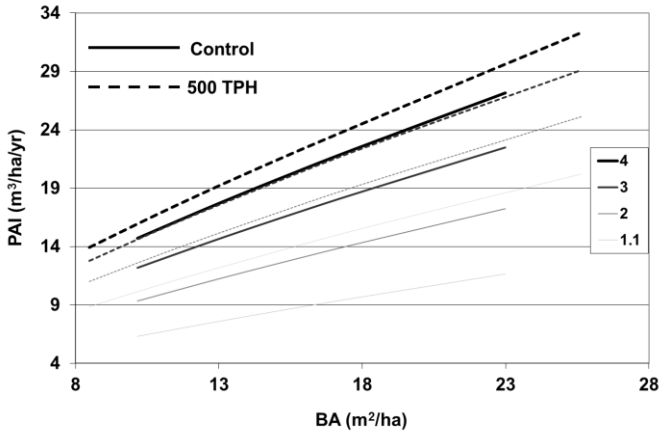

Figure 4 Implied effect of thinning to 500 TPH on pseudothecial abundance

Occlusion was much greater at lower levels of foliage retention, reaching nearly 43% on the most infected control plots (Fig 4). There were no treatment-level differences in the proportion of occluded stomates on one-year old needles. For two-year old needles, there was a significant decrease in the proportion of occluded stomates following thinning. For the 250 and 500 TPH thinnings, this amounted to absolute decrease in occlusion of ~1.9 and 2.7% respectively, regardless of initial foliage retention.

Discussion

Contrary to concerns about adverse effects of thinning in the presence of Swiss needle cast, there was no evidence of any significant decline in foliage retention induced by thinning, even in the most severely infected stands. Although foliage retention increased in the lower crowns of all but the most healthy trees following treatment, the increase was implied to be less in infected plots thinned to 500 TPH than in infected unthinned plots.

Pseudothecial abundance is greatest and foliage retention poorest in the upper crowns of trees, which suggests that conditions in the tree tops are more conducive to spore interception, spore germination, or pseudothecial development (Hansen et al. 2000). Both epidemiological

research and climate modeling have identified spring leaf wetness and winter temperatures as being directly related to successful *Phaeocryptopus* germination and growth, and subsequent needle loss (Zhao et al. 2011). Although leaf wetness is likely to be greater and more sustained in the lower canopy where wind speeds are lower and atmospheric drying is less effective, springtime humidity along the US Pacific coast is generally high. Temperatures conducive to fungal development can be also expected to be greater at the tops of trees than at the base of the crown (Zweifel et al. 2002). Whether there are differences in *Phaeocryptopus* ascospore deposition within the crown is unknown—while interception of ascospores by upper branches might result in decreased penetration of spores to lower branches, it is unknown what role through fall precipitation and successive dripping of intercepted precipitation from upper to lower foliage play in dispersal and deposition. Other research has linked excess foliar nitrogen and associated free amino acid (FAA) concentrations with increased levels of *Phaeocryptopus* (El Hajj et al. 2004). Although the nutritional requirements of *Phaeocryptopus* remain poorly understood, this proposed link, in concert with an observed increase in N concentration with increased canopy light exposure (Brooks et al. 1996), could partly explain the decreasing gradient in SNC severity with depth into crown.

Numerous changes occur within newly thinned stands that affect the environment vis-à-vis SNC. The fact that foliage retention within the lower crown of healthy stands increased following thinning suggests that in the absence of SNC or loosely held needles, increased wind speeds do not by themselves cause a net loss of needles. At the same time, increased wind speeds in the lower canopy would presumably result in lower humidity and more effective drying of needles, thus negatively impacting fungal germination and needle colonization. Thinning can increase temperatures in the lower canopy (Rambo and North 2009), resulting in more rapid pseudothecial development (Capitano 1999) of older, previously infected needles. Sudden exposure of shade foliage can also lead to photoinhibition (Powles and Bjorkman 1982) and premature abscission (Tucker and Emmingham 1977), and this effect would be expected to be greater in the more heavily shaded lower foliage of trees with higher foliage retention, as observed in our thinned Douglas-fir plots.

Because pre-commercial thinning in young Douglas-fir stands is generally performed from below, a question remains as to how well the results from this study apply after such a treatment. In progeny tests subject to SNC, therefore, the larger and better-growing trees may not necessarily exhibit better foliage retention (Johnson 2002). These results suggest that smaller trees within a stand may be smaller only in part due to greater genetic susceptibility, and that their growth rate per se may render them less able to resist the disease. On the stand level, the presence of these smaller trees would tend to lower the growth rate for a given initial basal area, as illustrated by the stand-level thinning response of all trees relative to the thinning response of only the largest 500 Douglas-fir TPH.

Another reason for the improvement in volume growth per unit initial basal area within the thinned Douglas-fir stands can be inferred from stand dynamics within SNC-infected control plots, where species other than Douglas-fir tend to be common. Because the pre-commercial thinning treatment for this study preferentially removed both subordinate Douglas-fir and other species that were highly competitive with Douglas-fir, residual trees in several impacted plots benefitted.

It is well known that thinning increases the amount of light available to residual trees (Brix 1993). Thinning is also known to increase leaf area throughout the crown, but especially in the lower crown (Brix 1981). Because SNC-infected trees carry relatively large amounts of their foliage mass in the lower portions of the crown, even before thinning, and because illumination

increases dramatically in those crown portions following thinning (Han 2006), it can be inferred that residual trees in an infected stand experience a larger relative increase in light capture.

Analysis of the largest 500 or 250 TPH in each stand revealed a notable difference in the performance of the 500 and 250 TPH thinning treatments. Periodic annual increment of the largest trees (250 or 500 TPH) improved after thinning to 500 TPH thinning, but didn't differ significantly from the control when thinned to 250 TPH. The heavier thinning may also have resulted in greater thinning shock (Harrington and Reukema 1983) than the light thinning. Given the small number of 250 TPH treatments, and their non-representation in severely impacted stands, conclusions about net PAI of stands with low initial foliage retention and thinned to 250 TPH require further testing.

Analysis of pseudothecial abundance indicates that pre-commercial thinning can reduce the pseudothecial abundance in two-year old needles. Whether this is part of the explanation for the improved growth within thinned stands is unknown, although fewer plugged stomates should increase gas exchange. Although there was not a significant interaction with foliage retention, the 2-3% absolute reduction in fruiting bodies represents a larger percentage of unplugged stomates within severely infected stands than within healthier stands. That said, the reduction in plugging with thinning is small, and is likely to provide only a small part of the benefit of thinning.

Literature Cited

Brix. H. 1981. Effects of thinning and nitrogen fertilization on branch and foliage production in Douglas-fir. Can. J. For. Res. **11**: 502–511.

Brix, H. 1993. Fertilization and thinning effect on a Douglas-fir ecosystem at Shawnigan Lake: a synthesis of project results. FRDA Rep. 196. Pacific Forestry Centre, Forestry Canada, Victoria, B.C., and Research Branch, British Columbia Ministry of Forests, Victoria, B.C.

Brooks, J.R., Sprugel, D.G., and Hinckley, T.M. 1996. The effects of light acclimation during and after foliage expansion on photosynthesis of Abies amabilis foliage within the canopy. Oecologia 107:21-32.

Bruce, D. and DeMars, D. J.. 1974. Volume equations for second-growth Douglas-fir. USDA-FS Pacific Northwest Research Station, Portland, Oregon. Res. Note PNW-239. 5 p.

El-Hajj, Z, Kavanagh, K. Rose, C., and Kanaan-Atallah, Z. 2004. Nitrogen and carbon dynamics of a foliar biotrophic fungal parasite in fertilized Douglas-fir. New Phytologist. 163: 139–147.

Han Q., Araki M., and Chiba Y. 2006. Acclimation to irradiance of leaf photosynthesis and associated nitrogen reallocation in photosynthetic apparatus in the year following thinning of a young stand of *Chamaecyparis obtusa*. Photosynthetica 44:523–529

Hansen, E. M., Stone, J. K., Capitano, B. R., Rosso, P., Sutton, W., Winton, L., Kanaskie, A., and McWilliams, M. 2000. Incidence and impact of Swiss needle cast in forest plantations of Douglas-fir in coastal Oregon. Plant. Dis. 84: 773–778.

Harrington, C.A., and Reukema, D.L. 1983. Initial shock and long-term stand development following thinning in a Douglas-fir plantation. For. Sci. 29:33–46.

Johnson, G. R. 2002. Genetic variation in tolerance of Douglas-fir to Swiss needle cast as assessed by symptom expression. Silvae Genetica. 51: 80–86.

Littell , R.C. , Milliken, G.A., Stroup, W.W., Wolfinger, R.D., Schabenberber, O. 2006. SAS for Mixed Models. 2nd ed . SAS Institute Inc , Cary, NC , 814 pp .

Powles, B., and Bjorkman, O. 1982. Photoinhibition of photosynthesis: Effect on chlorophyll fluorescence at 77K in intact leaves and in chloroplast membranes of Nevium oleander. Planta 156:97-107.

Rambo, T. R. and North, M. P. 2009. Canopy microclimate response to pattern and density of thinning in a Sierra Nevada forest. *Forest Ecology and Management* 257:435–442.

Tucker, G.F., Emmingham, W.H. 1977. Morphological changes in leaves of residual western hemlock after clear and shelterwood cutting. *Forest Science* 23:195-203.

Zhao, J. Mainwaring, D.B., Maguire, D.B., and Kanaskie, A. 2011. Regional and annual trends in Douglas-fir foliage retention: correlations with climatic variables. *In Review.*

Zweifel, R., Bohm, J.P., and Hasler, R., 2002. Midday stomatal closure in Norway spruce—reactions in the upper and lower crown. Tree Phys. 22: 1125-1136.

Table 1. Initial attributes (1998, after thinning) of Douglas-fir plots included in the SNCC pre-commercial thinning study.

Variable	Units	Control mean (stdev)	500 TPH mean (stdev)	250 TPH mean (stdev)
Douglas-fir tree density	trees ha^{-1}	1020.8 (313.3)	472.4 (36.0)	242.6 (15.8)
Douglas-fir basal area	m^2ha^{-1}	15.76 (6.32)	8.51 (2.89)	5.99 (2.51)
Douglas-fir breast height age	yrs	10.9 (2.4)	10.6 (2.3)	11.1 (3.1)
Douglas-fir QMD	cm	14.1 (3.1)	15.1 (3.0)	17.4 (4.6)
Douglas-fir top height	m	11.66 (2.06)	11.49 (1.95)	12.28 (2.84)
Douglas-fir site index	m at 50 yrs	43.0 (6.7)	43.4 (6.3)	44.4 (4.0)
Basal area of other conifers	m^2ha^{-1}	1.75 (6.14)	0	0
Basal area of broadleaved species	m^2ha^{-1}	1.21 (1.14)	0	0
Total tree density	trees ha^{-1}	1496.6 (950.2)	491.5 (50.0)	247.0 (20.2)
Total plot basal area	m^2ha^{-1}	18.72 (8.79)	8.51 (2.89)	5.99 (2.51)
Total basal area removed	m^2ha^{-2}	0	10.50 (7.29)	12.23 (7.40)
Foliage retention	years	2.43 (0.52)	2.46 (0.62)	2.80 (0.30)
Periodic annual increment	$m^3ha^{-1}yr^{-1}$	17.26 (6.84)	15.08 (6.78)	12.29 (4.96)

Table 2: Parameter estimates and standard errors for model describing net periodic annual volume growth of Douglas-fir after precommercial thinning (equation [1]).

		All trees		Largest 500 TPH		Largest 250 TPH	
Parameter	Variable	Estimate	SE	Estimate	SE	Estimate	SE
β_0	intercept	-4.1087	0.1.2362	-3.5544	1.2796	-3.8987	0.9558
β_1	$\ln(FR_0)$	0.5604	0.1061	0.5965	0.1174	0.5606	0.09286
β_2	$\ln(BA_{DF})$	0.6331	0.04291	0.6836	0.05272	0.7660	0.04497
β_3	$\ln(BA_{ODF})$			0.000338	0.004003	-0.00324	0.005491
β_4	$\ln(BA_{OS})$	0.00419	0.00313	0.006856	0.003567	0.004597	0.002350
β_5	I_{250}	0.2704	0.2163			0.3323	0.2650
β_6	I_{500}	0.4912	0.09236	0.6302	0.1179	0.6785	0.0797
β_7	$\ln(FR_0)\cdot I_{250}$	-0.2580	0.1871			-0.08211	0.1846
β_8	$\ln(FR_0)\cdot I_{500}$	-0.3196	0.08481	-0.3367	0.09250	-0.3745	0.07216
β_9	$\ln(SI)$	1.2045	0.3399	0.9839	0.3536	0.9951	0.2658

Simulation of mixed stands of SNC-infected Douglas-fir and western hemlock

Doug Mainwaring, Doug Maguire, David Hann, Junhui Zhao

Introduction

Swiss needle cast (SNC) is a disease caused by the endemic foliar fungus *Phaeocryptopus gaeumannii* (Rohde) Petrak. The disease leads to significant growth losses in Douglas-fir (*Pseudotsuga menziesii* (Mirb.) Franco) by plugging the stomates of needles, thereby inhibiting gas exchange, and, if plugging is severe enough, causing premature needle abcission. Previous analyses have established a direct correlation between the number of years of foliage attached to trees (foliage retention), and the tree's growth potential (Maguire et al. 2011). This correlation has enabled the estimate of a quantitative relationship between foliage retention and stand level growth losses (Maguire et al. 2011). While this has been used to provide an estimate of stand-level SNC damage, it hasn't enabled forest managers to predict the effect of SNC on the development of individual trees, or on the subsequent stand dynamics within infected stands. A large dataset of individual tree measurements and accompanying stand-level estimates of foliage retention enabled development of a quantitative relationship between the expected growth of trees in the absence of SNC (as estimated by the regional growth model ORGANON) and actual measured growth. Through the auspices of the Center for Intensive Planted-forest Silviculture, equations have been developed which adjust ORGANON-estimated diameter and height growth increments with a foliage retention-based modifying function. This report provides examples of ORGANON output using these modifying functions, and demonstrates the effects of applying these modifiers on tree and stand development.

Methods

Data

Data for the development of a modifying function was compiled from four studies established within the Oregon Coast Range, and were distributed from Coos Bay to Astoria. These studies were established specifically to investigate the influence of SNC on symptom expression and growth loss, with and without thinning. These studies include 1) the Growth impact study (GIS), established in 76 10-30 year old plantations, and measured 5 times from 1998-2008; 2) The Pre-commercial thinning study (PCT) established in 23 8-17 year old stands, and measured 5 times from 1998-2008; 3) the commercial thinning study (CT), established in 30 25-60 year old stands, and measured three times between 2002-2006; and 4) the retrospective commercial thinning study (RCT), established in 41 30-60 year old stands in 2002 and remeasured once in 2006. Development of the modifying function was led by David Hann and Junhui Zhao.

Simulations

The primary objective of this report is to demonstrate the effect that applying the SNC modifier has on stand dynamics. The chosen method was to perform ORGANON projections of a mixed species stand of Douglas-fir and western hemlock at different levels of foliage retention.

The tree list for simulating within ORGANON came from an SMC type 1 site. The stand was 13-years old (total age) with a site index of 120 ft in 50 years. For the Douglas-fir comparisons,

this tree list was projected to a total age of 58 years, assuming no SNC presence, as well as SNC-reduced foliage retentions of 2.5, 2.0, 1.5, and 1.0 years.
The same tree list was used for western hemlock simulations using the following method: A random selection of 33.3% of the trees in the tree list was made and the species of these trees was changed from Douglas-fir to western hemlock. To account for expected height differences, heights of the species-converted trees were reduced by 10%. The site index of the western hemlock trees was determined using the site index conversion equation within ORGANON, which reduces the Douglas-fir site index value by approximately 10%.

Results

The relationship between reduced foliage retention and reductions in diameter and height growth from the latest fits are shown in figure 1. When applying these within ORGANON, decreasing foliage retention benefitted western hemlock relative to Douglas fir (figs. 2-3). In addition, as foliage retention decreased, western hemlock benefitted with increased diameter growth for a given height. (fig.4).

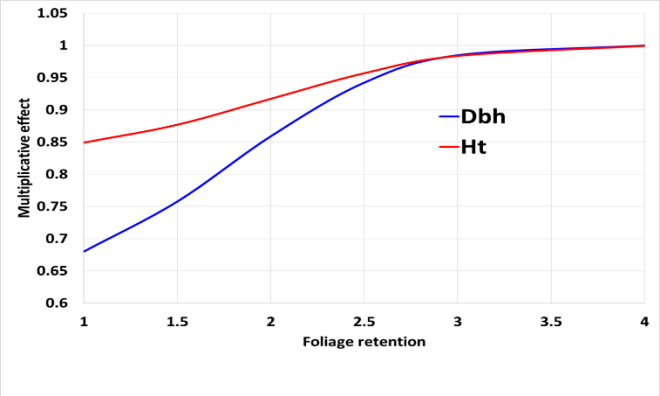

Figure 1 Multiplicative effect of foliage retention on ORGANON dbh and ht increment

The relative benefit to western hemlock from decreased Douglas-fir foliage retention, and the resulting competitive disadvantage to Douglas-fir in a severely infected mixed stand is demonstrated by the reduced the quadratic mean diameter of DF relative to that within a pure DF stand (figure 5).

The effect of SNC on the projected TPA of a mixed DF:WH stand is slightly negative for Douglas-fir, with a decrease of about 30 TPA of suppressed trees at age 58 (figure 6), which is due to the diminished position of Douglas-fir relative to western hemlock.
In a healthy stand, Scribner volume of Douglas-fir exceeds that of western hemlock until after age 50. Conversely, in an infected stand, hemlock volume always exceeds that of Douglas-fir, and, as with QMD and TPA, benefits from the poor development of Douglas-fir (figure 7).

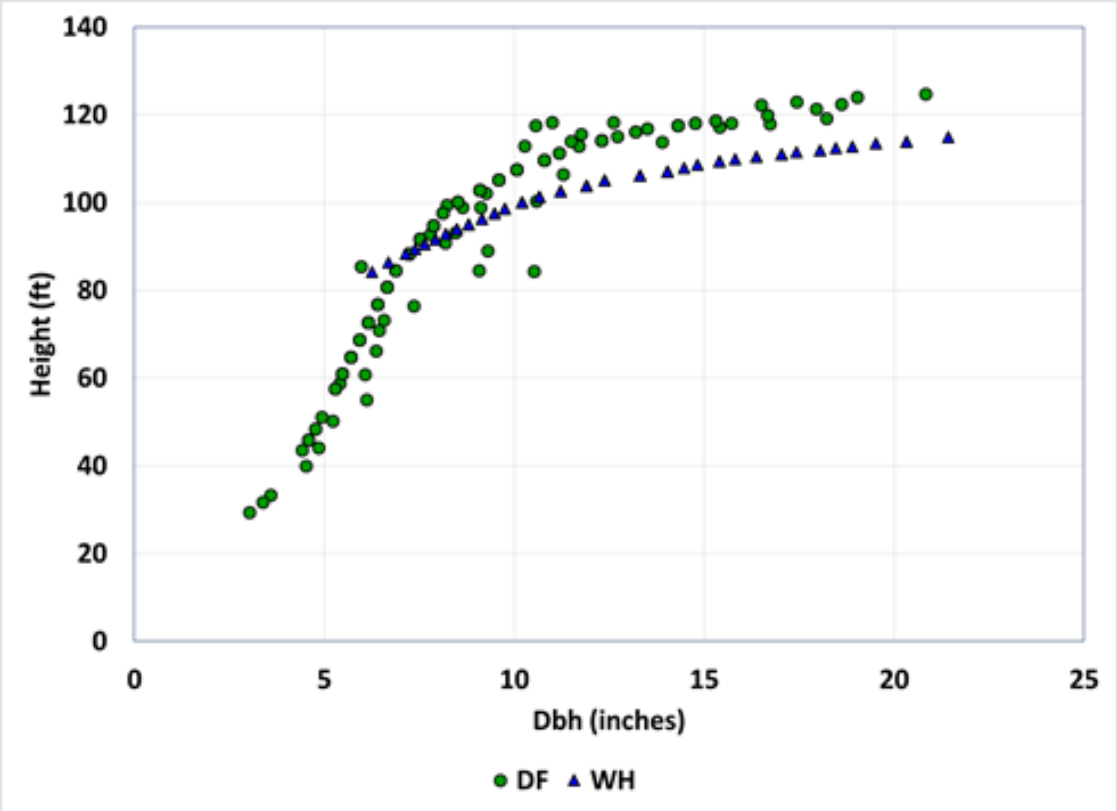

Figure 2 Projected height:diameter relationship of a healthy,mixed DF, WH stand

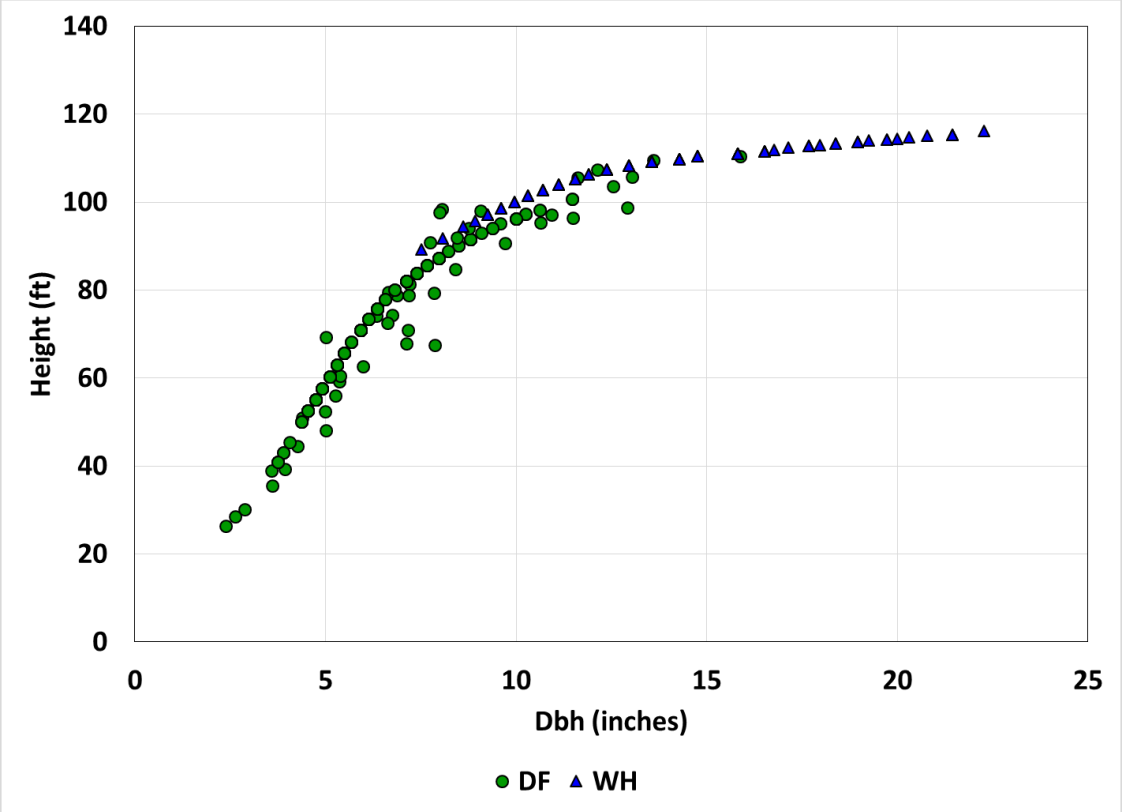

Figure 3 Projected height:diameter relationship of a mixed DF:WH stand with DF foliage retention=1.0 yr

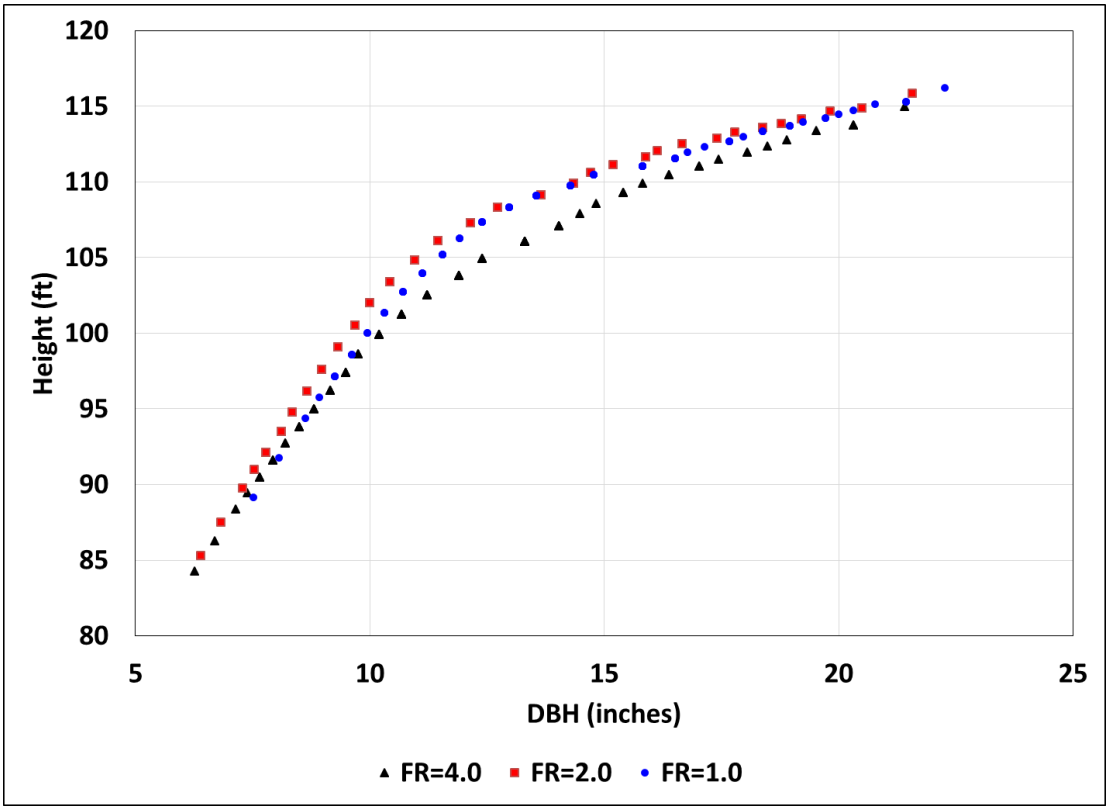

Figure 4 Multiplicative effect of foliage retention on ORGANON dbh and ht increment

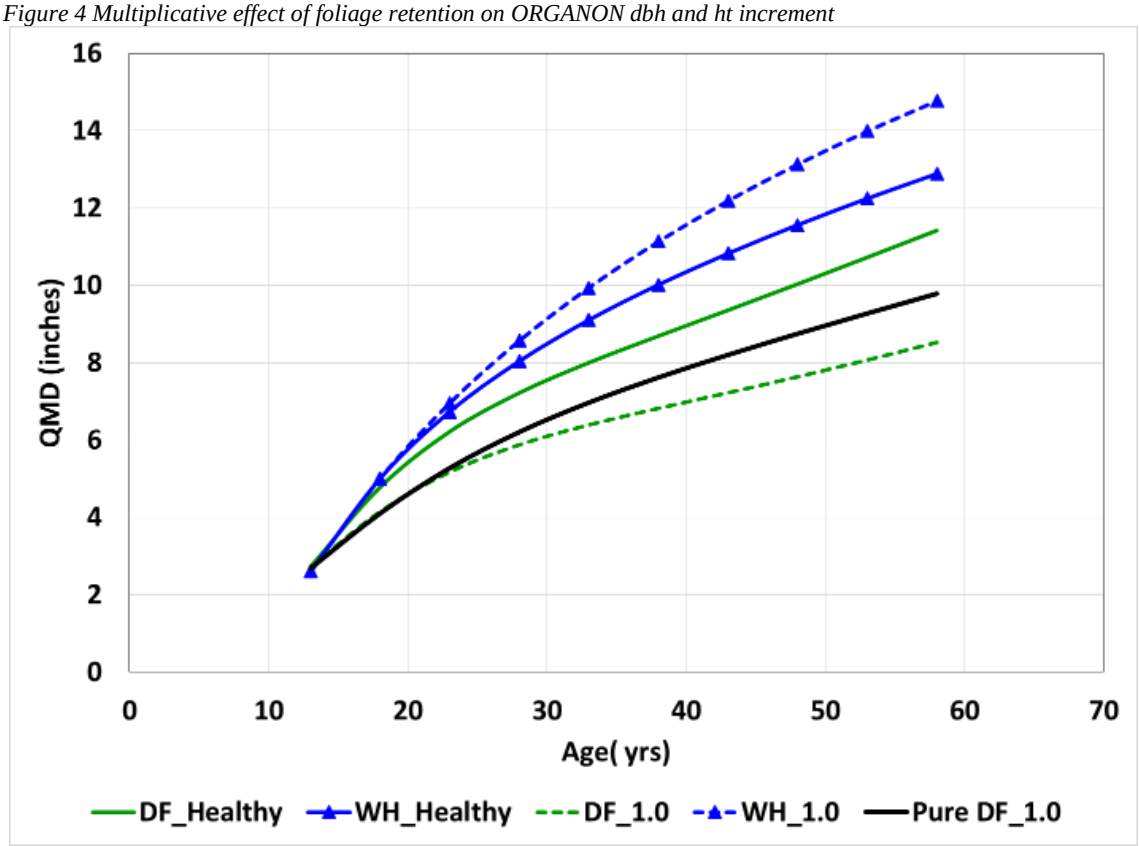

Figure 4 QMD by age for projected healthy, infected mixed DF:WH stands, and an infected pure stand of DF

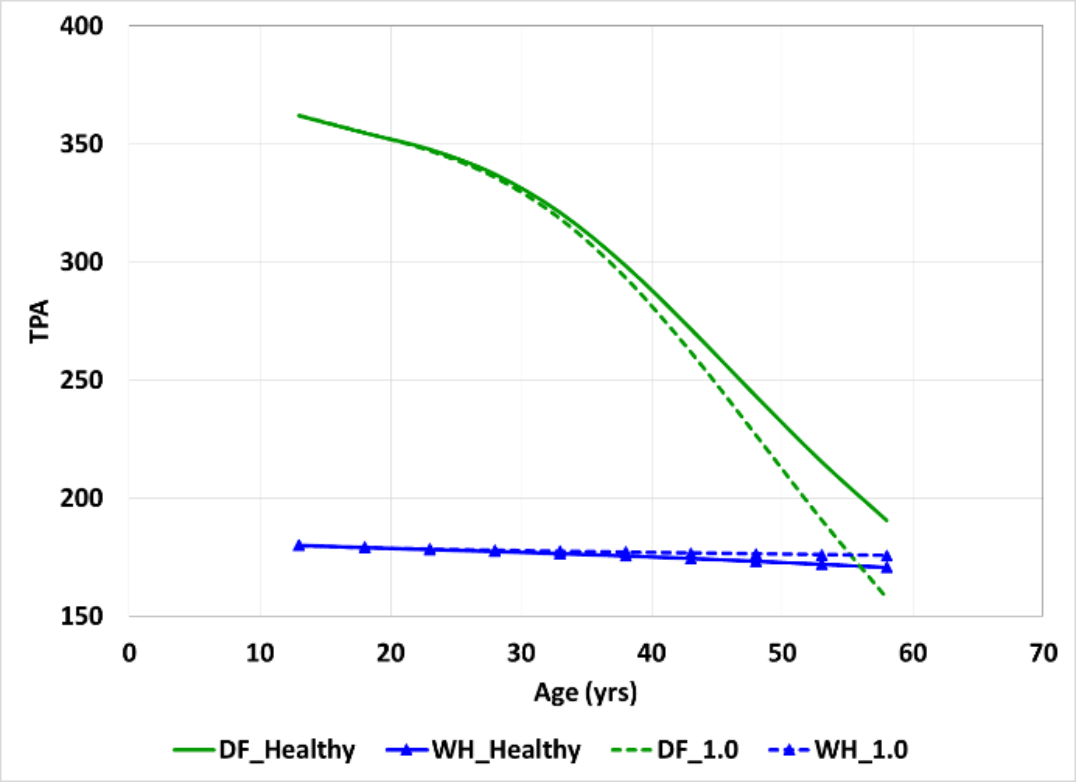

Figure 5 Projected TPA of healthy and infected mixed stands of DF and WH

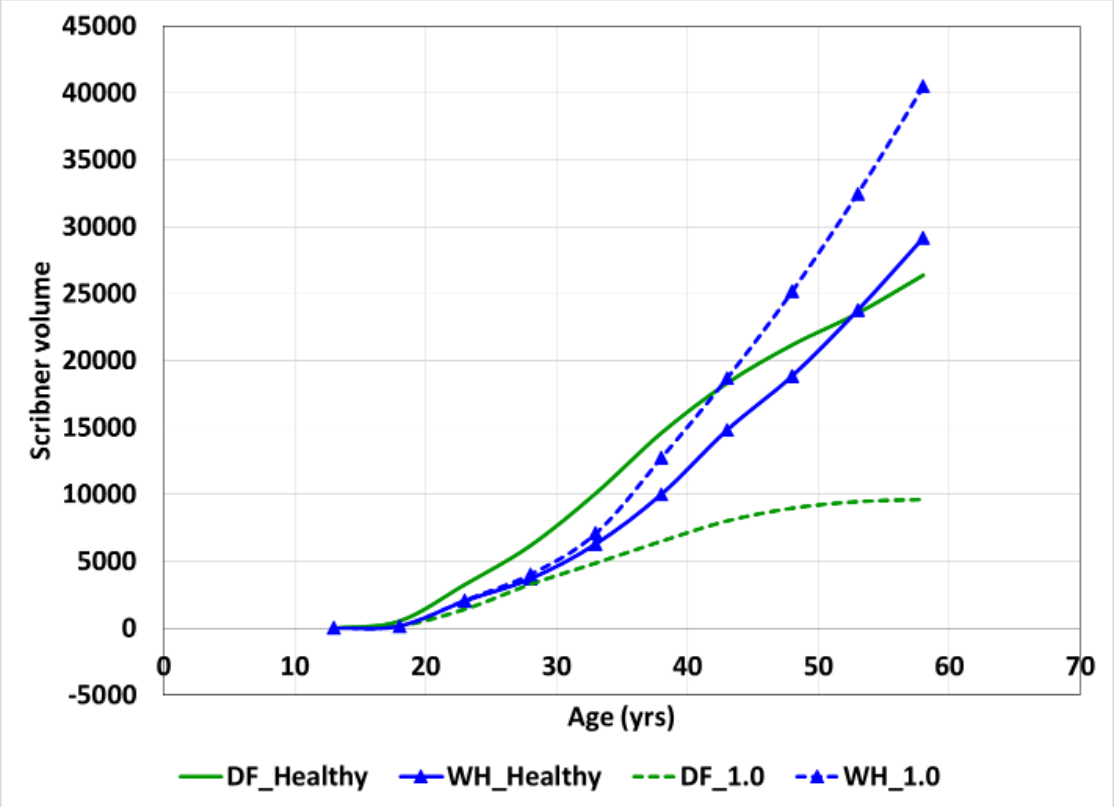

Figure 6 Projected Scribner volume of healthy and infected mixed stands of DF and WH

Effect of Seed Source and Growing Environment on Douglas-fir Foliage Diseases and Other Damaging Agents

Constance Harrington and Brad St. Clair, USDA Forest Service, Pacific Northwest Research Station

The Douglas-fir Seed Source Movement Trial is a reciprocal transplant study in which trees from 60 populations from 12 regions are planted back into test sites representative of nine of those regions. These common garden tests are located on 3 latitudinal bands in southwestern Oregon, north central Oregon and southern Washington. Each latitudinal band has a site near the coast and two inland sites – one at a lower elevation and one at a higher elevation. The 12 seed-source regions include the three latitudinal transects in Washington and Oregon as well as a fourth transect in northern California that includes the coast, the Klamath Mountains and the northern Sierra Mountains. The nine test sites cover diverse environments and are on private and public land ownership. Two-year old seedlings were planted in late fall 2008 or early spring 2009.

The trees have been measured annually for height and diameter (2009-2014) and their condition or presence of damaging agents coded. Assessments have been made of the timing of vegetative budburst on all sites and a subset of sites has been used for assessments of reproductive budburst, drought hardiness, cold hardiness, leader extension, and cambial growth. Observations have been made of tree damage including stem or branch breakage, dieback, needle loss, and insect damage. In 2014 the PNW Research Station funded a Joint Venture Agreement with David Shaw, Oregon State University, to fund a graduate student (Nicholas Wilhelmi) to study these plantings for the presence of Swiss needle cast and Rhabdocline as well as other common damaging agents on young Douglas-fir. The Swiss Needle Cast Cooperative and the Bureau of Land Management will provide additional resources to help with formal damage surveys which are planned for completion in the spring and early summer of 2015. Other agencies may also help in assessing these plantings which should provide a very robust data set to use in testing current recommendations for planting Douglas-fir and addressing general questions on the effects of genotype and environment on the occurrence of foliage diseases and other damaging agents. Questions to be addressed include: (1) Are local genotypes the best choice for minimizing the impacts of needle cast diseases and other damaging agents? and (2) How do environmental conditions influence the expression and impact of these agents?

Populations | **Planting Locations**

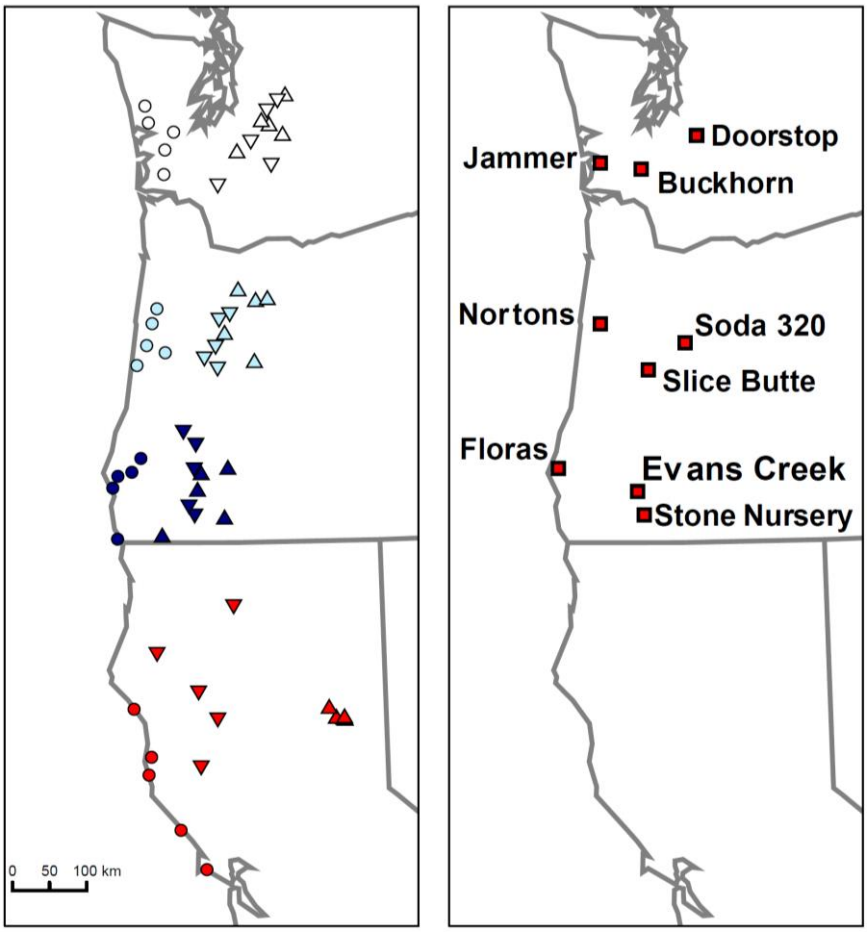

Genetic Diversity and Population Subdivision in *Phaeocryptopus gaeumannii* in the Pacific Northwest

Patrick Bennett and Jeffrey Stone, OSU Botany and Plant Pathology

Introduction

The focus of this research is to determine the distributions of the two lineages of *Phaeocryptopus gaeumannii* in the Pacific Northwest, first described by Winton (2006) in relation to disease severity. A second objective is to determine whether the two lineages are sufficiently divergent to constitute separate species and to reevaluate the taxonomic placement of *P. gaeumannii*. The two lineages are provisionally designated as Lineage 1 and Lineage 2.

While both lineages of *P. gaeumannii* are capable of causing Swiss needle cast, there is some evidence to suggest that these lineages may differ in their ability to cause disease, and that the relative proportions of either lineage present at a given site may influence disease severity (Winton et al. 2001). Controlled inoculation experiments are in progress, which will allow us to determine the relative virulence of the two lineages.

The area affected by SNC has been expanding steadily in the Coast Range since 1996 and seems likely to continue to do so. Therefore, it is increasingly important to assess disease risk by applying genotypic data to predictive models. This work will establish baseline abundance and proportion estimates for each lineage and correlate their distributions with disease severity in controlled inoculations as well as field-based disease observations assessed by ODF-USFS aerial surveys.

Methods

Population Genetics

During the 2014 sampling season, foliage samples were collected from Douglas-fir trees at 15 sites in the SNCC monitoring network (Ritokova et al. 2013). Five trees were selected randomly at each site, and second and third-year internodes were sampled from secondary branches in the upper crown. One tree per site was sampled more intensively, with secondary branches collected in the lower, mid, and upper-crown.

Needles were returned to the lab and examined for presence of *P. gaeumannii* pseudothecia. Needles bearing pseudothecia were affixed to the lids of Petri dishes with the abaxial surface facing down and incubated to allow discharge of ascospores onto the agar surface. Within 48 hours of incubation, germinating ascospores were isolated individually onto malt agar and the single-ascospore isolates incubated at 17 °C for 2-6 months to obtain sufficient growth for DNA extraction and long-term storage.

Mycelium from these cultures was removed from the Petri dishes, transferred to 1.5 mL microfuge tubes with extraction buffer, frozen in liquid nitrogen, and macerated by shaking in a mini bead-beater with glass beads. Genomic DNA was then extracted from these samples using the Qiagen DNeasy Plant kit. These samples were used in a multiplex PCR protocol designed to amplify the ten microsatellite loci identified by Winton et al. (2007; Table 2). The amplified microsatellite PCR products were then submitted to the OSU Center for Genome Research and Biocomputing (CGRB) for genotyping by capillary electrophoresis on the ABI 3730 BioAnalyzer (Applied Biosystems). Allele sizes for the microsatellite loci were determined using GeneMapper 4.0 (Applied Biosystems).

Study sites were considered local populations for the purpose of this analysis. Genetic diversity, allele frequencies, and population subdivision were estimated using GenAlEx 6.5 (Peakall and Smouse 2012), and the R statistical computing package *Poppr 1.1.2* (Kamvar et al. 2014). The *aboot* function in *Poppr* was used to construct UPGMA dendrograms based on comparisons of pairwise genetic distance. An analysis of molecular variance (AMOVA) was used to compare the genetic variation within and between populations.

Inoculations

A total of 270 2-year-old Douglas-fir seedlings from two different seed sources, previously unexposed to *P. gaeumannii* inoculum, were artificially inoculated with macerated *P. gaeumannii* mycelium (Table 1). Eight different *P. gaeumannii* isolates (representing four genotypes of each lineage) were used as inoculum sources. Macerated mycelium of each isolate was applied to 15 seedlings of each seed source (Table 1). Cultures of each isolate were grown in 50 mL liquid 2% malt broth in Erlenmeyer flasks fitted with cotton stoppers. These liquid cultures were incubated with shaking for 6-8 weeks prior to inoculation. To prepare the inoculum, these cultures were vacuum filtered and the concentration of mycelium of each isolate was standardized by wet weight. The samples were then macerated with an immersion blender for 60-80 seconds each in 9 mL sterile water. Blender blades were flame-sterilized between different isolates. The concentration of macerated fragments was determined with the aid of a hemacytometer and sterile water was used to adjust the concentration of mycelial fragments of each isolate to 1.0×10^5 fragments per mL. The proportion of viable hyphal fragments in the inoculum also was estimated by serial dilution plating of the inoculum on 2% malt agar to confirm that all trees received equivalent inoculum concentrations. An airbrush was used to apply ten mL of this hyphal suspension to the foliage of each tree. Control trees received airbrush applications of sterile water. All seedlings were incubated in a misting chamber with intermittent mist to maintain high RH for seven days following inoculation, and then moved outdoors for incubation.

In late Apr-May 2015, disease severity will be assessed by estimating the proportions of stomata occluded by pseudothecia in samples of 90 needles per inoculation group (i.e. 3 needles per seedling). Foliage retention will also be measured for 10 shoots per seedling, measured as the percentage of the one-year-old year needle cohort retained.

Table 1. 2014 isolates and seed sources used for inoculation.

	Seed Source	
	Starker	**Campbell River**
Lineage 1[a]		
NT 019	15	15
BC1.3.2	15	15
BC12.2.2	15	15
MP 002	15	15
Lineage 2		
MP008	15	15
NT054	15	15
BC5.2.4	15	15
H3.3.1	15	15
CONTROL (uninoculated)	15	15

[a]NT= Newport/Toledo, BC= Beaver Creek, MP= Mary's Peak, H= Hebo.

Table 2. Primer sequences, numbers of alleles, size ranges, and repeat motifs for polymorphic microsatellite loci identified in Winton et al. 2007.

Loci	Primers[a]	Alleles	Size Range (bp)	Repeat Motif
Multiplex 1				
Pgdi1	**F:** TCCCCGCCTATATTTCTC	13	93-106	(CA)18
	R: (FAM) CCGAATCGATTTGCTAGG			
Pgdi2	**F:** ATTCCAGAGCCATACCGTTG	25	229-256	(AG)26
	R: (HEX) AGGTGGATGAGGGATGTTTG			
Pgdi3	**F:** GGGGATGCTGGAATGTATGT	17	328-350	(TC)18
	R: (NED) GCACATTGCTCAGTGCTCTC			
Pgdi4	**F:** GGCATCGCAGTCAACTTA	25	441-492	(GT)17
	R: (FAM) CGAGCCGAACCTTTAGTT			
Pgdi5	**F:** ATAGTATATTACACCAGG	27	336-404	(AG)4GA(AG)5AA(AG)3AAAGAA(AG)3 AAAGAC(AG)8AAAGAC(AG)11 GA(AG)4GG(AG)5AA(AG)5GG(AG)2
	R: (HEX) CAACAGCACATCGCAACA			
Multiplex 2				
PgTri1	**F:** TGGAGACCATTAACCCTGGA	21	374-434	(CAT)22(CTT)19
	R: (FAM) TTGGGAGGGTATTGAGGTTG			
PgTri2	**F:** AGGCAGAGAAGGGAGAGGAG	50	258-400	(GAC)4[(GAA)3(GAC)3]9GAA(GAC)2
	R: (HEX) TCTGCAAGACCGTCATCATC			
PgTri6	**F:** CCCTTCCCAATCACTTCTCA	74	268-391	(CAA)24
	R: (NED) GGACTGCTTTGGGTGATGTT			
Multiplex 3				
PgTri7	**F:** ATGCTATCCCTCCCCAACTC	27	373-420	(TTC)8TTT(CTT)7
	R: (FAM) TGCGAAGCGTGTAAATTCTG			
PgTet1	**F:** CATCCGCTCCATTTCATTCT	67	200-324	(AATC)13
	R: (HEX) TGGCGACGGAGTTGATAATA			

[a]F = forward primer, R = reverse primer. FAM = blue fluorescent dye, HEX = green fluorescent dye, NED = yellow fluorescent dye.

Results and Discussion

Genetic Diversity, Population Subdivision

A total of 803 isolates were obtained from 15 sites in the SNCC plot network, including 550 from ten sites in the Tillamook group, 136 from three sites near Florence and 107 from two WDNR sites in southern Washington (Table 3). To date 384 of these isolates have been

genotyped. One of the microsatellite loci (PgTri1) failed to amplify in our multiplexed PCR protocol, so all data presented here represent the genotypes based on nine of the ten original microsatellite loci identified by Winton et al. (2007).

The preliminary analysis suggests that Lineage 1 is more abundant overall in western Oregon, with an estimated 80% of all isolates sampled belonging to Lineage 1. Lineage 1 isolates were detected at all sites sampled, while Lineage 2 isolates were absent, or present in low abundance, at many sites. The microsatellite loci analyzed appear to be highly polymorphic, i.e. there are numerous different alleles present at each locus in both lineages over the entire sampling area. Of the total 384 isolates analyzed, 348 distinct multi-locus genotypes were detected. The expected heterozygosity (a measure of the frequency of different microsatellite alleles in a population) is quite high ($H_E > 0.5$) in most of the populations sampled, further indicating a high degree of polymorphism at these microsatellite loci (Figure 2, Table 5).

The results of the AMOVA test indicate high genetic variance within lineages (87%), and low genetic variance between lineages (13%; Table 4). Estimates of population differentiation were calculated using the PhiPT parameter, (a modification of Wright's F-statistic). The results of these analyses indicate significant genetic differentiation between the two lineages (PhiPT= 0.131, $p = 0.01$).

Reproductive Isolation

Pairwise comparisons of genetic distance (number of shared microsatellite alleles) and comparisons of allele frequencies between lineages indicate a strong reproductive barrier. The UPGMA dendrograms indicate that there is no gene flow occurring between the two lineages (Figure 3). These analyses support the conclusion that Lineages 1 and 2 constitute separate biological species; they do not interbreed although their ranges overlap.

Dispersal

The dendrograms also indicate that isolates from a particular site in the plot network may be more similar to isolates from distant sites than they are to other isolates from within the same site. This suggests that there may be some long-distance dispersal of genetic material between distant sites. Genotypes of Lineage 2 isolates from the WDNR plots were very similar to Lineage 2 isolates from Tillamook and Florence, OR. Whether this reflects natural dispersal or is due to human-aided movements of plant material remains to be determined.

Lineage Distributions

Lineage 2 is most abundant at sites near Tillamook, but occurs further inland in sites in southwestern Oregon. Lineages 1 and 2 coexist in approximately equal proportions along the western Coast Range near Tillamook, and Lineage 2 decreases in abundance with increasing distance inland (Figure 1). Our sampling to date did not recover any Lineage 2 isolates at the most eastern site in the Tillamook group, 25–35 miles inland. However, no such pattern occurred as far south as Florence, with sites 15–25 and 25–35 miles from the coast containing 23% and 21% Lineage 2, respectively (Table 3). Although we did not obtain samples from sites near the central coast the results from more inland sites in the Florence site group indicate that Lineage 2 is more abundant in the southern Oregon Coast Range compared to sites from the same longitude near Tillamook. Only two Lineage 2 isolates out of the 20 genotyped to date were recovered from the DNR sites in southwestern Washington.

Table 3. Numbers and proportions of each lineage at each site sampled in 2014.

Site	Owner	Name	Distance from Coast (miles)	Total Spores Isolated	# Isolates Analyzed	L1	L2	Proportion L2
T-01	Stimson	Wedding Ring	0-5	70	49	23	26	0.53
T-02	Stimson	Rockaway	0-5	39	6	3	3	0.50
T-03	Campbell	CG172	0-5	44	7	6	1	0.14
T5-1	Campbell	CG111	5-15	45	0			
T5-3	Stimson	Mill Creek	5-15	46	12	11	1	0.08
T5-5	ODF	ODFT	5-15	37	24	19	5	0.21
T15-1	Campbell	PGS	15-25	74	43	27	16	0.37
T15-2	Stimson	Olson	15-25	55	5	5	0	0
T25-2	Stimson	SLFG1	25-35	70	56	56	0	0
T25-3	Stimson	SLFG2	25-35	70	53	53	0	0
F15-1	Starker	Swamp Creek	15-25	49	28	25	3	0.11
F15-3	Starker	Haines Rd	15-25	19	15	8	7	0.47
F25-2	Starker	Honey Grove	25-35	68	52	41	11	0.21
DNRS25-1	WDNR	Cat Scratch	25-35	55	0			
DNRL25-2	WDNR	East Slope	25-35	52	20	18	2	0.10
CarnWA		Carnation, WA		10	8	8	0	0
Total: 15				**803**	**384**	**308**	**76**	**0.20**

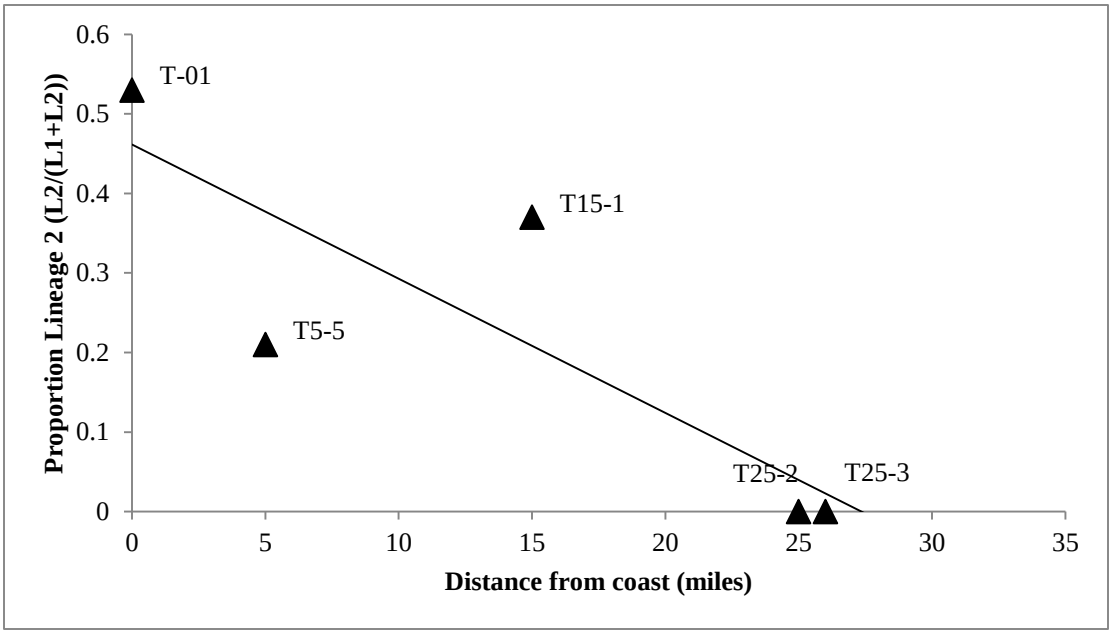

Figure 1. Scatterplot showing the proportions of Lineage 2 at several Tillamook sites with varying distances from the coast. T-01: n= 49, T5-5: n= 24, T15-1: n= 43, T25-2: n= 56, T25-3: n= 53. R^2= 0.713.

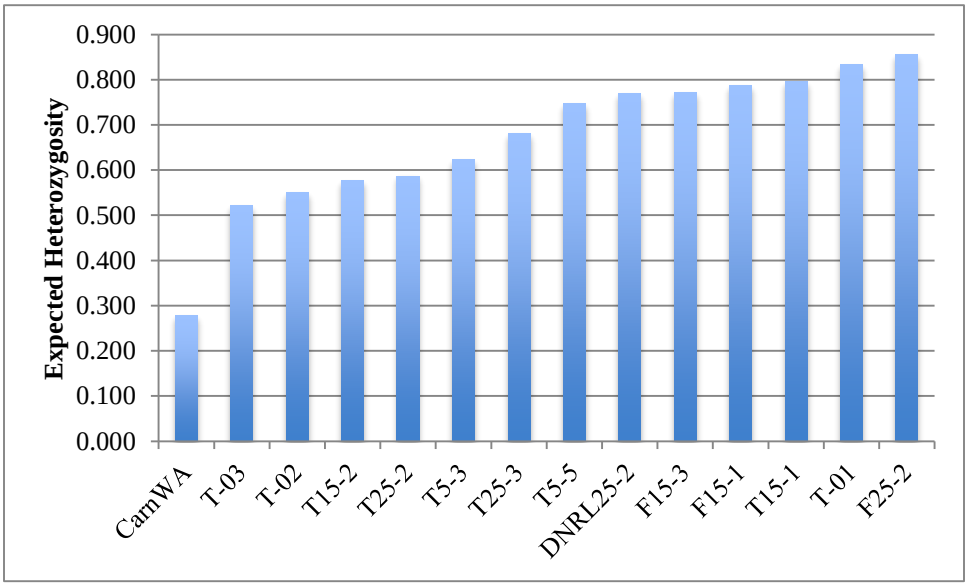

Figure 2. Estimates of expected heterozygosity (H_E) based on allele frequencies at each site. T= Tillamook, F= Florence. DNRL= WA Department of Natural Resources, CarnWA= Carnation, WA. H= $[1 - \Sigma (p_i{}^2)]$.

Table 4. Summary Analysis of Molecular Variance (AMOVA) table.

Summary AMOVA Table					
Source	**df**	**SS**	**MS**	**Est. Var.**	**%**
Among Pops	14	645548.378	46110.598	1476.429	13%
Within Pops	369	3615875.955	9799.122	9799.122	87%
Total	383	4261424.333		11275.551	100%

Table 5. Summary of population parameters and diversity indices.

	Na[a]	**%P[b]**	**I[c]**	**H[d]**
CarnWA	2.222	66.67%	0.487	0.278
T-03	3.333	100.00%	0.950	0.522
T-02	3.000	88.89%	0.944	0.550
T15-2	3.111	100.00%	0.997	0.578
T25-2	8.222	100.00%	1.360	0.587
T5-3	5.222	100.00%	1.300	0.623
T25-3	9.333	100.00%	1.585	0.681
T5-5	8.778	100.00%	1.769	0.747
DNRL25-2	9.222	100.00%	1.863	0.769
F15-3	6.556	100.00%	1.660	0.772
F15-1	10.222	100.00%	1.930	0.787
T15-1	11.556	100.00%	1.947	0.796
T-01	11.889	100.00%	2.101	0.834
F25-2	16.333	100.00%	2.338	0.857
Mean	7.786	96.83%	1.516	0.670

[a]**Na** = # of alleles
[b] **%P** = percentage of polymorphic loci
[c] **I** = Shannon Information Index= - [Σ (p_i ln (p_i)],
[d]**H** = Diversity= [1 – Σ (p_i ^{2})] (Where p_i is the frequency of the *i*th allele for the population & Σ p_i^2 is the sum of the squared population allele frequencies).


100
Lineage 1
Lineage 2

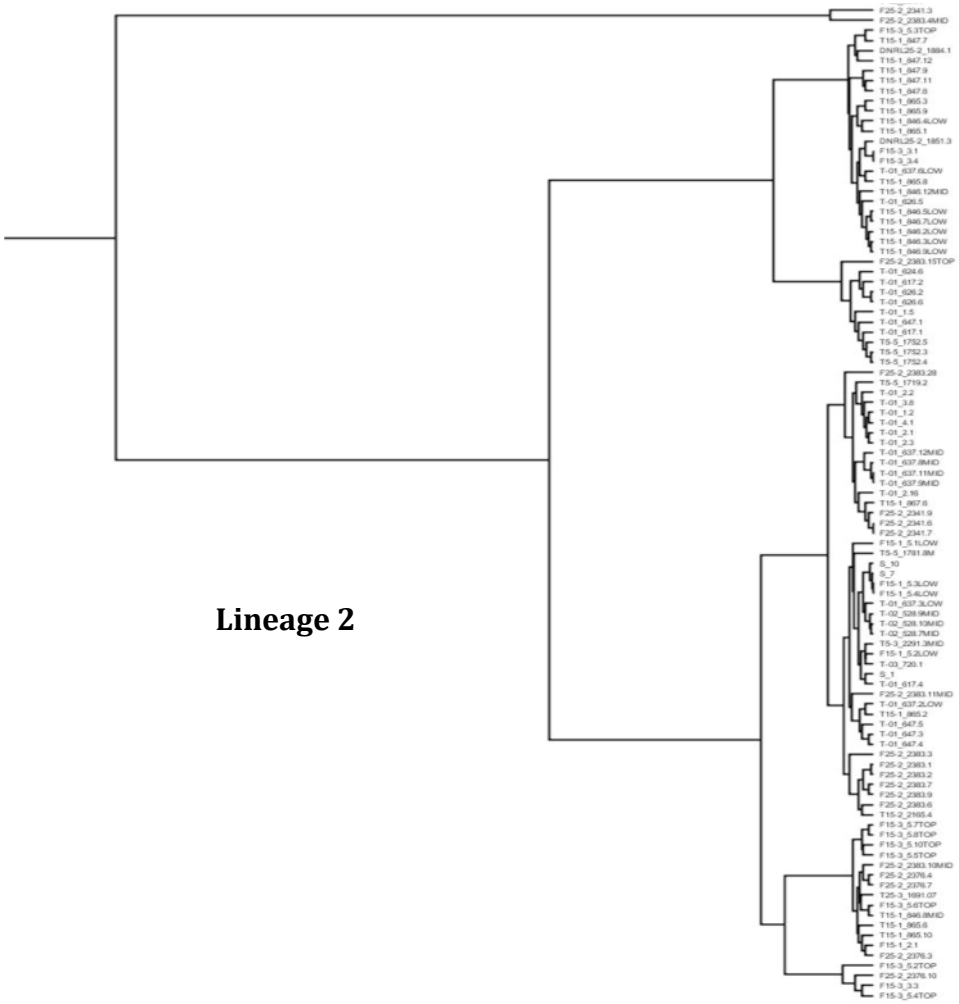

Figure 3. Dendrogram depicting similarity between isolates in the microsatellite data set based on pairwise comparisons of Nei's genetic distance. 100% bootstrap support for split between Lineage 1 and Lineage 2.

Literature Cited:

Kamvar, Z.N., J.F. Tabima, and N.J. Grunwald. 2014. Poppr: an R package for genetic analysis of populations with clonal, partially clonal, and/or sexual reproduction. PeerJ 2:e281

Peakall, R. and P.E. Smouse. 2012. GenAlEx 6.5: genetic analysis in Excel. Population genetic software for teaching and research-an update. Bioinformatics 28, 2537-2539.

Ritokova, G., D. Shaw, D. Maguire, D. Mainwairing, J. Browning, W. Littke, M. Gourley, G. Filip, A. Kanaskie. 2013. SNCC Research and Monitoring Plot Network. Swiss Needle Cast Cooperative Annual Report. Oregon State University, Corvallis, OR.

Winton, L.M. 2001. Phylogenetics, population genetics, molecular epidemiology, and pathogenicity of the Douglas-fir Swiss needle cast pathogen *Phaeocryptopus gaeumannii*. Thesis, Oregon State University, Corvallis, OR.

Winton, L.M., E.M. Hansen, and J.K. Stone. 2006. Population structure suggests reproductively isolated lineages of *Phaeocryptopus gaeumannii.* Mycologia 98:781–791.

Winton, L.M., E.M. Hansen, and J.K. Stone. 2007. Polymorphic microsatellite markers for the Douglas-fir pathogen *Phaeocryptopus gaeumannii*, causal agent of Swiss Needle Cast disease. Molecular Ecology Notes 7: 1125–1128.

Regional effects of Swiss needle cast disease and climate on growth of Douglas-fir in western Oregon

E. Henry Lee[1], Peter A. Beedlow[1], Ronald S. Waschmann[1], David T. Tingey[2], Charlotte Wickham[3], Steve Cline[1]

[1] US Environmental Protection Agency, 200 SW 35th Street, Corvallis, OR 97330

[2] Retired

[3] Oregon State University, Department of Statistics, Corvallis, OR 97332

Summary

The fungal pathogen, *Phaeocryptopus gaeumannii*, occurs wherever Douglas-fir is found but disease damage is believed to be limited to the Coast Range and is of no concern outside this region (Shaw et al., 2011). However, knowledge remains limited on the spatial distribution of Swiss Needle Cast (SNC) impacts in the Pacific Northwest. We examined the spatial distribution of SNC impacts on mature Douglas-fir trees using time series intervention analysis of intra-annual tree ring width chronologies from nine study sites in western Oregon. The sites were located in mature forest stands on the west slope of the Coast Range to mid- and high-elevations on the west slope of the Cascade Mountains of Oregon (Figure 1).

All sampled stands experienced significant radial growth reductions in Douglas-fir that could not be accounted for by current and previous-year seasonal climatic factors (Figure 2). The spatiotemporal patterns of growth impact from SNC disease were synchronous across the region, displayed periodicities of 25-30 years, and were strongly correlated with winter and summer temperatures and summer precipitation. In warm environments on the west slopes of the Coast Range, summer temperature and/or precipitation was more limiting to fungal development than winter temperature (Figure 3); in cool environments at high elevations, winter temperature was the primary limiting factor.

Our findings show that SNC impacts occur wherever Douglas-fir is found in western Oregon and is not limited to the coastal fog zone. In the 20th century, SNC impacts at low- to mid-elevations were least severe during the warm phase of the Pacific Decadal Oscillation (PDO, 1924-1945) and most severe in 1984-1986, following the cool phase of the PDO (1945-1977). At high elevations on the west slope of the Cascade Mountains, SNC impacts were the greatest in the 1990s and 2000s due to warmer winter temperatures associated with climate change (Figure 4). Our findings of a 25-35 year disease impact cycle combined with aerial surveys indicating record acreage exhibiting disease symptoms for the past four years suggest that the next peak impact will occur in 2014-2016, following the last peak in 1984-1986. Warmer winters will increase disease severity at higher elevation, north along the coast from northern Oregon to British Columbia, and inland sites where current winter temperatures limit fungal growth, as predicted in Lee et al. (2013).

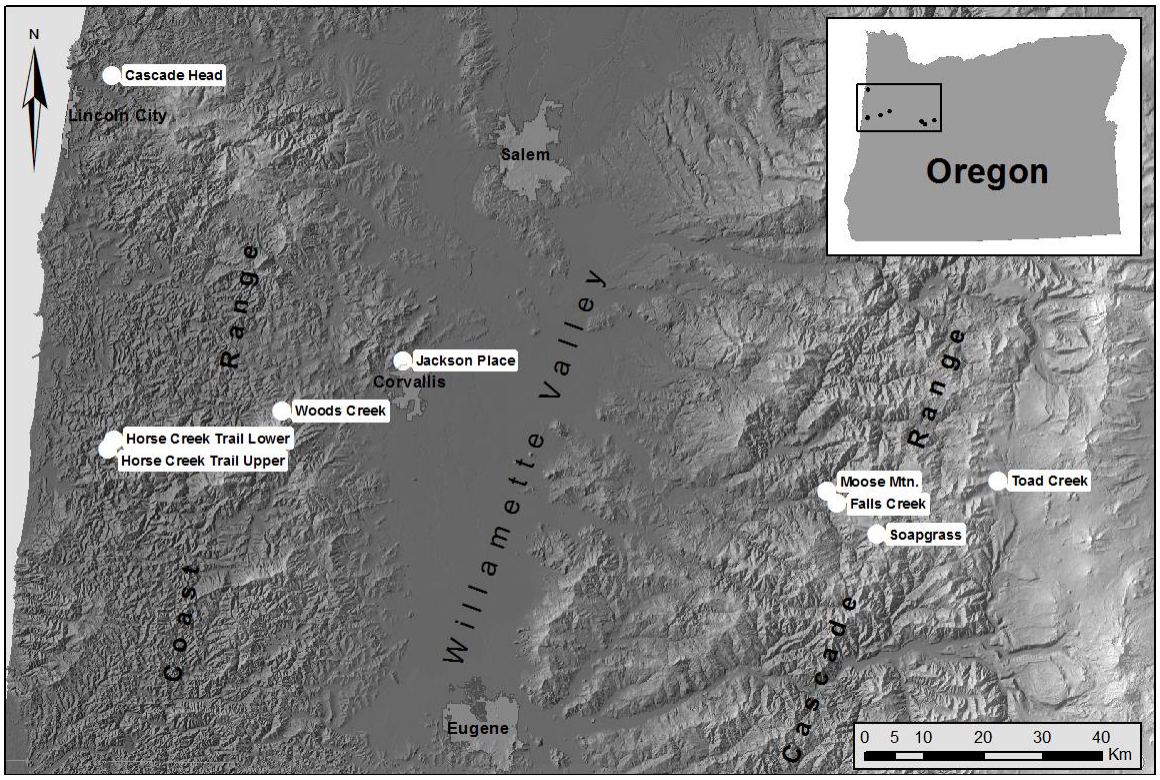

Figure 1. Tree core samples were collected from nine field sites located in mature Douglas-fir stands on the west and east sides of the Coast Range, in the Willamette Valley, and on the west side of the Cascade Mountains.

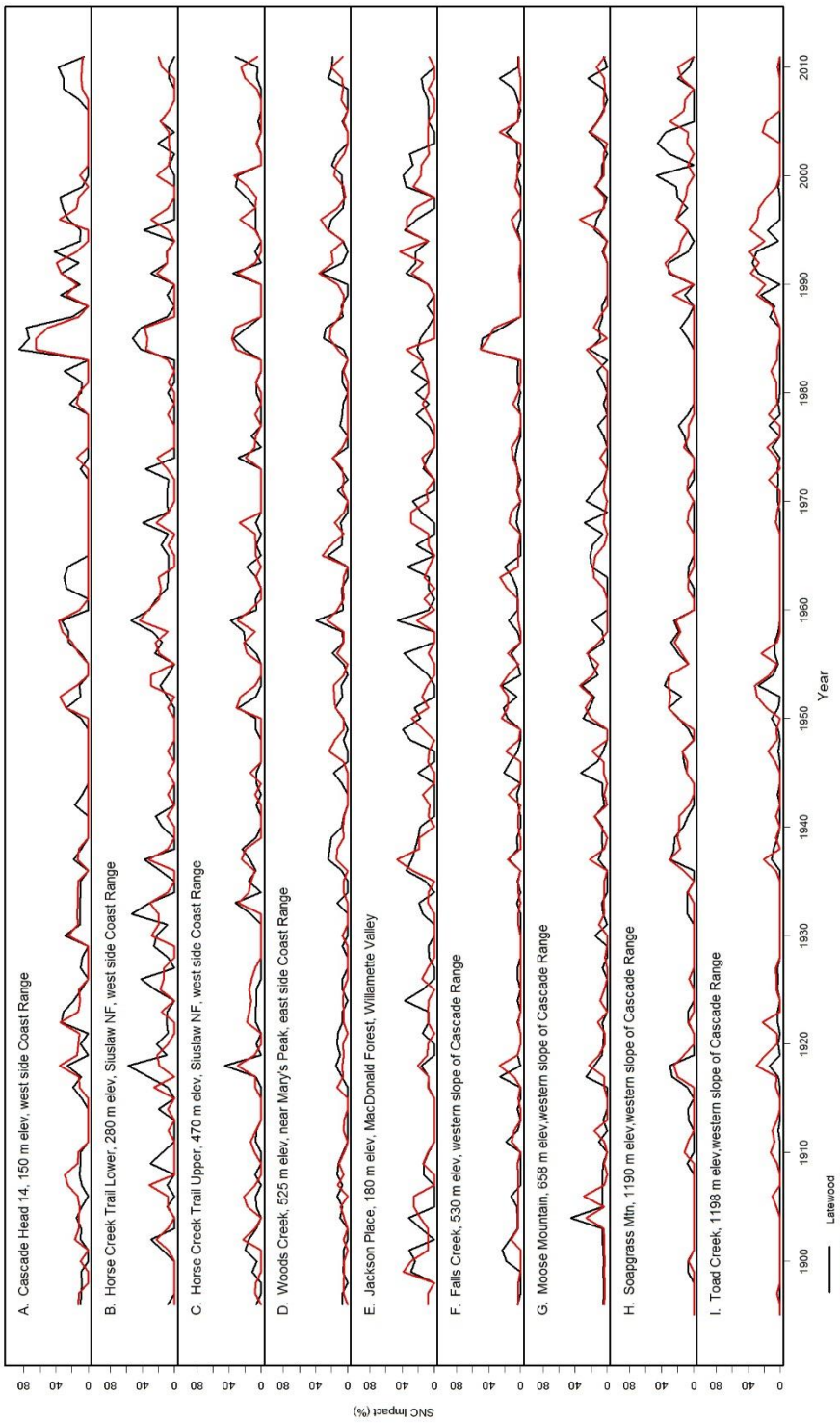

Figure 2. Tree-ringwidth based reconstruction of Swiss needle cast impacts 1895-2011 at nine study sites located in mature forest stands in western Oregon. SNC impacts have a ~30 year periodicity that is synchronous across the region as indicated by the peak impacts in 1918, 1959, and 1984.

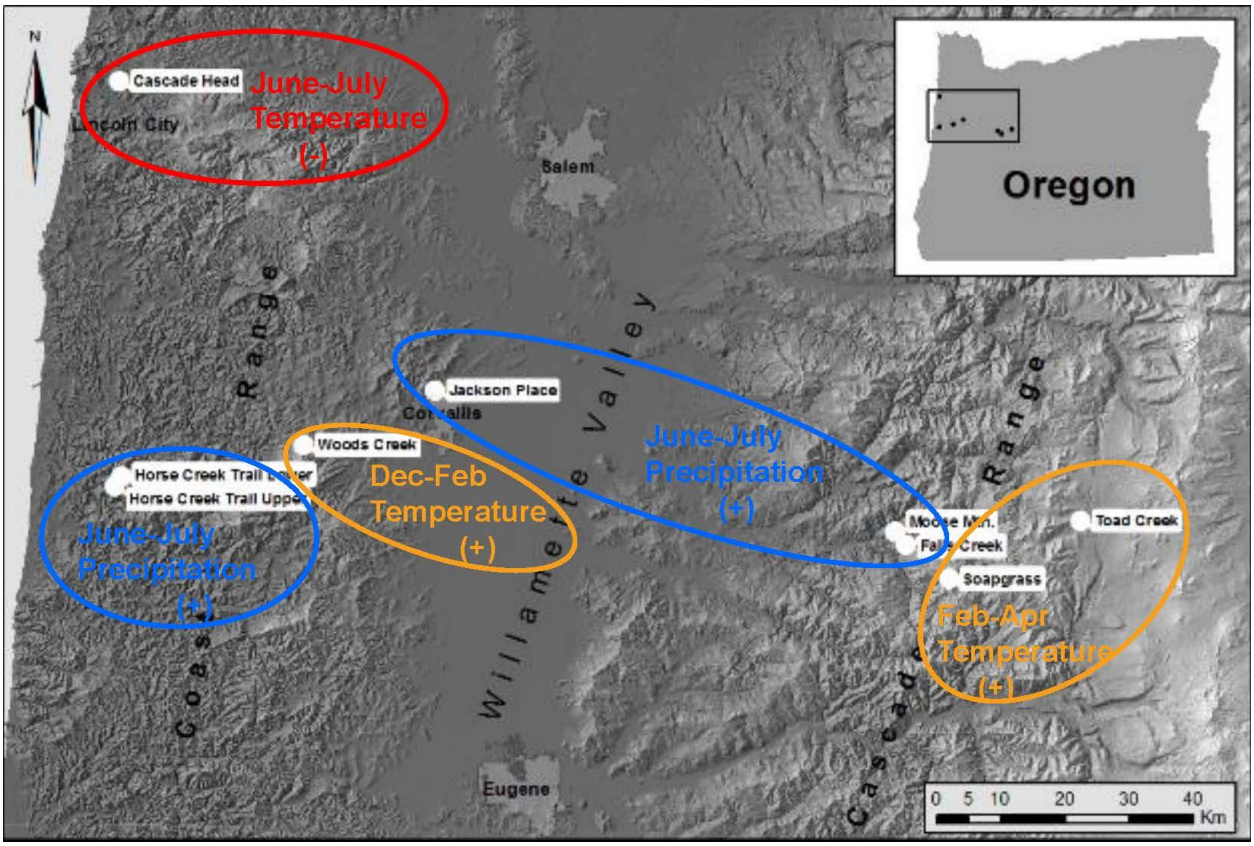

Figure 3. Winter temperature and summer temperature and precipitation limit fungal development depending upon location, topography, aspect, and site conditions. Summer conditions are the primary limiting factor in warm environments while winter conditions are more limiting in cool environments based on their associations with the low-frequency SNC impacts at each site.

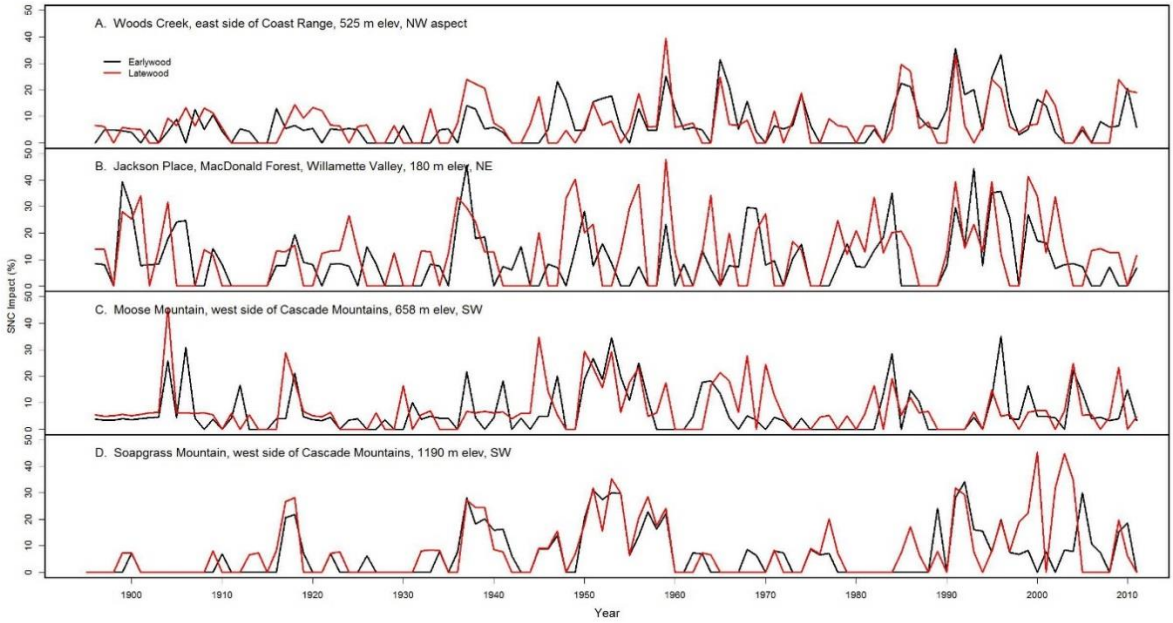

Figure 4. SNC impacts display an increasing trend 1895-2011 at several inland sites, most notably at Soapgrass Mountain, a high-elevation site on west slopes of the Cascade Mountains of Oregon. SNC impacts at Soapgrass were unprecedented in the 1990s and 2000s due to warmer winters associated with climate change.

The needle damage done

A nuanced approach is the best treatment for Swiss needle cast on Douglas fir

By David Shaw, Alan Kanaskie and Gabriela Ritokova

Swiss needle cast (SNC) is a foliage disease of Douglas fir caused by the fungus *Phaeocryptopus gaeumannii*, a common native ascomycete that occurs wherever Douglas fir is found. The fungus is specific to Douglas fir.

Mortality is rare, but premature loss of foliage reduces growth in forest plantations. In Christmas trees and nursery stock the disease can impact aesthetics, crown fullness and color, and tree health (Figure 1).

History of the disease

Swiss needle cast was first described in Switzerland in 1925. The disease was then noted in other parts of Europe, and is now known to be a potentially significant disease wherever Douglas fir is grown outside its native range.

The fungus that causes SNC was shown to be ubiquitous in native Douglas fir forests and not considered a significant threat to forest health. In the 1970s, however, SNC was recognized as a problem in Christmas tree plantations in western Washington and Oregon.

SNC has become increasingly apparent in the coast ranges of Oregon and Washington since the 1970s. It became so severe by the mid 1990s as to prompt formation of a research organization at Oregon State University — the Swiss Needle Cast Cooperative — to investigate the problem and find management solutions.

The spread of SNC

Swiss needle cast is visible as yellowish crowns and thin crown foliage (Figure 2). An aerial survey conducted in 2014 (Mulvey et al., 2013) estimated 586,249 acres of forests and plantations showing symptoms of SNC in Oregon, and another 228,500 acres in Washington. Therefore, we estimate more than 4,000,000 acres are affected by the disease, from Bandon, Oregon, to the Northern Olympic Peninsula and inland 20–35 miles. Surveys south of Bandon to Eureka, California, indicate no significant SNC in that region.

The total economic impact of SNC to Oregon's economy has been estimated at $128 million per year. This amount is based on a 20 percent growth reduction of Douglas fir in 10–70-year-old stands, equal to more than 190 million board feet per year.

Over the past 20 years, Swiss needle cast has intensified across coastal Oregon and Washington, as well as inland plantations in the foothills of the Cascades, especially in low-elevation forests of valley bottoms and toe slopes near rivers and streams, but also in high-rainfall areas.

Environmental factors

Although the fungus occurs everywhere, the disease develops according to different geographic, seasonal and management settings.

The Swiss Needle Cast Cooperative managed a plot system through the western mid-slope of the Oregon ▶

Figure 1. This Douglas fir tree has symptoms of Swiss needle cast: low foliage retention, thin crown and yellowish foliage. PHOTO BY DAVID SHAW

Figure 2. Yellowish foliage, a common symptom of Swiss needle cast, as seen from an aerial view of a Douglas fir plantation. PHOTO BY ROB FLOWERS, OREGON DEPARTMENT OF FORESTRY

Cascades for 10 years, and found very low incidence of SNC. Several different disease-modeling efforts were initiated; most indicated that trees become more susceptible to the disease at lower elevations and with closer proximity to the coast. When these two factors are removed from models, variations on seasonal rainfall, and especially temperature, became important.

One modeling group developed a "continentality" index: climates that are colder in winter and hotter in summer, with more seasonal temperature variation and less summer rainfall, result in fewer disease symptoms.

SNC is an unusual foliage disease because the fungus does not cause mortality of cells and leaves directly. The fungus appears to live as an endophyte within the needle. Disease develops when the fungus forms spore dispersal structures called pseudothecia (Figure 4), which emerge from and clog the air pores (stomates) on the underside of the needle. The disease develops from carbon starvation because the stomates cannot let water out or carbon dioxide in. Needles are typically lost after greater than 50 percent of the stomates are plugged.

In the coastal and inland sites, disease development is related to the formation of pseudothecia on one- and two-year-old needles, resulting in significant foliage loss. In natural forests of the Cascades where needles persist on the tree for more than 5 years, pseudothecia is found on the oldest needles, but not younger ones.

Bud break occurs in late April and early May for Douglas fir, with 4–6 weeks for branch elongation. Current-year foliage is more susceptible to *P. gaeumannii*, although older foliage may also be infected.

The fungus spreads via sexual reproduction, and unlike other foliage fungi, does not have asexual spores to aid in intensification. Spores are dispersed from living foliage.

Consistently wet needles — a common occurrence near the coastal fog zone during late spring and summer (May–August) — allow spores to successfully germinate on the needle surface and hyphae to grow into the needles through stomates. Warm winter temperatures probably allow the fungus to develop faster in the intercellular spaces of the needles and form pseudothecia sooner.

In Christmas tree farms and nursery settings, the disease symptoms (needle loss and yellowing) occur mostly in the lower, mid and inner crown. Due to humidity gradients, the wetter areas of the crown are thought to be more susceptible to SNC.

However, in the coastal epidemic area, the disease is most severe in the upper crown, which leads to the hypothesis that leaf wetness is not a controlling influence in the region — they are always wet during spore dispersal!

Severity of SNC has an effect on wood quality. The impact of the disease is determined by growth rate and proportion of early wood, the first wood produced in spring.

Scientists compared severely infected trees that were treated with fungicides to those that were not. They also investigated wood characteristics across a gradient of SNC intensity. These studies showed that trees with severe SNC had narrower sapwood, narrower growth rings, higher modulus of elasticity, higher wood density, greater proportion of latewood, and lower sapwood moisture content, including narrower tracheid cell-wall thickness.

The lack of older foliage and an associated reduction in early-wood production drives the increase in wood density and stiffness.

Douglas fir has no apparent resistance to infection; all needles become infected under the right environmental conditions. In one study, fungal biomass within the

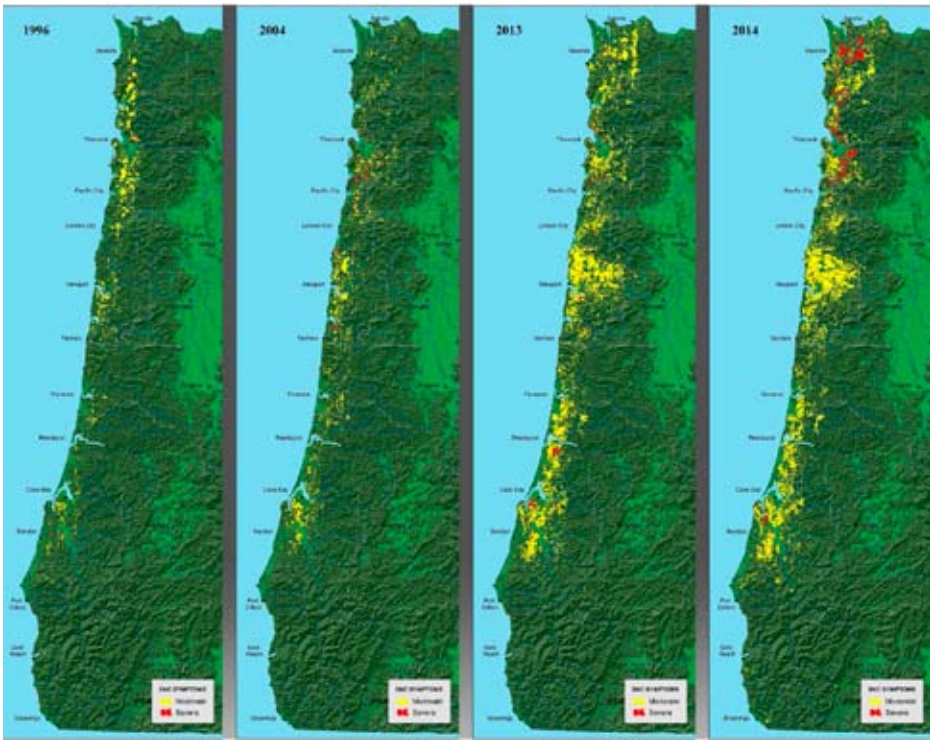

Figure 3. Aerial survey maps of coastal Oregon from 1996–2014. Yellow indicates moderately infected plantations; red, heavily infected. SOURCE: OREGON DEPARTMENT OF FORESTRY AND USFS FOREST HEALTH PROTECTION, AERIAL DETECTION SURVEY

needle was similar between trees, although families differed in growth rate.

Regional genetic differences of the tree have a big influence on disease susceptibility. Research from British Columbia and northern Washington indicated that there was variation in disease expression between the interior Rocky Mountain variety of Douglas fir (*Pseudotsuga menziesii* var. *glauca*) and the coastal form (*P. m.* var. *menziesii*) when trees were grown together in provenance trials. The coastal form was less impacted by disease in coastal areas, presumably because it has adapted to grow in wetter conditions.

Soil nutrients, especially high nitrogen levels, have been implicated in disease incidence. There is a strong negative correlation between foliar nitrogen concentration and foliage retention. It has been proposed that excess nitrogen in the foliage may be stored in the form of soluble amino acids, which promote the growth and development of *P. gaeumannii*.

In addition, nutrient availability varies across the Oregon Coast Range, with lower nitrogen and higher calcium availability east of the crest, and higher nitrogen and lower calcium availability closer to the coast where SNC becomes severe.

In one study in Idaho, nitrogen fertilization of Douglas fir was shown to increase nitrogen leaf content, *P. gaeumannii* biomass and SNC severity. In another study of approximately 20-year-old Douglas fir trees in western Oregon, no relationship was found between disease severity and trees that were treated with a variety of nutrients and untreated trees.

SNC in managed settings

Management of the disease in forest plantations involves a nuanced approach that depends on geographic location, measured stand impacts, stand age and structure. It should also include evaluation of qualitative models and needle retention, along with quantitative measurement of growth impacts.

Fungicides in the forest environment will work, but they are not recom- ▶

mended and un-economical. Silvicultural techniques, such as thinning and vegetation management, have been shown to have no impact on disease severity, but will influence stand development and individual tree growth.

In Christmas tree and nursery settings, an integrated pest management strategy is required and may involve fungicide applications during spore dispersal (Chastagner, 1997). Monitoring is important, and should begin at least 3 or 4 years before planned harvest.

For the marketplace, it is important to protect foliage from infection and maintain 2–3 years of healthy foliage. Therefore, fungicides do not need to be used until 3 years prior to harvest.

Several fungicides are registered for treatment of SNC: products containing chlorothalonil are most commonly used. Other strategies include canopy-drying

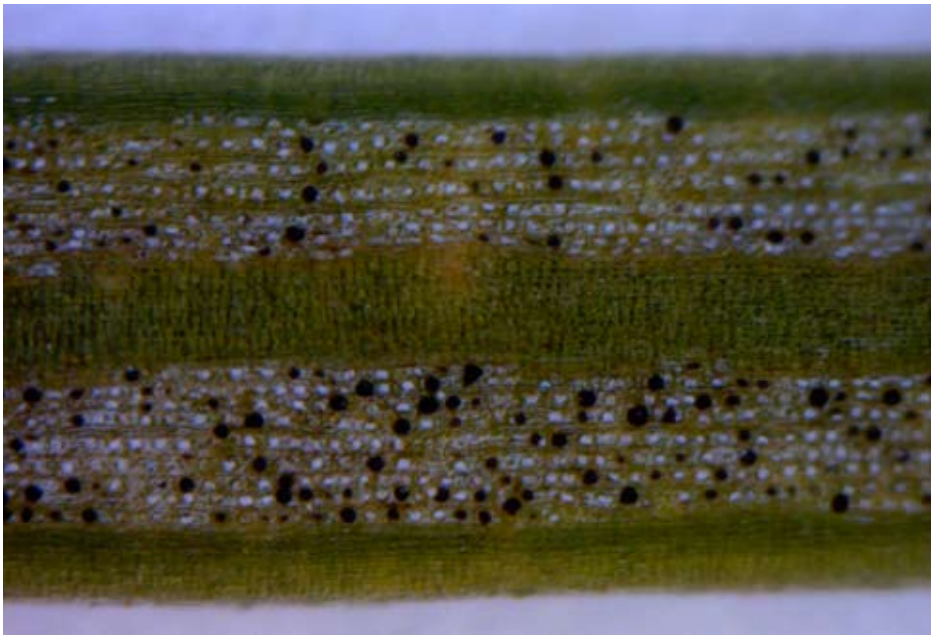

Figure 4. Underside of Douglas fir needle. Two bands of stomates are visible, one on each side of the midrib. Note the black spore-producing bodies (pseudothecia) that clog the stomates. PHOTO COURTESY OF SWISS NEEDLE CAST COOPERATIVE

techniques, such as vegetation management and wider spacing of trees, as well as avoiding plantings adjacent to Douglas fir forests.

In conclusion

Swiss needle cast has emerged as one of the most important disease issues in the Pacific Northwest. Management must be careful to identify that *P. gaeumannii* is causing harm and not just present. The Swiss Needle Cast Cooperative will continue its investigation of this disease.

David Shaw is an associate professor in the Department of Forest Engineering, Resources, and Management, and is a forest health specialist with Forestry and Natural Resources Extension at Oregon State University in Corvallis, Oregon, and serves as director of the Swiss Needle Cast Cooperative. He can be reached at dave.shaw@oregonstate.edu.

Alan Kanaskie is a forest pathologist with the Oregon Department of Forestry in Salem, Oregon. He can be reached at alan.kanaskie@state.or.us.

Gabriela Ritokova is a faculty research assistant in the Department of Forest Engineering, Resources, and Management at Oregon State University in Corvallis, Oregon. She can be reached at gabriela.ritokova@oregonstate.edu.

References

Chastagner, G.A. (1997). Christmas tree diseases, insects, and disorders in the Pacific Northwest: Identification and management. Washington State University Cooperative Extension, Publication #MISCO186.

Mulvey, R.L., D.C. Shaw, G.M. Filip, and G. Chastagner. (2013). Swiss needle cast. U.S. Department of Agriculture, Forest Service. *Forest Insect and Disease Leaflet 181.*

Shaw, D.C., G.M. Filip, A. Kanaskie, D.A. Maguire, and W. Littke. (2011). Managing an epidemic of Swiss needle cast in the Douglas-fir region of Oregon: the Swiss Needle Cast Cooperative. *Journal of Forestry* 109:109–119.

Vertical Foliage Retention in Douglas-Fir Across Environmental Gradients of the Western Oregon Coast Range Influenced by Swiss Needle Cast

Author(s): David C. Shaw , Travis Woolley and Alan Kanaskie
Source: Northwest Science, 88(1):23-32. 2014.
Published By: Northwest Scientific Association
DOI: http://dx.doi.org/10.3955/046.088.0105
URL: http://www.bioone.org/doi/full/10.3955/046.088.0105

David C. Shaw[1], Department of Forest Engineering, Resources and Management, 280 Peavy Hall, Oregon State University, Corvallis, Oregon 97331

Travis Woolley, Department of Forest Engineering, Resources and Management, 280 Peavy Hall, Oregon State University, Corvallis, Oregon 97331

and

Alan Kanaskie, Oregon Department of Forestry, 2600 State Street, Salem, Oregon 97208

Vertical Foliage Retention in Douglas-fir Across Environmental Gradients of the Western Oregon Coast Range Influenced by Swiss Needle Cast

Abstract

We investigated the vertical pattern of foliage retention of Douglas-fir (*Pseudotsuga menziesii*) in the western Oregon Coast Range where Swiss needle cast, a foliage disease caused by *Phaeocryptopus gaeumannii,* is causing foliage loss and growth impacts. Swiss needle cast reduced foliage retention more in the upper crown than the lower crown within the epidemic area, which is unusual as foliage diseases usually reduce foliage retention most in the lower crown. We hypothesized that as foliage retention increased across environmental gradients that it would also increase in the upper crown at a greater rate than the lower crown. We randomly selected 72 sites from a population of Douglas-fir plantations in the northwest Oregon Coast Range. We estimated foliage retention from the lower, mid and upper crown of 10 trees per plot. We fitted a two-level hierarchical model with tree and stand level predictors to model changes in foliage retention with changing environmental gradient for foliage in each of three vertical crown positions. We found that the vertical pattern of foliage retention was generally similar throughout the study area with lowest retention in the upper crown, and highest retention in the lower crown. Foliage retention increased with increasing distance from the coast, which is correlated with increased elevation and decreased temperature and site productivity. These findings are consistent with our current understanding of conifer foliage retention. No apparent shift occurs from whole crown to lower crown impacts in our study area as foliage retention increases and approaches normal.

Keywords: Douglas-fir, foliage retention, hierarchical modeling, foliage disease

Introduction

Foliage retention in determinant growth conifers, expressed as the number of years of foliage cohorts retained on a stem, varies due to environmental and biological factors. Foliage retention in conifers is known to increase with increasing elevation and decreasing site productivity (Ewers and Schmid 1981, Schoettle 1990, Reich et al. 1995, Reich et al. 1996), or increasing latitude and decreasing temperature (Xiao 2003). Fertilization with urea (N) has also been shown to reduce foliage retention (Brix 1983, Balster and Marshall 2000). Within a healthy tree crown, the upper crown typically has the lowest foliage retention and the lower crown has the highest foliage retention (Schoettle and Smith 1991, Reich et al. 1995).

Foliage diseases that affect conifers cause reductions in foliage retention, with greater reduction of foliage occurring where the spores landing on foliage have the greater chance of survival. This is typically in the lower portions of the crown (Tatter 1989, Scharpf 1993, Goheen and Willhite 2006) due to higher humidity. Foliage diseases also appear to be most prevalent in certain landscape settings, such as on north slopes and in wetter areas where humid air settles (Goheen and Willhite 2006, Shaw et al. 2009).

Swiss needle cast (Swiss needle cast), a foliage disease of Douglas-fir, (*Pseudotsuga menziesii*) caused by *Phaeocryptopus gaeumannii*, has reached epidemic proportions in the state of

[1]Author to whom correspondence should be addressed.
E-mail: dave.shaw@oregonstate.edu

Oregon, USA along the Pacific coast and west slope of the Oregon Coast Range—referred to hereafter as the epidemic area (Shaw et al. 2011). The disease is most severe near the coast and at low elevations. The severity of Swiss needle cast has been linked to warm winter temperature and consistent spring/summer leaf wetness (Hansen et al. 2000, Rosso and Hansen 2003, Manter et al. 2005). Swiss needle cast symptoms include early loss of foliage, thinning and chlorosis of the crown, and reduced tree growth. Within the epidemic area, Douglas-fir foliage retention is thought to be directly affected by *P. gaeumannii* (Hansen et al. 2000, Manter et al. 2001, Winton et al. 2003). Tree growth has been directly linked to foliage retention (Maguire et al. 2011), and effects of foliage retention have been incorporated into the forest growth model ORGANON (Maguire et al. 2002, Garber et al. 2007).

Zhao et al. (2011) investigated the correlation of regional and annual trends in foliage retention with 85 different climatic variables. They found that average foliage retention in western Oregon Douglas-fir was correlated with a temperature-based continentality index, mean annual precipitation, winter temperature, summer temperature, and spring or summer precipitation when distance from coast and elevation were excluded. Zhao et al. (2012) then investigated the climatic influences on needle cohort survival associated with Swiss needle cast in coastal Douglas-fir. They found that needle survival was positively correlated with maximum summer temperature, and negatively associated with minimum winter temperature and spring precipitation.

Typically, Swiss needle cast causes foliage loss in the lower and inner portion of the crown, where humidity is higher (Merrill and Longenecker 1973, Chastagner and Byther 1983, Scharpf 1993). However, Hansen et al. (2000) concluded that disease severity, measured as the density of Swiss needle cast reproductive structures emerging from the stomates (pseudothecia) was greater and foliage retention was lower in the upper crown for the first three cohorts of foliage at seven Douglas-fir plantations near Tillamook, Oregon. These coastal Oregon forests have unique environmental conditions where summer precipitation and fog cause similar leaf wetness throughout the entire crown during the Swiss needle cast spore dispersal period from late May through August.

Manter et al. (2003) also studied vertical patterns of Swiss needle cast in Douglas-fir crowns in coastal Oregon. They sampled one branch each from the north-top, north-bottom, south-top, and south-bottom quadrants of the crown of three infected trees at each of five Swiss needle cast impacted sites near the coast. The highest pseudothecia density (disease severity) and greatest relative foliage loss were found on the south-top, followed by north-top quadrant. Manter et al. (2003) also compared trees from north and south aspects across three sample sites representing the gradient from the western coast to the eastern drier Willamette Valley margin. They found higher levels of infection and symptom severity on trees growing on south slopes in the western Coast Range. Weiskittel et al. (2006) investigated the influence of Swiss needle cast on foliage mass, foliage age-class structure, and vertical foliage distribution at twenty-one Douglas-fir plantations (10- to 60-year-old) across a gradient of disease severity within the Swiss needle cast epidemic area. Reduction in the total mass of foliage in each age class was associated with increasing Swiss needle cast severity. As would be expected, this resulted in an increased relative mass in the younger age classes. The older age classes (4- to 5-year-old) were skewed to the lower crown, while younger age classes (1- to 3-year-old) were proportionally more abundant in the upper crown.

Methods for estimating foliage retention vary among studies. Hansen et al. (2000) and Manter et al. (2003) used a disease assessment technique where they focused on the first three years of cohorts because impacts to these cohorts reflect disease impacts to the host. They estimated the percent of retained foliage in each cohort and found that an average of 87% of the foliage was retained in all three cohorts. Schoettle (1990) used leaf longevity, defined as the age of the oldest leaves that are firmly attached to the stem of a shoot. A leaf longevity of 10 years indicates presence of leaves in 11 annual cohorts, including the current

year. Reich et al. (1996) also assessed needle longevity or retention by counting annual needle cohorts. However, a cohort was only counted if > 50% of the needles in a cohort were retained. With this technique, leaf longevity represents an average needle life span. In addition, Reich et al. (1996) recognized difference in vertical patterns and averaged needle longevity from the upper and lower crown. In contrast, Xiao (2003) defined leaf longevity as the time in years that current-year foliage of individual trees is expected to live given the observed mortality rate using a life table approach.

An understanding of foliage retention patterns is important to management of the disease. For example, thinning (density reduction) and vegetation control are suggested as management options to reduce foliage disease in conifer plantations. However, research in the Swiss needle cast epidemic area has so far shown thinning and vegetation management does not aid in control of the disease (Crane 2002, Mainwaring et al. 2005). Similar insights have been gained in studies of Swiss needle cast in New Zealand (Hood and Sandberg 1979). However, the lack of response to thinning may only be the case in the high severity area and it should still be suggested for low severity sites (higher foliage retention) if relative impacts of disease are greater in the lower crown than the upper.

The objective of our research was to examine whether the vertical pattern of foliage retention in Douglas-fir within the Swiss needle cast epidemic area on the western slope of the Oregon Coast Range varies across an environmental gradient of increasing elevation and decreasing temperature and productivity as one moves inland. We hypothesized that the change in foliage retention across environmental gradients would be greater in the upper crown than in the lower crown due to lessening of disease severity as one moves out of the coastal fog zone.

Methods

Study Sites and Data Collection

We used an existing plot system of Douglas-fir plantations in the northwest Coast Range of Oregon. This plot system was originally designed to assess tree growth impacts resulting from *P. gaeumannii* infection (Maguire et al. 2002). These plots were measured annually from 1998-2003 and have become a foundation for monitoring Swiss needle cast (Shaw et al. 2011). A single permanent 0.02 ha plot was randomly established within each of 76 Douglas-fir plantations between 10 and 30 years of age, located north of Newport (N44°35', W124°00'), south of Astoria (N46°10', 123°50'), and within 31 km of the coast and on sites ranging in elevation from 45 m to 518 m (Figure 1). These plantations were randomly selected from a large database that included all major landowners with Douglas-fir plantations within the given geographic and age constraints. Height, height to live crown base, and foliage retention was measured for 10 tallest trees per plot (dominant or co-dominant trees), and tree diameter at breast height (DBH) was measured for all trees, annually from 1998-2003 (Table 1). Estimates of foliage retention were obtained in the year 2000. Results are reported for a total of

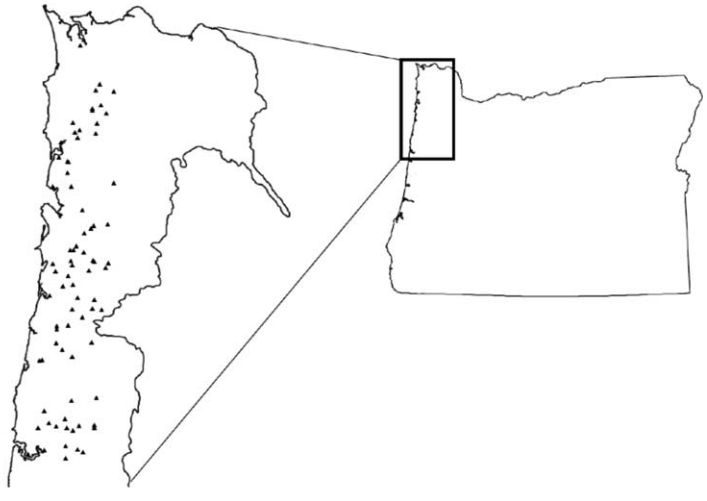

Figure 1. Map showing Growth Impact Study field sites (triangles) on which foliage retention was measured. Plots are located in the northern half of the Oregon coastal ecoregion between Newport and Astoria.

TABLE 1. Mean and range of stand attributes for 76 permanent growth impact study plots in the northern Oregon coast range mountains.

Stand Attribute	Mean	Range
DBH (cm)	25.9	11.8 – 40.0*
Douglas-fir Density (trees/ha)	688	148 – 1,927
Douglas-fir Basal Area (m^2/ha)	15.77	2.03 – 37.24
Total Basal Area (m^2/ha)	19.25	2.84 – 54.97
Site Index (Height at 50 yr, m)	41.0	24.4 – 52.1
Average Foliage retention (yr)	2.26	1.12 – 3.4*
Elevation (m)	230	45 – 518
Aspect (°)	180.8	0 – 356
Distance from Coast (km)	9.5	0.6 – 19.8

* +/- 2 standard deviations

72 stands and 676 trees. Two sites were excluded from the analysis because their elevations were well above the range of the remaining sites and were located on the east side of the Coast Range crest, beyond the scope of our study. Two sites were lost to disturbance.

The purpose of obtaining foliage retention estimates was to determine the amount of foliage present and its impact on tree growth (Maguire et al. 2011). Therefore, our estimate of foliage retention was not foliage longevity. The foliage retention estimate was made by observing the amount of foliage present and estimating the number of cohorts where a full complement would fit. For example, if year 1 and year 2 had full cohorts, year 3 had 0.8 cohort and year 4 had 0.5 cohort then foliage retention = 3.3. Foliage retention was determined in spring (April) prior to current year budbreak (early May). The live crown was divided into thirds (lower, middle, upper) with the base of the live crown defined as the lowest live branch. A single secondary, or lateral branch, off a primary branch in the center of each crown third was examined. A two person crew (rarely a third person substituting) did the needle retention estimates to maintain consistency.

Data Analysis

The relationship of foliage retention to environmental measurements (distance from coast, elevation, aspect) was modeled using a two-level hierarchical linear model (Bryk and Raudenbush 1992; Singer 1998) with both tree- and stand-level predictors. This method accounts for multi-level variation due to measurement of explanatory variables at different scales than the response variable. The tree level model assumed the relationship of foliage retention to DBH within a stand did not differ among crown positions within a tree, but allowed the mean foliage retention to change as a function of position within the tree canopy. Although DBH in general is known to impact foliage retention, the general variation in DBH among trees in our study was not great (Figure 2) and it is difficult to interpret the degree to which DBH actually

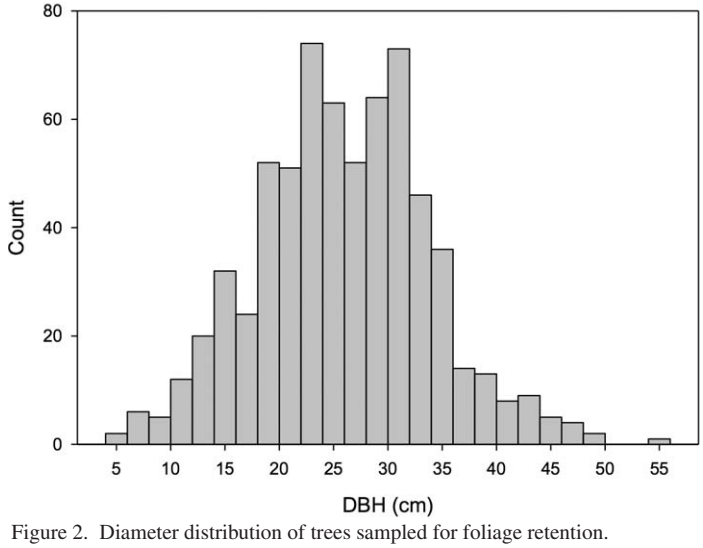

Figure 2. Diameter distribution of trees sampled for foliage retention.

influences foliage retention. Therefore we held the effect constant in our models. The model translates to a constant slope model with different intercepts for each crown position and can be written as:

$$Y_{ijk} = \beta_{0i} + \beta_{1i} I_{b,ijk} + \beta_{2i} I_{m,ijk} + \beta_3 DBH_{ijk} + \varepsilon_{ijk}$$

where Y_{ijk} is the mean foliage retention of the i^{th} position in the j^{th} tree in the k^{th} stand, and I_b is an indicator of whether the measurement was made in the bottom position and I_m is an indicator of whether the measurement was made in the middle position. By convention, the intercept, β_0 represents the mean foliage retention of the top position. In this model, each tree was repeatedly measured (at 3 positions) and residuals were assumed to be multivariate normal with an unstructured 3 by 3 variance-covariance matrix. Tree level covariates included DBH and canopy position.

The second level model represented the hypothesis that the mean foliage retention of each position was dependent on stand level variables. The second level model was

$$\begin{aligned} \beta_{0i} &= \gamma_{00} + \gamma_{01} X_i + \lambda_{0i} \\ \beta_{1i} &= \gamma_{10} + \gamma_{11} X_i + \lambda_{1i} \\ \beta_{2i} &= \gamma_{20} + \gamma_{21} X_i + \lambda_{2i} \\ \beta_{3i} &= \gamma_{30} + \gamma_{31} X_i + \lambda_{3i} \end{aligned} \begin{bmatrix} \lambda_{0i} \\ \lambda_{1i} \\ \lambda_{2i} \\ \lambda_{3i} \end{bmatrix} \sim MVN \begin{bmatrix} 0 \\ 0 \\ 0' \\ 0 \end{bmatrix} \begin{bmatrix} \tau^2_{00} & \tau_{01} & \tau_{02} & \tau_{03} \\ \tau_{01} & \tau^2_{11} & \tau_{12} & \tau_{13} \\ \tau_{02} & \tau_{12} & \tau^2_{22} & \tau_{23} \\ \tau_{03} & \tau_{13} & \tau_{23} & \tau^2_{33} \end{bmatrix}$$

where X_i represents a stand level variable or variables, and residuals are multivariate normal with mean 0 and in a 4 by 4 unstructured variance-covariance matrix. Stand level covariates were elevation, aspect, and distance from coastline. Aspect was measured as an azimuth (0-360°) and transformed for analysis using a cosine transformation (cosine[(aspect/360)*2π]) resulting in continuous values between 1 (0° or 360°) and -1 (180), thus removing the disjunction between 0° and 360°. Values of DBH, elevation, and distance from coast were centered to either the mean values within a stand (DBH), or the mean values across all stands (distance and elevation). This approach provides more interpretable model coefficients (Singer 1998).

Explanatory variables at the tree (canopy position and DBH) and stand (elevation, distance from coast, and cos_aspect) levels were used to develop 18 *a priori* candidate models (Table 2). Models included combinations and interactions of explanatory variables at both the tree and stand level, based on *a priori* hypotheses These models were then compared using Akaike's Information Criterion (AIC) to select the best model (Burnham and Anderson 2002). Models were ranked by the change in AIC (Δ_i). and Akaike's weight (W_i, the weight of evidence in favor of a model being the best model within the entire set being tested given the data [Burnham and Anderson 2002]). Estimated proportional reduction in variance of ($\tau^2_{00}, \tau^2_{11}, \tau^2_{22}, \tau^2_{33}$) after inclusion of tree level and/or stand level explanatory variables provided evidence of the importance of these variables in explaining variance in foliage retention.

All regression analyses were performed using the MIXED procedure with maximum likelihood estimation methods in SAS v9.2 (SAS Institute Cary, NY). The CORR procedure was also used prior to model selection to determine correlation between explanatory variables. Variables with significant correlations were not included in the same model. Because stand age and tree diameter were moderately correlated ($r = 0.57$), stand age was not used as a stand level variable in model selection.

Results

The highest ranked models of foliage retention included canopy position (lower, middle, upper), tree diameter, and distance from coast (Table 3). Foliage retention averaged 1.603 (0.038) for the upper crown, 2.37 (0.051) for the mid crown, and 2.85 (0.068) for the lower crown. The lowest foliage retention occurred in the upper third of the canopy and the highest occurred in the lower third of the canopy (Figure 3, 4). Variation in foliage retention was lowest in the upper canopy and highest in the lower canopy (Table 4). One hundred percent of cumulative weight (W_{aic}) was given to the top 10 ranked models, which all included canopy position, DBH, and distance from coast.

We chose the top-ranked model to indicate the most relevant variables explaining foliage retention due to its relative simplicity and because the interaction between canopy position and distance from coast is biologically meaningful in relation

TABLE 2. Rankings based on AIC values and explanatory variables for the 18 a priori candidate modelsand the NULL model.

Rank	Variables	AIC	Δ_{aic}	W_{aic}
1	CP, DBH, DIST, CP*DIST	2835.2	0.0	0.23
2	CP, DBH, DIST	2835.8	0.528	0.18
3	CP, DBH, DIST, ELEV	2836.4	1.156	0.13
4	CP, DBH, DIST, ASP	2836.9	1.631	0.10
5	CP, DBH, DIST, ASP, DIST*ASP	2837.0	1.807	0.09
6	CP, DBH, DIST, ELEV, DIST*ASP	2837.4	2.148	0.08
7	CP, DBH, DIST, ELEV, ASP	2837.5	2.220	0.08
8	CP, DBH, DIST, ELEV, DIST*ELEV	2838.4	3.203	0.05
9	CP, DBH, ASP DIST, ELEV, ELEV*ASP	2839.3	4.035	0.03
10	CP, DBH, ASP DIST, ELEV, DIST*ELEV	2839.5	4.265	0.03
11	CP, DBH, ELEV	2848.2	12.917	0.00
12	CP, DBH, ELEV, ASP	2849.3	14.106	0.00
13	CP, DBH, ASP, ELEV*ASP	2851.4	16.152	0.00
14	CP, DBH, ELEV, CP*ELEV	2851.5	16.302	0.00
15	CP, DBH^	2852.1	16.842	0.00
16	CP, DBH, ASP	2853.4	18.180	0.00
17	CP, DBH, ASP, DBH*ASP	2855.0	19.780	0.00
18	CP, DBH, ASP, CP*ASP	2857.3	22.027	0.00
19	NULL	3022.2	187.0	0.00

^Tree level variables only

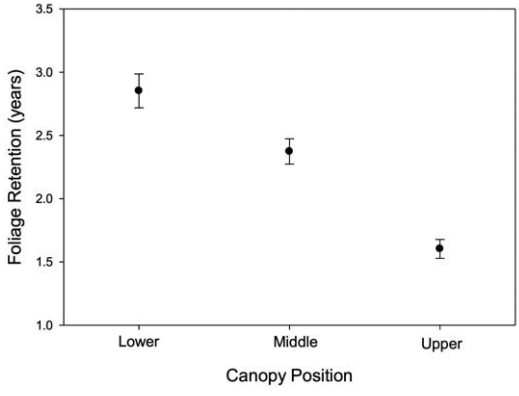

Figure 3. Mean foliage retention estimates in three canopy positions for trees of average DBH in the Swiss needle cast infected area of the western Oregon coast range. Error bars indicate 95% confidence intervals.

to our original hypotheses (Table 2). All *a priori* models with distance as an explanatory variable were included in this top 10. Delta AIC values (Δ_{aic}) showed that there was little difference among the top eight models. The second-ranked and simplest model included only canopy position, DBH, and distance from coast. The model including elevation in addition to canopy position, DBH, and distance from coast, was ranked third among the pool of possible models.

At the stand level, distance from coast was the most important of the stand variables ($F_{1,66.1}$ = 26.06, p<0.001), but there is some evidence that its effect differs with position in the canopy ($F_{2,70.1}$ = 2.33, p = 0.105; Figure 3).When considering trees of average DBH, foliage retention in the lower canopy was found to increase by 0.40 years (95% CI: 0.21-0.58 years) every 10 km increase in the distance from the coast. In the mid-canopy, foliage retention was found to increase by 0.33 years (95% CI: 0.19-0.46 years) for every 10 km increase in distance from the coast, and in the upper canopy, foliage retention was found to increase by 0.25 years (95% CI: 0.14-0.35 years) for every 10 km increase in distance from the coast. Foliage retention does increase at a greater rate in the upper crown than in the lower crown, but this difference does not appear meaningful across the study area.

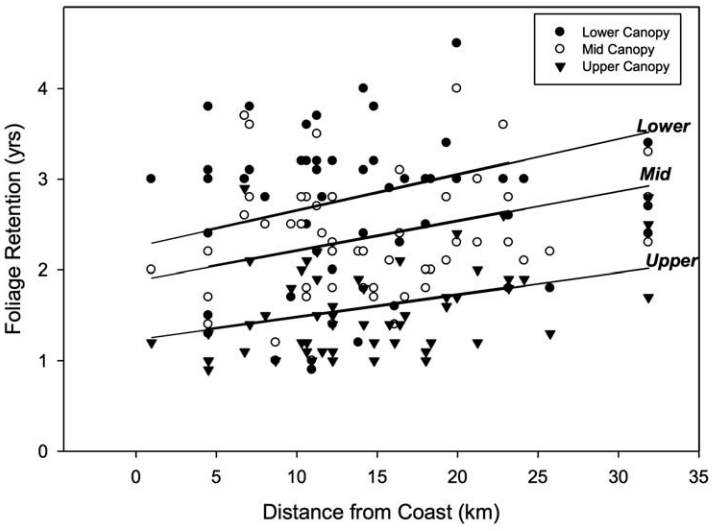

Figure 4. Foliage retention for lower, middle, and upper canopy positions illustrating the relationship of foliage retention and distance from the coastline for trees of average DBH.

In individual tree canopies (i.e., tree level factors) in 10-30 year-old Douglas-fir stands on the Oregon coast range, DBH was a significant factor explaining foliage retention patterns ($F_{1,39.5} = 9.71$, $p = 0.003$) (Table 3). Holding the other model variables constant, foliage retention increases by 0.1 years (95% CI: 0.04-0.17) for every 10 cm increase in DBH. In addition to DBH, foliage retention varies by canopy position (lower, middle, and upper positions).

Discussion

The vertical pattern of foliage retention was generally consistent throughout the study area with lowest retention in the upper crown and highest retention in the lower crown. Foliage retention in all crown positions increased with distance from the coast (Figure 4). Contrary to our hypothesis, we could detect little difference in the rate of increase in foliage retention with distance to the coast among the three crown positions. The top 10 models (all within ~4 AIC units of each other; Table 3), were similar to one another, all of them involving crown position, DBH and distance from coast, but differing either by inclusion of an additional stand level variable or by allowing the effect of distance

TABLE 3. Rankings based on AIC values for the top three hierarchical models and both the level 1 model (no stand level covariates) and the NULL model (intercept only). $\boldsymbol{T}$ = estimated variance among trees in FR in each crown position. Proportional variance reduction = $(T_1 - T_2)/T_1$.

Rank	Variables	AIC	Δ_{aic}	W_{aic}	$\boldsymbol{T}$(Crown Position)	Proportional variance reduction relative to NULL	Proportional variance reduction relative to Level 1
1	CP, DBH, DIST, CP*DIST	2835.2	0.0	0.27 (Upper) 0.23 0.07 (Lower)	0.89 0.14 (Mid) 0.50	0.23 0.87 0.36	0.26
2	CP, DBH, DIST	2835.8	0.528	0.28 (Upper) 0.18 0.07 (Lower)	0.88 0.14 (Mid) 0.50	0.20 0.87 0.36	0.26
3	CP, DBH, DIST, ELEV	2836.4	1.156	0.28 (Upper) 0.13 0.07 (Lower)	0.88 0.14 (Mid) 0.50	0.20 0.87 0.36	NA
15	CP, DBH (Level 1)	2852.1	16.8	0.35 (Upper) 0.00 0.11 (Lower)	0.82 0.19 (Mid) 0.21	0.87	NA
19	NULL	3022.2	187.0	2.35 (Upper) 0.00 0.14 (Lower)	1.07 (Mid)	NA	NA

TABLE 4. Model coefficients for the top ranked model (SE in parentheses). The model is in the form of: FR= β_0 + β_1*DBH + β_2*Distance for each position. DBH is measured in cm and distance in kilometers.

Canopy Position	β_0 (Intercept)	β_1 (DBH)	β_2 (Distance)
Lower	2.852	0.011	0.040
	(0.068)	(0.003)	(0.009)
Middle	2.373	0.011	0.033
	(0.051)	(0.003)	(0.007)
Upper	1.603	0.011	0.025
	(0.038)	(0.003)	(0.005)

to differ among crown positions. There was no clear evidence that any one of these models was the best, implying that none of the factors besides the crown position, DBH, and distance from coast appear to be important in explaining much of the variation in vertical foliage retention patterns.

Distance from the coast was clearly more closely related to foliage retention in our analysis than was elevation (Table 3). This is consistent with our understanding of disease distribution and severity relative to winter temperature and coastal fog and rain during spring and summer (Hansen et al. 2000, Rosso and Hansen 2003, Manter et al. 2005) while needle retention and longevity are related to climatic factors also (Zhao et al. 2011, 2012). In our study area, elevation increases with distance from the coast, and is slightly correlated (r =0.36) with foliage retention patterns.

Separating out the interaction among elevation, distance from coast, and other environmental factors that influence foliage retention is very difficult. Zhao et al. (2011, 2012) did not include distance from coast and elevation in their models purposely to determine the influence of climate. Perakis et al. (2005) documented a strong soil and foliar nitrogen decline from the coastline moving inland, and lower nitrogen levels have been correlated with higher foliage retention (Brix 1983, Reich et al. 1995, Balster and Marshall 2000). The high nitrogen levels near the coast combined with mild winter temperature, longer growing season, greater summer precipitation and fog all interact to reduce foliage retention. Tree size is also known to influence relative vertical foliage distribution in Douglas-fir (Maguire and Bennett 1996) as well as overall foliage retention (Xiao 2003).

We held DBH constant in our model due to the fairly narrow distribution of DBH and tree age in our sample (Figure 2). Given that tree diameter is closely related to tree height, the relationship of foliage retention and tree diameter may be reflecting changes in tree height and subsequent changes in canopy architecture and microclimate as stand structure changes through stand development. Findings from Weiskittel et al. (2006) also support this conclusion; crown size and tree social position were both factors influencing patterns of foliage retention. We accounted for tree social position by only choosing dominant or co-dominant trees.

Foliage retention and/or leaf longevity in conifers is known to increase with increasing elevation and decreasing site productivity (Reich et al. 1992, 1996). Our results support this paradigm, although we did not explicitly account for site productivity. Tree height is often used to predict site productivity and Swiss needle cast has been shown to influence tree height, making site productivity difficult to measure. However, site productivity is generally thought to decrease with distance from coast and increasing elevation in the Oregon Coast Range (Perakis et al. 2005).

Merrill and Longenecker (1973), Chastagner and Byther (1983) and Scharpf (1993) all note that Swiss needle cast symptoms were most severe in the lower crown. We hypothesized that at high elevations far from the coast, where foliage retention in Douglas-fir is highest, the largest reduction in foliage retention would occur in the lower crown. This would be manifested as a smaller difference in foliage retention between upper and lower crowns at high elevations than at low elevations. This was not the case in our study area on the western slopes of the Coast Range of northwest Oregon, where we found no evidence of this effect but some slight evidence of an opposite effect with distance (Figure 3). In our Swiss needle cast study area, the difference in foliage retention between the upper and lower crowns was greater farther from the coast than near the coast.

Our approach to estimating foliage retention differed from those more interested in foliage longevity (Ewers and Schmid 1981, Schoettle 1990, Reich et al. 1995, and Reich et al. 1996) and disease biology (Hansen et al. 2000, Manter et al. 2003). However, we feel our approach is practical for estimates of foliage retention and may not be extremely different from estimates of foliage longevity. Our technique has been used to quantify foliage retention with respect to impact on tree growth (Maguire et al. 2011) and foliage retention is the basis for estimating growth deviations from normal using models such as ORGANON (Garber et al. 2007).

Our results show that on the west slope of the Oregon Coast Range the vertical pattern of foliage retention is similar across environmental gradients and it does not appear to fit the usual paradigm applied to trees influenced by foliage disease in general, or Swiss needle cast infestations in other regions. Typical foliage disease plantation treatments, such as thinning to dry out the stand and improve airflow, do not reduce Swiss needle cast severity (Mainwaring et al. 2005). Swiss needle cast management in the Oregon Coast Range therefore involves an integrated pest management strategy that incorporates both qualitative models using disease severity estimates based on foliage retention, quantitative tools to measure growth impacts, adaptive silviculture, economic models, and alternative species where appropriate (Shaw et al. 2011, Mulvey et al. 2013).

Acknowledgments.

The plot network used in this study was initiated by the Swiss Needle Cast Cooperative (D. Maguire and A. Kanaskie, Principal Investigators) with Oregon Department of Forestry support, and collaborations with forest landowners in the Oregon Coast Range. Data and needle retention estimates were graciously provided by Doug Mainwaring. Funding was provided by the Swiss Needle Cast Cooperative, Oregon State University. Manuela Huso provided statistical consultation and guidance.

Literature Cited

Balster, N. J. and J. D. Marshall. 2000. Decreased needle longevity of fertilized Douglas-fir and grand fir in the northern Rockies. Tree Physiology 20:11891-1197.

Brix, H. 1983. Effect of thinning and nitrogen fertilization on growth of Douglas-fir: relative contribution of foliage quantity and efficiency. Canadian Journal of Forest Research 13:167-175.

Bryk, A. S. and S. W. Raudenbush. 1992. Hierarchical Linear Models. Sage, Newbury Park, CA.

Burnham, K. P., and D. R. Anderson. 1998. Model Selection and Inference. A Practical Information-Theoretic Approach. Springer-Verlag, New York, NY.

Chastagner, G. A., and R. S. Byther. 1983. Infection period of *Phaeocryptopus gaeumannii* on Douglas-fir needles in western Washington. Plant Disease 67:811-813.

Crane, G. A. 2002. Effect of fertilization, vegetation control and sulfur on Swiss needle cast and growth of coastal Douglas-fir saplings. M.S. Thesis, Oregon State University, Corvallis.

Ewers, F. W., and R. Schmid. 1981. Longevity of needle fascicles of *Pinus longaeva* (Bristlecone pine) and other North American pines. Oecologia 51:107-115.

Garber, S., D. Maguire, D. Mainwaring, and D. Hann. 2007. Swiss Needle Cast ORGANON Module Update. *In* D. Shaw (editor), Swiss Needle Cast Cooperative Annual Report. College of Forestry, Oregon State University, Corvallis. Pp. 63-66.

Goheen, E. M. and E. A. Willhite. 2006. Field Guide to Common Diseases and Insect Pests of Oregon and Washington Conifers. USDA Forest Service, PNW Region, Portland, OR.

Hansen, E. M., J. K. Stone, B. R. Capitano, P. Rosso, W. Sutton, L.Winton, A. Kanaskie, and M. G. McWilliams. 2000. Incidence and impact of Swiss needle cast in forest plantations of Douglas-fir in coastal Oregon. Plant Disease 84:773-779.

Hood, I. A. and C. J. Sandberg. 1979. Changes within tree crowns following thinning of young Douglas-fir infected by *Phaeocryptopus gaeumannii*. New Zealand Journal of Forestry Science 9:177-184.

Maguire, D. A. and W. S. Bennett. 1996. Patterns in vertical distribution of foliage in young coastal Douglas-fir. Canadian Journal of Forest Research 26:1991–2005.

Maguire D. A., A. Kanaskie, W. Voelker, R. Johnson, and G. Johnson. 2002. Growth of young Douglas-fir plantations across a gradient in Swiss needle cast severity. Western Journal of Applied Forestry 17:86-95.

Maguire, D. A., D. B. Mainwaring, and A. Kanaskie. 2011. Ten-year growth and mortality in young Douglas-fir stands experiencing a range in Swiss needle cast severity. Canadian Journal of Forest Research 41:2064-2076.

Mainwaring, D., D. Maguire, A. Kanaskie, and J. Brandt. 2005. Growth responses to commercial thinning in Douglas-fir stands with varying severity of Swiss needle cast in Oregon, USA. Canadian Journal of Forest Research 35:2394-2402.

Manter, D. K., R. G. Kelsey, and J. K. Stone. 2001. Quantification of *Phaeocryptopus gaeumannii* colonization in Douglas-fir needles by ergosterol analysis. Forest Pathology 31:229-240.

Manter, D. K., L. M. Winton, G. M. Filip, and J. K. Stone. 2003. Assessment of Swiss needle cast disease: Temporal and spatial investigations of fungal colonization and symptom severity. Phytopathologische-Zeitschrift 151:344-351.

Manter, D. K., P. W. Reeser, and J. K. Stone. 2005. A climate-based model for predicting geographic variation in Swiss needle cast severity in the Oregon coast range. Phytopathology 95:1256-1265.

Merrill, W., and J. Longenecker. 1973. Swiss needle cast on Douglas-fir in Pennsylvania. Plant Disease Reporter 57:984.

Mulvey, R. L., D. C. Shaw, G. M. Filip, and G. A. Chastagner. 2013. Swiss Needle Cast. Forest Insect and Disease Leaflet 181. USDA Forest Service, Pacific Northwest Research Station, Portland, OR.

Perakis, S. S., D. A. Maguire, T. D. Bullen, K. Cromack, R. H. Waring, and J. R. Boyle. 2005. Coupled nitrogen and calcium cycles in forests of the Oregon Coast Range. Ecosystems 8:1-12.

Reich, P. B., M. B. Walters, and D. S. Ellsworth. 1992. Leaf life-span in relation to leaf, plant, and stand characteristics among diverse ecosystems. Ecological Mongraphs 62:365-392.

Reich, P. B., T. Koike, S. T. Gower, and A. W. Schoettle. 1995. Causes and consequences of variation in conifer leaf life-span. *In* W.K. Smith and T.M. Hinckley (editors), Ecophysiology of Coniferous Forests, Academic Press, New York, NY. Pp. 225-254.

Reich, P. B., J. Oleksyn, J. Modrzynski, and M. G. Tjoelker. 1996. Evidence that longer needle retention of spruce and pine plantations at high elevations and high latitudes is largely a phenotypic response. Tree Physiology 16:643-647.

Rosso, P. H., and E. M. Hansen. 2003. Predicting Swiss needle cast disease distribution and severity in young Douglas-Fir plantations in coastal Oregon. Phytopathology 93:790-798.

Received 02 May 2013
Accepted for publication 17 October 2013

Scharpf, R. F. 1993. Diseases of Pacific Coast Conifers. USDA, Forest Service, Agriculture Handbook 521. Pacific Southwest Research Station, Albany, CA.

Schoettle, A. W. 1990. The interaction between leaf longevity, shoot growth, and foliar biomass per shoot in *Pinus contorta* at two elevations. Tree Physiology 7: 209-214.

Schoettle, A. W., and W. K. Smith. 1991. Interrelation between shoot characteristics and solar irradiance in the crown of *Pinus contorta* spp. *latifolia*. Tree Physiology 9:245-254.

Shaw, D. C., G. Filip, A. Kanaskie, D. Maguire, and W. Littke. 2011. Managing an epidemic of Swiss needle cast in the Douglas-fir region of Oregon: The role of the Swiss needle cast cooperative. Journal of Forestry 109:109-119.

Shaw, D. C., P. T. Oester, and G. M. Filip. 2009. Managing Insects and Diseases of Oregon Conifers. Extension Manual 8980, Oregon State University Extension Service Press, Corvallis, OR.

Singer, J. D. 1998. Using SAS PROC MIXED to fit multilevel models, hierarchical models, and individual growth models. Journal of Educational and Behavioral Statistics 23:323-335.

Tattar, T. A. 1989. Diseases of Shade Trees. Academic Press, San Diego, CA.

Weiskittel, A. R., D. A. Maguire, S. M. Garber, and A. Kanaskie. 2006. Influence of Swiss needle cast on foliage age-class structure and vertical foliage distribution in Douglas-fir plantations in north coastal Oregon. Canadian Journal of Forest Research 36:1497-1508.

Winton, L. M., D. K. Manter, J. K. Stone, and E. M. Hansen. 2003. Comparison of biochemical molecular and visual methods to quantify *Phaeocryptopus gaeumannii* in Douglas-fir foliage. Phytopathology 93:121-126.

Xiao, Y. 2003.Variation in needle longevity of *Pinus tabulaeformis* forest at different geographic scales. Tree Physiology 23:463-471.

Zhao, J., D. B. Mainwaring, D. A. Maguire, and A. Kanaskie. 2011. Regional and annual trends in Douglas-fir foliage retention: correlations with climatic variables. Forest Ecology and Management 262:1872-1886.

Zhao, J., D. A. Maguire, D. B. Mainwaring, and A. Kanaskie. 2012. Climatic influences on needle cohort survival mediated by Swiss needle cast in coastal Douglas-fir. Trees 26:1361-1371.

Mycologia, 106(4), 2014, pp. 666–675. DOI: 10.3852/12-180

Relationships between Swiss needle cast and ectomycorrhizal fungus diversity

Daniel L. Luoma[1]
Joyce L. Eberhart
Department of Forest Ecosystems and Society, Oregon State University, Corvallis, Oregon 97331

Abstract: Swiss needle cast (SNC) is a disease specific to Douglas-fir (*Pseudotsuga menziesii*) caused by the ascomycete *Phaeocryptopus gaeumannii*. Here we examine characteristics of the EM fungus community that are potentially useful in predictive models that would monitor forest health. We found that mean EM density (number of colonized root tips/soil core) varied nearly 10-fold among sites of varying levels of SNC, while mean EM fungus species richness (number of species/soil core) varied by about 2.5 times. Strong relationships were found between EM and SNC parameters: EM species richness was positively correlated with both Douglas-fir needle retention (R^2 = 0.93) and EM density (R^2 = 0.65); EM density also was significantly correlated with Douglas-fir needle retention (R^2 = 0.70). These simple characteristics of the EM fungus community could be used to monitor forest health and generate predictive models of site suitability for Douglas-fir. Based on previous findings that normally common EM types were reduced in frequency on sites with severe SNC, we also hypothesized that some EM fungi would be stress tolerant-dominant species. Instead, we found that various fungi were able to form EM with the stressed trees, but none were consistently dominant across samples in the severely diseased areas.

Key words: anthropogenic disturbance, climate change, ecosystem health, *Phaeocryptopus gaeumannii*

Introduction

Swiss needle cast (SNC) disease is specific to *Pseudotsuga menziesii* (Mirb.) Franco (Douglas-fir) and is caused by the ascomycete *Phaeocryptopus gaeumannii* (T. Rohde) Petr. (Gaümann 1930 in Stone et al. 2008). SNC affects the foliage of Douglas-fir: symptoms include chlorotic needles and premature needle abscission, resulting in reduced leaf area index and vigor (Manter et al. 2000, McGuire et al. 2002, Weiskittel and McGuire 2007). *Phaeocryptopus gaeumannii* is native to the western United States and presumably was introduced in Europe, New Zealand and elsewhere via import of live Douglas-fir seedlings (Stone et al. 2007). It was the initial discovery of the disease in Douglas-fir plantations in Switzerland in the mid-1920s that engendered the name of the disease (Gaümann 1930). Until the mid-1980s, *P. gaeumannii* was considered an unimportant and minor pathogen (Boyce 1940, Hansen et al. 2000). Under most conditions, *P. gaeumannii* is a benign component of the tree canopy and does not contribute to premature needle shed or growth loss. Nevertheless, since the late 1980s and early 1990s SNC has caused an epidemic affecting hundreds of thousands of acres, across a wide variety of soil conditions, in the western Oregon Coast Range from Coos Bay to Astoria. Annual aerial surveys conducted by the Oregon Department of Forestry have shown a consistent increase in affected areas since the surveys began in 1996. The 2011 aerial survey mapped more than 160 000 ha with symptoms of SNC. Most diseased trees occurred within 29 km of the Pacific Ocean, but SNC symptoms extended up to 40 km inland (Kanaskie and McWilliams 2011). Stone et al. (2008) note the strong correlation of *P. gaeumannii* abundance and disease severity with climatic factors, particularly winter mean temperature. Growth losses in the area of epidemic infection generally are 20–50%, and annual growth losses are estimated to exceed $200 000 000 per year (Maguire et al. 2002).

It is important to consider the potential links between ectomycorrhizal (EM) fungi and SNC. Ectomycorrhizal fungi are essential for host plant nutrient uptake and play important roles in nutrient cycling in many forests (Cromack et al. 1979, Smith and Read 2008). For example, an estimated 50–70% of the net annual productivity may be translocated to roots and associated mycorrhizal fungi (Fogel and Hunt 1979, Vogt et al. 1982, Norton et al. 1990). Markkola et al. (2004) found reduced carbon allocation to roots after 100% defoliation and that fungal biomass in fine roots decreased when defoliation occurred in the year of harvest but not when the defoliation was conducted the previous year. They concluded that current photosynthates are particularly important for EM fungal symbionts.

Most of the dominant and economically important timber species in the Pacific Northwest are EM-dependent, including all members of the pine, oak and birch plant families (Smith and Read 2008). Douglas-fir alone is thought to have about 2000 EM fungal symbionts throughout its range (Trappe 1977) and appears unable to grow in soil without ectomycorrhizal fungi (Trappe and Strand 1969).

Submitted 15 May 2012; accepted for publication 2 Jan 2014.
[1] Corresponding author. E-mail: luomad@fsl.orst.edu

In a 2006 pilot study we found that Douglas-fir forests with moderate to high SNC (as measured by foliage retention) had 3–4 times fewer EM fungus species than similar Douglas-fir stands without appreciable SNC (Eberhart et al. 1996, Luoma et al. 2006) and had numbers of EM species comparable to that of sites that had experienced significant disturbance from clear-cutting and fire (Luoma and Eberhart 2006). We concluded that the degree of EM fungus diversity detected in the pilot study suggested that the belowground ecosystem was being strongly affected by SNC, alone or in combination with the previous removal of mature trees during timber harvest and postharvest silvicultural practices.

Here we present work that was undertaken to provide better understanding of relationships between EM fungus diversity and SNC in northwestern Oregon. We assumed the EM fungus community structure varied substantially across the landscapes in which SNC is found for many potential reasons, particularly those tied to variations in climate and soil conditions. We hypothesized that in comparing sites of similar age, structure and management history across a gradient of SNC disease, EM root-tip density and EM fungus species richness (at the scale of the soil core) would be inversely correlated with SNC severity (mean needle age cohorts, measured in years) due to reduced photosynthetic capacity accompanying increasing disease.

In addition, preliminary data suggested that some EM fungi were tolerated stress (sensu Grime 1979) because common Douglas-fir EM types formed by genera such as *Cenococcum* and *Rhizopogon* were less widespread in SNC-stressed stands than in other studies (Eberhart et al. 1996, Luoma et al. 2006). Because the diseased trees were mycorrhizal, albeit at low EM root-tip densities, we hypothesized that certain EM fungi (with important functional roles to keep Douglas-fir alive in the face of heavy SNC) may become more dominant on the roots that remain. Therefore we examined a second hypothesis that particular stress-tolerant EM fungi would be found as dominant members of the EM community. Specifically we hypothesized that (i) common mycorrhiza types of non-SNC affected trees, as measured by mean number of root-tips/soil core, will be less common on high SNC sites; (ii) A limited number of stress-tolerent fungi, possibly adapted to a reduced carbon supply, will be relatively more common, as measured by mean number of EM root-tips/soil core, on high SNC sites.

MATERIALS AND METHODS

Field sites.—The study sites (FIG. 1) varied by degree of SNC disease symptoms (TABLE I), and disease severity was measured by use of a needle retention index (Hansen et al. 2000). Stands were similarly managed, un-thinned and unfertilized Douglas-fir plantations that were about 20–25 y old at the time of sampling. Additional site information can be found in Stone et al. (2005), Mainwaring et al. (2007) and Mulvey et al. (2013). Foliage retention (mean needle age cohorts, measured in years) has been found to work well for predicting tree and stand growth (Maguire et al. 2002, 2011).

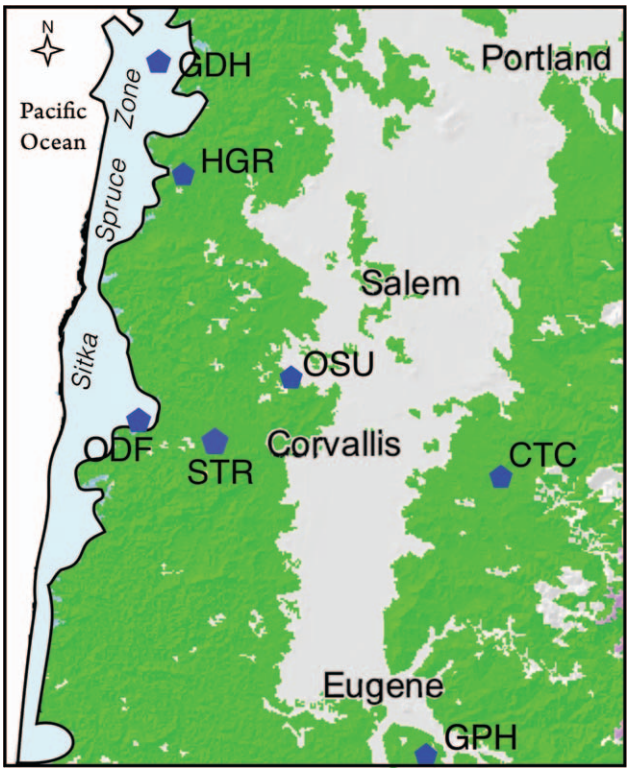

FIG. 1. Study site locations with reference to the *Picea sitchensis* (Sitka spruce) zone (light gray) in northwestern Oregon. The *Tsuga heterophylla* (western hemlock) zone, typically dominated by long-lived stands of Douglas-fir, is depicted in dark gray (after Franklin and Dyrness 1973). (Key in TABLE I.) Base map: Oregon Gap Analysis/Oregon Department of Forestry.

Study trees had been mapped and numbered by other researchers (Stone et al. 2005, Mainwaring et al. 2007, Mulvey et al. 2013). EM roots of Douglas-fir were obtained from 350 cc soil cores, 15 cm × 5.5 cm. At each site one soil core was taken from beneath the canopy of each of 10 trees chosen randomly from the list of prenumbered trees. Soil cores were located approximately 1 m from the base of each tree and on the side of the bole closest to the nearest neighboring Douglas-fir, so as to bias for maximum Douglas-fir root density. A total of 70 soil cores were obtained (10 trees/site × 7 sites) in Feb 2007. We also sampled two sites in 2008 that included the most severely diseased site, GDH, as well as another heavily affected site (Swede Hill) near GDH (TABLE I).

Laboratory.—Soil cores were kept cool in the field and stored at −20 C immediately after returning from the field.

TABLE I. Study sites with map codes (FIG. 1), year of sample, Douglas-fir density, disease severity index, variation in EM density and variation in EM fungus species richness among study sites

Land manager at time of study	Location	Map code	Year	Stems[1]	SNC index[2]	EM density[3,4]	Richness[4,5]
Giustina Land & Timber	Pleasant Hill	GPH	2007	921	3.62	478.6^{e} (106.6)	7.7^{d} (0.76)
Cascade Timber Consulting	Waterloo	CTC	2007	977	3.12	274.9^{d} (60.0)	5.9^{cd} (0.74)
Starker Forests	Burnt Woods	STR	2007	754	2.94	149.9^{abc} (42.4)	4.6^{bc} (0.76)
Oregon State University	McDonald Forest	OSU	2007	819	2.99	274.9^{cd} (105.0)	4.3^{abc} (0.65)
Oregon Dept. of Forestry	Elk City	ODF	2007	877	2.31	99.3^{ab} (27.5)	3.3^{ab} (0.60)
Hampton Affiliates	Grand Ronde	HGR	2007	683	2.17	236.6^{bcd} (92.9)	2.9^{ab} (0.48)
Green Diamond Resource	Hemlock	GDH	2007	724	1.70	65.8^{a} (20.0)	2.9^{a} (0.67)
Green Diamond Resource	Hemlock	GDH	2008	724	1.70	122.1 (21.5)	2.5 (0.37)
Green Diamond Resource	Swede Hill	GDH[6]	2008	430	1.59	123.5 (35.9)	2.3 (0.45)

[1] Stems = mean number of Douglas-fir trees per ha.
[2] SNC index = mean years needle retention (n = 10).
[3] EM density = mean number of live ectomycorrhizal root-tips per 350 cc soil core (n = 10). Non-EM tips were almost nonexistent (< 1 in 10 000).
[4] For the 2007 dataset, means across locations not sharing letters are significantly different at $P \leq 0.05$, standard errors are in parentheses. In 2008 the response variables did not differ (n = 10).
[5] EM richness = mean number of EM types per 350 cc soil core (n = 10).
[6] The Green Diamond "Swede Hill" site was in essentially the same location as the GDH site at the scale of the map.

When soil cores were thawed they were examined within 48 h. Roots were extracted from the soil cores by wet sieve-washing over a 1 mm grate. The contents of the sieve were spread evenly, with sufficient water to cover, in the bottom of a 38 × 17 × 2 cm tray that was divided into 36 compartments by an inserted Plexiglas partition (Eberhart et al. 1996). Roots were examined with a stereomicroscope at 15–30× magnification. Each EM type encountered was classified by morphological characteristics similar to those described in Ingleby et al. (1990) and Goodman et al. (1996) including color, texture, presence/absence of rhizomorphs and emanating hyphae. Morphotype identities were determined by comparison to the EM character database maintained by J. Eberhart (unpubl), some of which had been determined to genus or species by DNA sequencing (Luoma and Eberhart 2006). The total number of EM types per soil core and total number of mycorrhizal root tips in each core were recorded for 10 soil cores from seven sites in 2007 and two sites in 2008. Representative samples (a minimum of two tips each) of the predominant mycorrhiza types were saved in CTAB buffer for molecular analysis of the fungal DNA.

Molecular analysis.—For the most common EM morphotypes in the 2008 samples, we extracted DNA following the method described by Avis et al. (2003) with a plant DNA extraction kit (REDExtract-N-Amp Plant PCR Kit, Sigma, St Louis, Missouri). The ITS region (ITS1, 5·8S and ITS2) of the rRNA operon was amplified with primer set ITS1-F/ITS4 (White et al. 1990, Gardes and Bruns 1993). PCR was performed with the REDExtract-N-Amp Plant PCR Kit with PCR cycling conditions modified from Gardes and Bruns (1993). Cycling conditions included an initial denaturation at 94 C for 3 min followed by 35 PCR cycles (93 C, 35 s; 55 C, 53 s; 72 C, 30 + 05 s per cycle) and 72 C for 10 min. Amplified ITS products were visualized in 2% agarose gels stained with ethidium bromide under UV illumination.

For sequencing, samples producing a single PCR product were purified before sequencing with ExoSAP-IT (USB, Cleveland, Ohio). Sequencing was performed by the Center for Genome Research and Biocomputing Core Laboratory at Oregon State University with an ABI Prism 3730 genetic analyser (Applied Biosystems, Foster City, California) with the forward primer ITS1F. Sequences were identified by querying the GenBank database with the nucleotide-nucleotide (BLASTN) query option on the National Center for Biotechnology Information website (Altschul et al. 1997). We set a functional species match criterion at 98% sequence similarity over at least 500 bp with vouchered sporocarp sequences, although not all matches at that level of similarity had corresponding species determination. Taxon assignment of EM fungi to our morphotypes was made with the BLASTN results. These were added to the EM morphotype identities in the EM character database maintained by J. Eberhart. Our manually trimmed sequences were submitted to GenBank (TABLE II).

Statistical analysis.—Number of EM types per soil core (species richness) and total number of EM tips per soil core (feeder root density) were used as response variables. The data were used to test for gradient responses to SNC disease.

TABLE II. Morphotypes identified to lowest taxonomic level from EM collected at the Green Diamond sites in 2008 and sequenced for this study (ITS, 5.8S) including constancy (% of cores out of 20 with taxon present), number of root tips colonized, root-tip sample identification number, GenBank accession number, and maximum identity percentage of the best GenBank match used as the basis of the taxonomic assignment of the EM

Taxon	Constancy (%)	No. of tips colonized	Sample ID No.	GenBank accession No.	Maximum identity (%)
Amanita cf. *gemmata*	5	7	R3445	KC618515	99
Amphinema sp.	10	9	R3482, R3486	KC618523, KC618525	97–98
Clavulina cristata	15	197	R3433, R3434	KC618513, KC618514	98
Clavulinaceae	5	28	R3461	KC618521	99
Hydnotrya sp.	5	36	R3421	KC618507	94
Inocybe sp.	5	8	R3452	KC618517	100
Lactarius luculentus	20	170	R3426, R3428	KC618509, KC618510	99
Melanogaster sp.	5	11	R3483	KC618524	96
Pseudotomentella	5	113	R3460	KC618520	96
Russula nigricans	5	125	R3457	KC618519	99
Sebacinaceae	5	3	R3450	KC618516	99
Thelephoraceae	10	226	R3454, R3472	KC618518, KC618522	95–96
Tomentella sp.	10	109	R3431, R3432	KC618511, KC618512	99
Tomentella sublilacina	5	39	R3487	KC618526	99
Tylospora asterophora sp.	5	33	R3423	KC618508	99

ANOVA was used for comparisons across the sites. When appropriate, Fisher's protected least significant difference test was used to determine whether study site means differed from one another. Linear regression was used to examine gradient responses in EM density and EM fungus species richness to among-block variation in SNC severity (foliage retention). Linear regression also was used to measure the association between EM density and EM fungus type (species) richness. To address the second hypothesis, we examined the mean number of EM root-tips/soil core and constancy of EM types across soil cores on high SNC sites from the 2008 dataset. When necessary to meet the assumptions of normality and constant variance (Sabin and Stafford 1990), we transformed the dependent variables; EM density was square-root transformed, EM fungus richness was log-transformed. Analyses were carried out with StatView 5.1 software (SAS Institute 1999).

RESULTS

Fewer than 1 in 10 000 root tips were non-EM. Mean EM root density varied by nearly 10-fold among sites (TABLE I), while mean EM type (species) richness varied by about 2.5 times (TABLE I) in 2007. In the 2008 sample, these response variables were nearly identical for richness and root density (TABLE I) at the GDH and GDS sites; therefore the GDS data were not included in the regressions. Treating mean logEM richness as a dependent variable of mean EM density produced a regression model of: $Y = 0.417 + 0.001 * X$; $R^2 = 0.65$, $P = 0.03$ (FIG. 2). Mean square-root EM density treated as dependent on mean years needle retention produced a regression model of $Y = -1.583 + 5.932 * X$; $R^2 = 0.70$, $P = 0.02$ (FIG. 3). For the main 2007 sample, mean log EM richness treated as dependent on mean years needle retention produced a regression model of $Y = 0.002 + 0.232 * X$; $R^2 = 0.90$, $P = 0.001$ (FIG. 4). When data from the 2008 sample of the GDH site were added to that model, the EM richness vs. years needle retention model improved to $Y = 0.023 + 0.226 * X$; $R^2 = 0.92$, $P = 0.0001$ (FIG. 4).

From the 20 soil cores examined in the 2008 Green Diamond sample, a total of 31 EM types were identified by morphotyping and molecular methods. Fifteen of the 31 types were assigned to taxa with ITS sequencing (TABLE II). Twenty-four of the 31 EM types found at the Green Diamond site were recorded from one soil core each. An additional four EM types were recorded from only two soil cores each. Only one EM type (*Cenococcum geophilum*) was regularly represented in the Green Diamond soil cores with 40% constancy (8 of 20 cores). The *Lactarius luculentus* morphotype was found in four soil cores and was confirmed by ITS sequencing of samples from two soil cores. The *L. luculentus* type matched

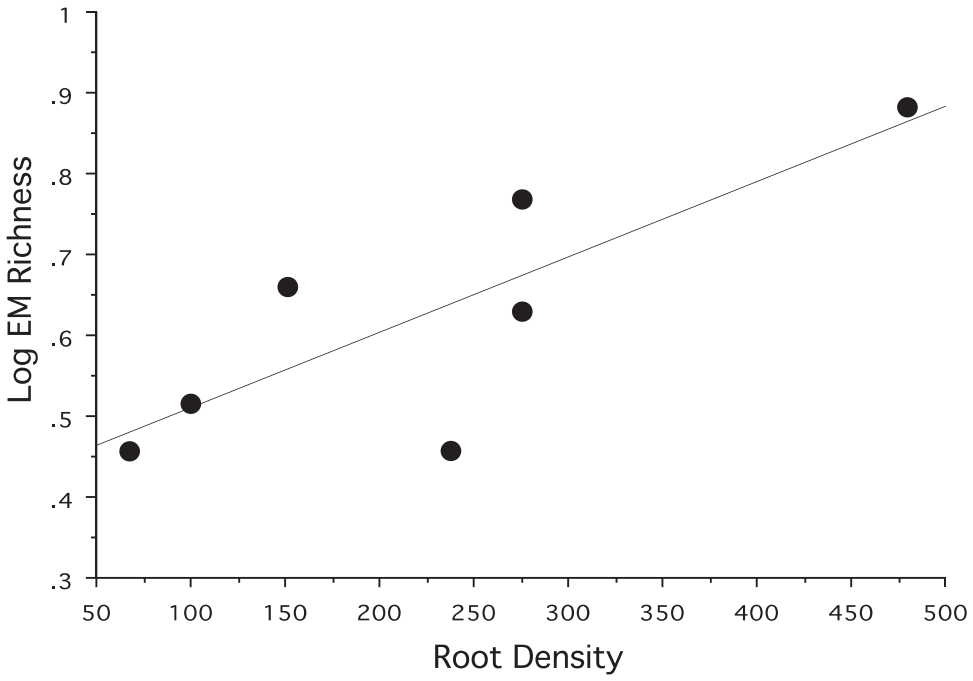

FIG. 2. Regression plot of mean EM type (species) richness (log transformed) against mean root density (R^2 = 0.65, P = 0.03, per site n = 10).

(100% similarity) within each core and between the cores. Two EM types that were tentatively assigned to the *L. luculentus* type based on morphology later were found to be different taxa when sequenced (*Tylospora* sp. and *Hydnotrya* sp.). Among EM morphotypes found in two different cores each, matches to their own types in the other core were at least 98% similar for four of the types. Two distinct single-core EM morphotypes matched at the family level (83–88%) between two soil cores. The eight

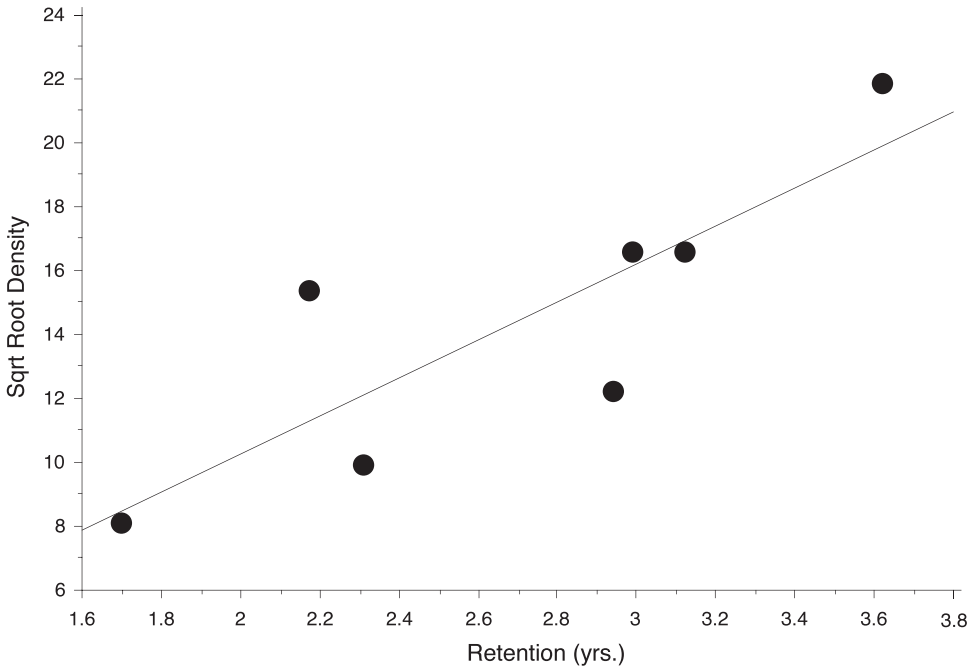

FIG. 3. Regression plot of mean EM root density (square-root transformed) against mean years needle retention (R^2 = 0.70, P = 0.02, per site n = 10).

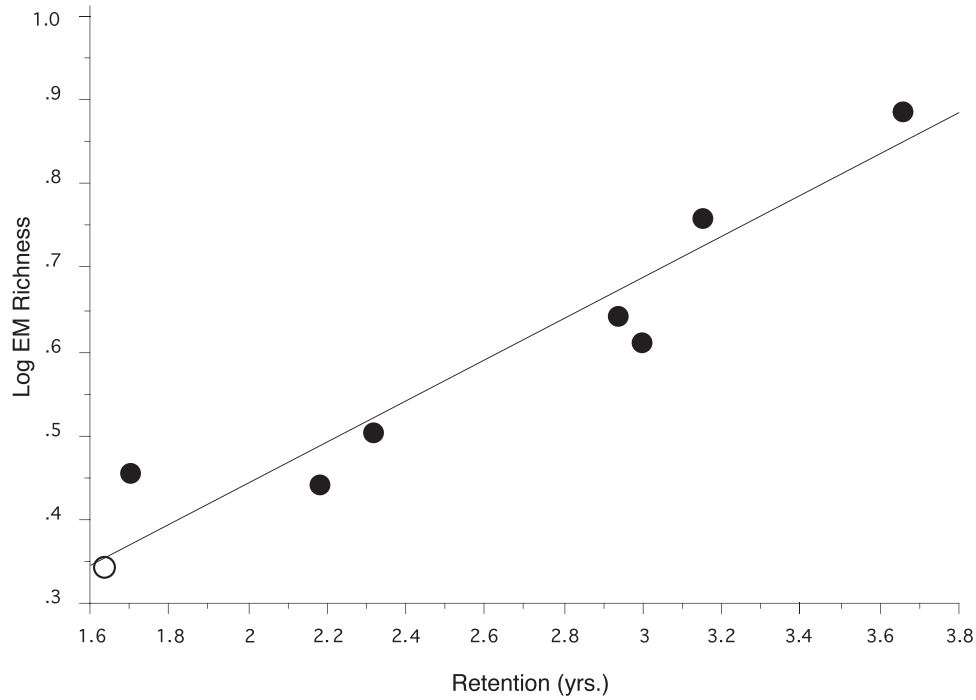

FIG. 4. Regression plot of mean EM type (species) richness (log transformed) against mean years needle retention (R^2 = 0.93, P = 0.0001, per site n = 10). Open circle represents the 2008 resample of the GDH site.

other single-occurrence EM morphotypes were distinct and did not match the other types, even at the family level based on the ITS sequences. Those results (13/15) produced a success rate of 87% at correctly discerning species-level morphotypes.

DISCUSSION

The hypothesis that EM density and species richness are correlated with SNC severity was supported. Across a gradient of SNC disease (as measured by mean years of needle retention), EM root-tip density and EM fungus species richness varied by factors of nearly 10 and 2.5 respectively. That EM fungus species richness was highly correlated with EM root-tip density is not surprising in that the root tips represent available habitat for EM fungi. The reductions in EM characteristics that we measured did not reveal threshold responses (FIGS. 2–4) to the amount of needle loss. Maguire et al. (2011) studied growth reductions in Douglas-fir stands across a gradient of SNC disease and similarly did not find threshold responses to needle loss. Their model predicts a growth loss of approximately 35% on our most severely diseased site (Green Diamond).

The 2007 data demonstrated a strong correlation between EM species richness and Douglas-fir needle retention (R^2 = 0.90). Addition of the 2008 GDH data was made to test the scope of inference of the model over time, especially at severely diseased sites. This allowed for the possibility that the model would show more variance. However, the results strengthened that correlation (FIG. 4) and the R^2 value increased to 0.93, which increases our confidence in the robustness of our model. In severely diseased SNC areas, the low values of EM root density that we observed were less strongly correlated with needle retention than was EM species richness. Even though 2008 root density was twice that observed in 2007 on the Green Diamond Hemlock site (but still low), species richness in 2008 was slightly lower. The 31 EM types (species) obtained from 20 soil cores contrasts with an expected number of 60–65 species found in 20 soil cores (of the same volume) from mature Douglas-fir stands in the Cascade Range not affected by SNC (Luoma et al. 2006 and unpubl data).

Despite much reduced EM fungus species richness on severely diseased SNC sites, we found that the proportion of the Douglas-fir root tips colonized by EM fungi remained at almost 100%. These results agree with the findings of Saikkonen et al. (1999), Cullings et al. (2005), and Kuikka et al. (2003), all of whom noted little response of EM colonization (proportion of root tips colonized) to defoliation. Our results also support the theoretical model proposed by Gange (2007) in which he predicted that mycorrhizal species richness would decline in the face of moderate to severe defoliation.

Our second hypothesis was that some EM fungus species could be more tolerant of a reduced carbon supply and therefore exhibit increased relative abundance in severely diseased SNC sites. However our results did not support this conclusion. Instead, various fungi were able to form EM with the stressed trees, with none consistently dominant across samples in the most severely diseased areas: the majority of distinct EM types (24 of 31) were found in only one core, and an additional four EM types were found in only two cores each. Thus no single EM type was dominant; only the *Cenococcum geophyllum* type was regularly represented in the soil cores (40% constancy, 8/20 cores). *Cenococcum geophyllum* (likely a species complex [Douhan et al. 2007]) is ubiquitous in PNW forests dominated by ectomycorrhizal trees. The next most common EM type was identified from its ITS sequence as *Lactarius luculentus* and was found with only 20% constancy (4/20 soil cores).

Neither of these EM types is considered a candidate for our concept of a stress-tolerant species (sensu Grime 1979) that would dominate a SNC site (i.e. a combination of relatively high constancy across cores and mean root-tip abundance within cores). The *Cenococcum* type has been reported as occurring with 97–100% constancy in soil cores from our region (Kolaczkowski 2005, Luoma et al. 2006) but its presence on severely diseased trees in this study is greatly reduced from that found in healthy Douglas-fir forests.

An alternative to the second hypothesis is that these results are consistent with a ''survival of the survivors'' scenario. We propose that, while the diversity of EM fungi decreases as SNC disease progresses, particular survivors (albeit not dominant) may reflect patterns of reverse establishment (i.e. community disassembly). With this hypothesis, the remaining EM species supporting Douglas-fir growth on these sites are able to persist simply due to variation in tolerance to SNC-caused decline (e.g. reduced carbohydrates) and the ability of EM fungi to (re-)colonize roots of trees affected by SNC. When compared to stands with little or no SNC, aggregate species richness (approximately a 50% reduction; data not shown) was not affected as severely as local, soil-core species richness (70–80% reduction, TABLE I and Luoma et al. 2006). Avis et al. (2008) note that variables such as species richness may demonstrate different responses to treatments in a soil core when contrasted with responses at a stand. The highly patchy soil environment may provide opportunities for particular EM species to persist due to each species' unique adaptive advantages in a given location. For instance, *Cenococcum* was able to maintain a well distributed presence across soil cores in the severely diseased stands but it was not dominant, in terms of constancy or abundance, to the extent that would be expected in healthy stands.

Although particular EM fungi did not become dominant, we did find some distinctive responses of EM fungi to SNC. Defoliation, presumably due to SNC, was strongly associated with a reduction in mycorrhizae of *Cenococcum geophilum* (8/20 cores), *Rhizopogon villosulus* (two cores), *Lactarius rubrilacteus* (zero cores), *Rhizopogon vinicolor* (zero cores), and *R. vesiculosis* (zero cores). These species have been found to be common EM associates of Douglas-fir in other studies (Luoma et al. 2006, Beiler et al. 2010). It is of interest to note that these species are thick-mantled EM types and their reduction in defoliated systems is similar to findings of Markkola et al. (2004) who noted that the most marked decline in thick-mantled mycorrhizae occurred with repeatedly defoliated seedlings. They concluded that carbon limitation strongly influenced EM fungus composition but not percentage of root tips colonized, which was maintained at about 97% (Markkola et al. 2004), similar to our study. Cullings et al. (2005) also noted that a *Cenococcum* sp. was significantly reduced (in sequence-based assessments of soil samples) by artificial defoliation of pine.

In addition to reduced carbon allocation to roots after 100% defoliation, Markkola et al. (2004) found that fungal biomass in the fine roots decreased when 100% defoliation occurred in the year of harvest but not when the defoliation was conducted the previous year. They concluded that current photosynthates are particularly important for EM fungal symbionts. Although not examined in our study, the initial response of EM fungi to reduced photosynthate might be a reduction in reproductive capacity. In an experiment to simulate pine sawfly (*Neodiprion sertifer*) herbivory, Kuikka et al. (2003) removed all 1 y old needles of *Pinus sylvestris* in each of two successive years and found that EM fungi reduced investment in reproduction (sporocarp production) in response to the short-term defoliation. Sporocarp biomass and species richness also were negatively affected by the defoliation (−300% and −100% respectively). They concluded that EM fungus symbionts were able to allocate proportionally less carbon to sexual reproduction due to resource limitation in the host. As with our findings, average mycorrhizal colonization percentage was high (93.5%) and did not differ between the defoliated and control treatments (Kuikka et al. 2003). A finding of a meta analysis by Barto and Rillig (2010) was that defoliation had little or no effect on EM root colonization percentage (although root density was not examined).

Carbon limitation and forest succession.—Picea sitchensis (Sitka spruce) is a long-lived but seral dominant

that generally outperforms Douglas-fir in the *Picea sitchensis* zone (Franklin and Dyrness 1973). The zone is typified by a wet and mild climate with minimal summer drought that is further ameliorated by frequent fog and low clouds. *Tsuga herterophylla* and *Thuja plicata* also are important tree species within this zone (Franklin and Dyrness 1973). The SNC epidemic area has substantial overlaps with the area covered by the *Picea sitchensis* zone (Stone et al. 2008, FIG. 1). Growth analyses of competing tree species by Kunstler et al. (2012) have identified leaf mass per unit area as an important functional trait related to species' niche similarity and competitive ability. The chronic infection of Douglas-fir needles with high *P. gaeumannii* has reduced growth of young Douglas-fir trees in the Sitka spruce zone, thereby providing a competitive advantage to spruce and hemlock during forest succession (Stone et al. 2008). The distribution of Douglas-fir in lower elevations of the western Oregon Coast Range was sporadic before initiation of commercial logging and conversion of large areas to plantation forestry. This led Stone et al. (2008) to conclude that the Sitka spruce zone exists in part as a result of Douglas-fir growing poorly due to Swiss needle cast disease. Stone et al. (2008) also note that winter temperature increases predicted for the Pacific Northwest correlate with an increased severity and distribution of SNC as a result of climate change. It appears that anthropogenic disturbance has interacted with regional climate change to perturb the health of forest ecosystems in northern coastal Oregon.

The hypothesis that net primary productivity is an important driver of competitive interactions between Sitka spruce and Douglas-fir can be applied to the belowground ecosystem as well. Direct measurements of carbohydrates in the EM of SNC affected Douglas-fir have not been made but should be, especially considering that Saffell (2013) found that as SNC symptoms increased, stem carbohydrate storage decreased linearly. To us, her results suggest that such a reduction would have a downstream effect on carbohydrates available to the roots. This could identify the specific mechanism involved in the decline of EM fungus diversity.

Our results and those of others suggest that reduced availability of carbohydrates to the roots of Douglas-fir could alter the species richness and abundance of the EM fungus community and reduce the presence of Douglas-fir host-specific EM fungus species. Molina et al. (1992) point out the ecological importance of EM host-specificity to plants' abilities to adapt or migrate in response to rapid climate change. We suggest that significant consequences for SNC affected forests include a serious potential for continuing decline in EM fungus species richness, even outside the Sitka spruce zone.

ACKNOWLEDGMENTS

The assistance of Dr Richard O'Hanlon, Emily Wittkop and Levi Davis with field and laboratory work is greatly appreciated. Financial support was provided by the Swiss Needle Cast Cooperative (http://sncc.forestry.oregonstate.edu). Our thanks to its members, past and present, for their support. Special thanks to Doug Mainwaring for providing much logistical support and important stand data from the SNC Co-op database. Comments of the anonymous reviewers and Dr Pete Avis are greatly appreciated.

LITERATURE CITED

Altschul SF, Madden TL, Schäffer AA, Zhang J, Zhang Z, Miller W, Lipman DJ. 1997. Gapped BLAST and PSI-BLAST: a new generation of protein database search programs. Nucleic Acids Res 25:3389–3402, doi:10.1093/nar/25.17.3389

Amaranthus MP, Trappe JM, Bednar L, Arthur D. 1994. Hypogeous fungal production in mature Douglas-fir forest fragments and surrounding plantations and its relation to coarse woody debris and animal mycophagy. Can J For Res 25:2157–2165, doi:10.1139/x94-278

Avis PG, McLaughlin DJ, Dentinger BC, Reich PB. 2003. Long-term increase in nitrogen supply alters above- and belowground ectomycorrhizal communities and increases the dominance of *Russula* spp. in a temperate oak savannah. New Phytol 160:239–253, doi:10.1046/j.1469-8137.2003.00865.x

———, Mueller GM, Lussenhop J. 2008. Ectomycorrhizal fungal communities in two North American oak forests respond to nitrogen addition. New Phytol 179:472–483, doi:10.1111/j.1469-8137.2008.02491.x

Barto EK, Rillig MC. 2010. Does herbivory really suppress mycorrhiza? A meta-analysis. J Ecol 98:745–753, doi:10.1111/j.1365-2745.2010.01658.x

Beiler KJ, Durall DM, Simard SW, Maxwell SA, Kretzer AM. 2010. Architecture of the wood-wide web: *Rhizopogon* spp. genets link multiple Douglas-fir cohorts. New Phytol 185:543–553, doi:10.1111/j.1469-8137.2009.03069.x

Boyce JS. 1940. A needle-cast of Douglas-fir associated with *Adelopus gaeumannii*. Phytopathology 30:649–659.

Cromack K, Sollins P, Graustein WC, Speidel K, Todd AW, Spycher G, Li CY, Todd RL. 1979. Calcium oxalate accumulation and soil weathering in mats of the hypogeous fungus *Hysterangium crassum*. Soil Biol Biochem 11:463–468, doi:10.1016/0038-0717(79)90003-8

Cullings K, Raleigh C, New MH, Henson J. 2005. Effects of artificial defoliation of pines on the structure and physiology of the soil fungal community of a mixed pine-spruce forest. Appl Environ Microb 71:1996–2000, doi:10.1128/AEM.71.4.1996-2000.2005

Douhan GW, Huryn KL, Douhan LI. 2007. Significant diversity and potential problems associated with inferring population structure within the *Cenococcum geophilum* species complex. Mycologia 99:812–819, doi:10.3852/mycologia.99.6.812

Eberhardt U, Walter L, Kottke I. 1999. Molecular and morphological discrimination between *Tylospora fibrillosa* and *Tylospora asterophora* mycorrhizae. Can J Bot 77:11–21.

Eberhart JL, Luoma DL, Amaranthus MP. 1996. Response of ectomycorrhizal fungi to forest management treatments—a new method for quantifying morphotypes. In: Azcon-Aquilar C, Barea JM, eds. Mycorrhizas in integrated systems: from genes to plant development. Luxembourg: Office for Official Publications of the European Communities. p 96–99.

Fogel R, Hunt G. 1979. Fungal and arboreal biomass in a western Oregon Douglas-fir ecosystem: distribution patterns and turnover. Can J For Res 9:245–256, doi:10.1139/x79-041

Franklin JF, Dyrness CT. 1973. Natural vegetation of Oregon and Washington. USDA Forest Service, Gen. Tech. Rep. PNW-8. Washington: US Government Printing Office. 417 p.

Gange AC. 2007. Insect-mycorrhizal interactions: patterns, processes and consequences. In: Ohgushi T, Craig TP, Price PW, eds. Ecological communities: plant mediation in indirect interaction webs. Cambridge, UK: Cambridge Univ. Press. p 124–144.

Gardes M, Bruns TD. 1993. ITS primers with enhanced specificity for basidiomycetes—application to the identification of mycorrhizae and rusts. Mol Ecol 2:113–118, doi:10.1111/j.1365-294X.1993.tb00005.x

Gaümann E. 1930. Über eine neue Krankheit der Douglasien. Schweiz Z Forstw 81:63–67.

Goodman DM, Durall DM, Trofymow JA, Berch SM, eds. 1996. A manual of concise descriptions of North American ectomycorrhizae. Victoria, Canada: Mycologue Publications and Canadian Forest Service.

Grime JP. 1979. Plant strategies and vegetation processes. New York: John Wiley & Sons. 222 p.

Hansen EM, Stone JK, Capitano BR, Rosso P, Sutton W, Kanaskie A, McWilliams MG. 2000. Incidence and impact of Swiss needle cast in forest plantations of Douglas-fir in coastal Oregon. Plant Dis 84:773–779, doi:10.1094/PDIS.2000.84.7.773

Harvey AE, Larsen MJ, Jurgensen MF. 1980. Partial cut harvesting and ectomycorrhizae: early effects in Douglas-fir-larch forests of western Montana. Can J For Res 10:438–435.

———, Page-Dumroese DS, Jurgensen MF, Graham RT, Tonn DR. 1997. Site preparation alters soil distribution of roots and ectomycorrhizae on out-planted western white pine and Douglas-fir. Plant Soil 188:107–117, doi:10.1023/A:1004299928220

Ingleby K, Mason PA, Last FT, Fleming LV. 1990. Identification of ectomycorrhizas. Institute of Terrestrial Ecology, Res. Pub. No. 5. London: HMSO. 112 p.

Kanaskie A, McWilliams M. 2011. Swiss needle cast aerial survey, 2011. In: Shaw D, ed. Swiss Needle Cast Cooperative Annual Report 2011. Corvallis: College of Forestry, Oregon State Univ. p 4–8.

Kolaczkowski O. 2005. Effects of spatially dispersed green-tree retention on ectomycorrhiza diversity (master's thesis). Corvallis: Department of Forest Science, Oregon State Univ. 62 p.

Kuikka K, Härmä E, Markkola A, Rautio P, Roitto M, Saikkonen K, Ahonen-Jonnarth U, Finlay R, Tuomi J. 2003. Severe defoliation of Scots pine reduces reproductive investment by ectomycorrhizal symbionts. Ecology 84:2051–2061, doi:10.1890/02-0359

Kunstler G, Lavergne S, Courbaud B, Thuiller W, Vieilledent G, Zimmermann NE, Kattge J, Coomes DA. 2012. Competitive interactions between forest trees are driven by species' trait hierarchy, not phylogenetic or functional similarity: implications for forest community assembly. Ecol Lett 15:831–840, doi:10.1111/j.1461-0248.2012.01803.x

Lilleskov EA, Fahey TJ, Horton TR, Lovett GM. 2002. Belowground ectomycorrhizal fungal community change over a nitrogen deposition gradient in Alaska. Ecology 83:104–115, doi:10.1890/0012-9658(2002)083[0104:BEFCCO]2.0.CO;2

Luoma DL, Eberhart JL. 2006. Are differences in the ectomycorrhiza community correlated with Swiss needle cast severity? In: Shaw D, ed. Swiss needle cast cooperative annual report 2006. Corvallis: College of Forestry, Oregon State Univ. p 60–64.

———, ———, Molina R, Amaranthus MP. 2004. Response of ectomycorrhizal fungus sporocarp production to varying levels and patterns of green-tree retention. Forest Ecol Manage 202:337–354, doi:10.1016/j.foreco.2004.07.041

———, Stockdale CA, Molina R, Eberhart JL. 2006. The spatial influence of Douglas-fir retention trees on ectomycorrhiza diversity. Can J For Res 36:2561–2573, doi:10.1139/x06-143

Maguire DA, Kanaskie A, Voelker W, Johnson R, Johnson G. 2002. Growth of young Douglas-fir plantations across a gradient in Swiss needle cast severity. West J Appl For 17:86–95.

———, Mainwaring DB, Kanaskie A. 2011. Ten-year growth and mortality in young Douglas-fir stands experiencing a range in Swiss needle cast severity. Can J For Res 41:2064–2076, doi:10.1139/x11-114

Mainwaring D, Maguire D, de Ross J. 2007. Douglas-fir foliage age class dynamics and nutrient flux. In: Shaw D, ed. Swiss needle cast cooperative annual report 2007. Corvallis: College of Forestry, Oregon State Univ. p 35–40.

Manter DK, Bond BJ, Kavanagh KL, Rosso PH, Filip GM. 2000. Pseudothecia of Swiss needle cast fungus, *Phaeocryptopus gaeumannii*, physically block stomata of Douglas fir, reducing CO_2 assimilation. New Phytol 148:481–491, doi:10.1046/j.1469-8137.2000.00779.x

Markkola A, Kuikka K, Rautio P, Härmä E, Roitto M, Tuomi J. 2004. Defoliation increases carbon limitation in ectomycorrhizal symbiosis of *Betula pubescens*. Oecologia 140:234–240, doi:10.1007/s00442-004-1587-2

Molina R, Horton TR, Trappe JM, Marcot BG. 2011. Addressing uncertainty: how to conserve and manage rare or little-known fungi. Fungal Ecol4, 134–146, doi:10.1016/j.funeco.2010.06.003

———, Massicotte H, Trappe JM. 1992. Specificity phenomena in mycorrhizal symbiosis: community-ecological

consequences and practical implications. In: Rourledge AMF, ed. Mycorrhizal functioning, an integrated plant-fungal process. New York: Chapman & Hall. p 357–423.

Mulvey RL, Shaw DC, Maguire DA. 2013. Fertilization impacts on Swiss needle cast disease severity in western Oregon. Forest Ecol Manage 287:147–158, doi:10.1016/j.foreco.2012.08.050

Norton JM, Smith JL, Firestone MK. 1990. Carbon flow in the rhizosphere of Ponderosa pine seedlings. Soil Biol Biochem 22:449–455, doi:10.1016/0038-0717(90)90177-2

Sabin TE, Stafford SG. 1990. Assessing the need for transformation of response variables. Publication 20. Corvallis: Forest Research Laboratory, Oregon State Univ. 31 p.

Saffell B. 2013. Impacts of Swiss needle cast on Douglas-fir tree-ring stable isotopes and tree carbohydrate reserves [master's thesis]. Corvallis: Department of Ecosystems and Society, Oregon State Univ. 102 p.

Saikkonen K, Ahonen-Jonnarth U, Markkola AM, Helander M, Tuomi J, Roitto M, Ranta H. 1999. Defoliation and mycorrhizal symbiosis: a functional balance between carbon sources and belowground sinks. Ecol Lett 2:19–26, doi:10.1046/j.1461-0248.1999.21042.x

SAS Institute . 1999. Statview Software 5.0.1. Cary, North Carolina: SAS Institute.

Smith SE, Read DJ. 2008. Mycorrhizal symbiosis. 3rd ed. London: Academic Press. 804 p.

Stone J, Chastagner G, Kanaskie A. 2005. Control of Swiss needle cast in forest plantations by aerially applied elemental sulfur fungicide. In: Shaw D, ed. Swiss needle cast cooperative annual report 2005. Corvallis: College of Forestry, Oregon State Univ. p 12–17.

Stone JK, Coop LB, Manter DK. 2008. Predicting effects of climate change on Swiss needle cast disease severity in Pacific Northwest forests. Can J Plant Pathol 30:169–176, doi:10.1080/07060661.2008.10540533

Trappe JM. 1977. Selection of fungi for ectomycorrhizal inoculation in nurseries. Ann Rev Phytopathol 15:203–222, doi:10.1146/annurev.py.15.090177.001223

———, Strand RF. 1969. Mycorrhizal deficiency in a Douglas-fir region nursery. Forest Sci 15:381–389.

Vogt KA, Grier CC, Meier CE, Edmonds RL. 1982. Mycorrhizal role in net primary production and nutrient cycling in *Abies amabilis* ecosystems in western Washington. Ecology 63:370–380, doi:10.2307/1938955

Waters AJ, McKelvey KS, Zabel CJ, Oliver WW. 1994. The effects of thinning and broadcast burning on sporocarp production of hypogeous fungi. Can J For Res 24:1516–1522, doi:10.1139/x94-196

Weiskittel AR, Maguire DA. 2007. Response of Douglas-fir leaf area index and litterfall dynamics to Swiss needle cast in north coastal Oregon, USA. Ann For Sci 64:121–132, doi:10.1051/forest:2006096

White TJ, Bruns TD, Lee S, Taylor J. 1990. Amplification and direct sequencing of fungal ribosomal RNA genes for phylogenetics. In: Innis MA, et al. eds. PCR protocols. London: Academic Press. p 315–322.

Wright E, Tarrant RF. 1958. Occurrence of mycorrhizae after logging and slash burning in the Douglas-fir forest type. Research Note PNW-160. Portland: USDA Forest Service, Pac. NW For. Range Exp. Sta. 7 p.

Tree Physiology Advance Access published February 18, 2014

Tree Physiology 00, 1–11
doi:10.1093/treephys/tpu002

Research paper

Seasonal carbohydrate dynamics and growth in Douglas-fir trees experiencing chronic, fungal-mediated reduction in functional leaf area

Brandy J. Saffell[1], Frederick C. Meinzer[2,5], David R. Woodruff[2], David C. Shaw[3], Steven L. Voelker[4], Barbara Lachenbruch[1] and Kristen Falk[3]

[1]Department of Forest Ecosystems and Society, Oregon State University, Corvallis, OR 97330, USA; [2]USDA Forest Service, Pacific Northwest Research Station, 3200 SW Jefferson Way, Corvallis, OR 97331, USA; [3]Department of Forest Engineering, Resources, and Management, Oregon State University, Corvallis, OR 97330, USA; [4]Department of Biology, Southern Oregon University, Ashland, OR 97520, USA; [5]Corresponding author (Rick.meinzer@oregonstate.edu; fmeinzer@fs.fed.us)

Received August 13, 2013; accepted December 27, 2013; handling Editor Michael Ryan

Stored non-structural carbohydrates (NSCs) could play an important role in tree survival in the face of a changing climate and associated stress-related mortality. We explored the effects of the stomata-blocking and defoliating fungal disease called Swiss needle cast on Douglas-fir carbohydrate reserves and growth to evaluate the extent to which NSCs can be mobilized under natural conditions of low water stress and restricted carbon supply in relation to potential demands for growth. We analyzed the concentrations of starch, sucrose, glucose and fructose in foliage, twig wood and trunk sapwood of 15 co-occurring Douglas-fir trees expressing a gradient of Swiss needle cast symptom severity quantified as previous-year functional foliage mass. Growth (mean basal area increment, BAI) decreased by ~80% and trunk NSC concentration decreased by 60% with decreasing functional foliage mass. The ratio of relative changes in NSC concentration and BAI, an index of the relative priority of storage versus growth, more than doubled with increasing disease severity. In contrast, twig and foliage NSC concentrations remained nearly constant with decreasing functional foliage mass. These results suggest that under disease-induced reductions in carbon supply, Douglas-fir trees retain NSCs (either actively or due to sequestration) at the expense of trunk radial growth. The crown retains the highest concentrations of NSC, presumably to maintain foliage growth and shoot extension in the spring, partially compensating for rapid foliage loss in the summer and fall.

Keywords: growth limitation, non-structural carbohydrates, *Phaeocryptopus gaeumannii*, *Pseudotsuga menziesii*, Swiss needle cast.

Introduction

Recent trends in drought-related tree mortality on a global scale have led to many questions regarding the role of non-structural carbohydrate (NSC) content as an indicator of overall tree vigor and demand for photosynthate (Sala et al. 2010, McDowell 2011, Ryan 2011, Johnson et al. 2012, Sala et al. 2012, Wiley and Helliker 2012). A first step toward resolving the uncertainty surrounding these issues could be achieved by developing a greater understanding of the different functions that may be performed by carbohydrate reserves stored within trees.

Traditionally, NSC accumulation has been viewed as a purely passive process signifying that the supply of photosynthate exceeds the demand from carbon sinks such as growth and respiratory metabolism. We are now aware that tree carbohydrate storage is multi-faceted, exhibiting patterns that suggest storage is partly passive and partly active (Chapin et al. 1990, Hoch et al. 2003, Körner 2003, Würth et al. 2005). Active

storage is defined as a prioritization of carbon allocation to storage over other carbon-dependent processes when resources are limited (Sala et al. 2012). Research by Bustan et al. (2011) has suggested that there is an active component to storage, such that in years of heavy fruit production the NSC content was not reduced in olive trees. In addition, Silpi et al. (2007) found that tapping rubber trees for carbon-rich latex actually caused NSC concentrations to increase at the apparent expense of growth.

Large carbohydrate reserves have been reported in mature trees across different climate types (Hoch et al. 2003, Würth et al. 2005), as well as different ecosystems and seasons (Hoch et al. 2002, Körner 2003), suggesting that trees allocate a substantial amount of assimilated carbon to storage (Hoch et al. 2003). Furthermore, it has been observed that trees have higher than average NSC concentrations and reduced growth during prolonged periods of mild-to-moderate stress such as long-term water deficit (Galvez et al. 2011, Muller et al. 2011, Woodruff and Meinzer 2011*a*) and low temperatures (Hoch and Körner 2009). Based on current knowledge, there are a few explanations for why trees do not mobilize their carbohydrate reserves for growth (Sala et al. 2012). First, during periods of environmental stress, such as water deficit, reduced cell turgor in expanding tissues would result in a constraint on sink strength resulting in reduced growth (Woodruff and Meinzer 2011*b*, Nikinmaa et al. 2013). Because growth is more sensitive to water deficit than photosynthesis is, photosynthesis would continue despite sharply reduced allocation to growth, resulting in an accumulation of NSCs (Muller et al. 2011). Second, carbohydrate reserves may become sequestered and no longer available for export due to compartmentalization that restricts their propensity to be loaded into the phloem (Quick et al. 1992) or impedes the access of enzymes to starch (Srichuwong and Jane 2007). Third, there may be an evolutionary advantage for trees to actively maintain a minimum level of carbohydrate reserves to support metabolism or to provide solutes for maintaining cell turgor and vascular integrity in an often stochastic and unpredictable environment, where water availability and growing conditions are not always optimal for plant functioning (Sala et al. 2012, Wiley and Helliker 2012).

Under conditions of water stress, it is difficult to determine whether the build up of NSCs is due to passive accumulation resulting from reduced sink demands, sequestration or active storage. To better understand the role of carbon storage in tree physiology, we must determine the extent to which storage is prioritized over growth in the absence of potentially confounding factors such as those resulting from water stress. The Douglas-fir (*Pseudotsuga menziessi* (Mirb.) Franco) disease called Swiss needle cast provides a unique natural experiment to examine the relative priorities of growth versus carbon storage in the absence of drought-related reductions in carbon assimilation, and water and phloem transport capacity. The disease is most prominent along the Oregon coast, a region with high rainfall and a maritime climate with a low risk of drought. Its prevalence and severity decrease sharply with increasing distance from the coast along a gradient of decreasing humidity and precipitation (http://sncc.forestry.oregonstate.edu/survey-maps). The pathogen that causes Swiss needle cast is an ascomycete (*Phaeocryptopus gaeumannii* (T. Rohde)) that colonizes Douglas-fir foliage. The spores are released in May and June, near the time of bud break for Douglas-fir, when they land and germinate on current-year needles (Stone et al. 2008). After about a year of incubation (in the most extreme cases of disease) during which the mycelia colonize the surface and inside of the needle, the mycelia produce fruiting bodies (pseudothecia) that block stomata. This blockage causes a significant decrease in stomatal conductance and photosynthesis (Manter et al. 2000). Once ~25–30% of stomata are blocked, the needle reaches a negative carbon balance, becomes chlorotic and abscises from the tree (Manter et al. 2000). There is a strong relationship between needle loss and the amount of pseudothecia present on the foliage of trees with Swiss needle cast (Manter et al. 2003), as well as between needle loss and reduced growth in diseased trees (Maguire et al. 2002, 2011). Growth can be reduced by as much as 20–50% in diseased stands (Maguire et al. 2002, Johnson et al. 2003, 2005). The fungus does not release any toxins, or cause any sort of known structural damage to the needle besides limiting the diffusion of carbon dioxide through the stomata and inside the needle. The disease has not yet been shown to result in tree mortality, and affected trees live for decades under a chronic reduction in carbon supply (Maguire et al. 2011).

The impact of Swiss needle cast on tree carbohydrate reserves is unknown, but if NSC accumulation in Douglas-fir has an active component, then this competing sink for photosynthate would exacerbate the impact of disease on growth and other carbon-dependent processes of lower or shared priority with storage. Swiss needle cast affords the opportunity to test for the relationship between growth, carbohydrate storage and disease symptoms because the disease involves a substantial reduction in carbon assimilation under conditions of low water stress at sites where the disease is prevalent. If NSC reserves remain largely undepleted under severe disease symptom severity, this result would provide evidence for prioritization of storage over growth, or that NSC has been sequestered. Additionally, if Swiss needle cast causes a greater relative decline in growth compared with NSC reserves, this would also provide evidence for prioritization of storage or storage sequestration as carbon assimilation is reduced. Finally, if NSC reserves become substantially depleted, this provides evidence for the ability of stored NSC to be mobilized when needed to maintain the physiological functioning and survival of trees.

The goals of this research were to: (i) determine how Swiss needle cast influences the partitioning of assimilated carbon between growth and carbohydrate reserves and to determine whether differences in disease severity influence the relative partitioning of carbon between these two sinks; (ii) identify any seasonal differences in the impact of the disease on the partitioning of carbon between growth and reserves; and (iii) establish the extent to which carbohydrate reserves are mobilized under natural conditions of high demand for carbon and low water stress. Based on previous research, we hypothesized that relative reductions in the growth of diseased trees would be greater than relative reductions in NSC reserves, and that seasonal fluctuations in NSC would be smallest in the most heavily diseased trees.

Materials and methods

Field site and sampling

A single Douglas-fir stand containing trees with a broad range of Swiss needle cast symptom expression was selected from an Oregon Department of Forestry unit (named Prairie Hill, 45.5°N 123.8°W) located on the Oregon coast near Tillamook at ~134 m above sea level. The region has a Pacific maritime climate with most of the mean annual precipitation of ~2800 mm falling between October and May. The mean annual temperature is ~10.1 °C, ranging from a mean of 5.7 °C in January to 15.3 °C in July. During the summer period from June to September, the mean precipitation is ~278 mm, the mean relative humidity hovers around 80% and the mean vapor pressure deficit generally remains <0.5 kPa (PRISM Climate Group, http://prism.oregonstate.edu, data summarized from 1980 to 2011). Previous studies along a coastal to interior transect have shown that Douglas-fir and other tree species growing in coastal sites similar to the one we selected do not experience significant variation in their predawn water potential during the growing season (Runyon et al. 1994). The development of Swiss needle cast is favored by conditions that include high humidity and precipitation and relatively mild temperatures (Rosso and Hansen 2003, Latta et al. 2009, Zhao et al. 2011). Although *P. gaeumannii* spores have been detected in more interior stands that experience substantial summer drought, Douglas-fir trees in these stands do not show Swiss needle cast symptoms. Thus, selecting different stands along a climatic gradient to obtain a range of disease symptom expressions would have inevitably introduced several potentially confounding environmental variables into our study. Instead, we regressed tree response variables against a two-component index of symptom severity for the co-occurring trees at our study site (see below).

The stand was initially planted in 1990, with trees successively inter-planted through 1997. Trees were selected that ranged in planting date from 1990 to 1995, so the largest age difference between trees would be 5 years. The stand resides in a region of the Oregon coast where disease had been present for ~20 years before our study took place in 2012, so it is likely that the trees exhibited disease symptoms since planting. We non-randomly selected 15 trees (Table 1), with five trees roughly fitting into each of the three categories of overall needle retention (0–1.0, >1.0–2.0 and >2.0 years). Needle retention for each tree was estimated using a standard protocol in the field where we visually divided the crown into thirds and averaged the most common needle retention among branches in each third, and finally averaged the mean needle retentions of each third (e.g., Maguire et al. 2002).

In June of 2012, we collected two 5 mm cores to pith from opposite sides of each tree with an increment borer for annual growth measurement. We marked the sapwood boundary on each core to determine the average sapwood width. Cores

Table 1. Individual characteristics of the sampled trees in ascending order by basal area increment (BAI).

Tree ID	Mean BAI (cm^2)	DBH (cm)	Height (m)	Age (years)	Pseudothecia count[1] (%)	Mean foliage mass[1] (g)
7	3.4 (1.2)	9.1	14.0	19	36 (9)	0.05 (0.06)
1	4.8 (1.3)	10.2	17.9	20	25 (2)	0.23 (0.09)
3	4.9 (3.0)	9.9	20.1	15	27 (5)	0.25 (0.02)
5	5.0 (1.8)	11.5	14.5	20	22 (3)	0.24 (0.03)
8	5.7 (4.1)	10.5	8.7	17	17 (6)	0.19 (0.02)
13	6.7 (3.4)	12.1	15.9	14	29 (3)	0.36 (0.14)
14	6.8 (2.9)	12.7	14.7	18	23 (2)	0.18 (0.12)
10	7.6 (1.6)	14.0	15.4	20	35 (2)	0.06 (0.02)
9	9.1 (4.7)	13.5	11.0	16	22 (5)	0.36 (0.04)
2	14.1 (2.2)	18.5	23.1	20	5 (1)	0.36 (0.06)
15	16.8 (4.5)	21.5	20.6	19	22 (3)	0.66 (0.10)
4	16.8 (1.9)	18.3	23.0	17	16 (3)	0.34 (0.04)
12	17.5 (2.9)	19.1	24.1	17	13 (3)	0.50 (0.09)
11	23.3 (9.1)	21.2	18.4	21	5 (2)	0.62 (0.17)
6	26.3 (5.4)	25.8	17.9	20	9 (1)	0.36 (0.05)

Parentheses contain one standard deviation from the mean. DBH, diameter at breast height.
[1]One-year-old foliage.

were stored in paper straws for transport to the laboratory. One-year-old foliage was collected from three branches located in the sun-exposed lower-mid crown of each tree to assess the presence and abundance of pseudothecia on the needles (described below).

For NSC analyses, trunk sapwood tissue was sampled with an increment borer to a depth of 2 cm at 1.3 m height on opposite sides of each tree. Foliage and twig wood were sampled from two branches located in the sun-exposed lower-mid crown of each tree. The branches were divided immediately into segments representing growth from Years 2011, 2010 and 2009 (i.e., 1-, 2- and 3-year-old tissues). Foliage was removed from the twigs, and the total foliage mass (at field moisture content) was recorded for each segment from each branch and averaged for each branch, and then each tree (mean foliage mass, g). All samples (two trunk samples, and foliage and twig samples from 2011, 2010 and 2009) were immediately placed into sealed plastic bags and onto dry ice in a cooler. Sampling was always conducted between late morning and early afternoon. We did not attempt to sample roots because it would not have been possible to associate a given sample with a specific individual without conducting extensive, destructive excavations. In view of our previous observations showing substantial seasonal variation in NSC content in Douglas-fir trees (Woodruff and Meinzer 2011*a*), sampling took place three times over a seasonal cycle in 2012: around bud break (June 18), mid-summer (July 31) and late summer (September 4).

Disease severity assessment

The presence and abundance of fungus on 1-year-old foliage was determined by visual estimates of pseudothecia emerging from stomata using standard techniques (e.g., Manter et al. 2005). Estimates of the percentage of stomata that were occluded with pseudothecia (i.e., pseudothecia counts) for each of the three branches collected in the field were calculated by averaging pseudothecia counts from three positions of 10 randomly selected needles per branch. At each position, one on each longitudinal third of the needle, pseudothecia counts were conducted by selecting a region within each position with a random number table and visually counting the number of pseudothecia emerging from 50 consecutive stomata above the needle midrib and 50 consecutive stomata below the needle midrib (100 stomata total in each position). The percentage of pseudothecia-occluded stomata of each needle was averaged across 10 needles per branch, and averaged again across the three branches per tree to calculate the tree pseudothecia count.

To account for the amount of functional 1-year-old foliage remaining on a tree relative to its pseudothecia count, we created an index for disease symptoms by multiplying the percentage of non-occluded stomata (100 – % occluded stomata) by the average 1-year-old foliage dry mass per growth increment for each tree (i.e., functional foliage mass, g). We intentionally used the functional foliage mass as a measure of disease severity instead of the needle retention technique (described above) due to its advantages of being an integrated measure of two symptoms (pseudothecia abundance and foliage mass) and therefore more objective and precise in quantifying disease severity.

Chemical analyses

Trunk sapwood, twig wood and foliage samples were stored in a –20 °C freezer before being microwaved for 90 s to stop all enzymatic activity, oven dried for 72 h at 65 °C and ground to a fine powder with a ball mill. The dried and ground tissue samples were analyzed for the content of four components: starch, sucrose, glucose and fructose together, and total NSC following the procedure described by Woodruff and Meinzer (2011*a*). Deionized water was added to the samples, which were then heated in covered vials over steam for 90 min to extract NSC. After enzymatic conversion of glucose and fructose to gluconate-6-phosphate, the concentration of free glucose was determined photometrically on a 96-well microplate photometer (Multiscan FC, Thermo Scientific, Waltham, MA, USA). Samples were analyzed before and after enzymatic treatments of sucrose digestion by invertase (45 min reaction) and starch and sucrose digestion by amyloglucosidase (15-h reaction). Photometric analysis was based on the absorbance of samples at 340 nm in the solution with reference to the absorbance of a glucose reference solution. The combination of glucose and fructose content was determined from the photometric analysis of sample solutions without invertase or amyloglucosidase enzymatic treatment. Sucrose content of the samples was determined by subtracting the combination of glucose and fructose content from the glucose concentration of sample solutions following invertase enzyme treatment. Total NSC was determined from the amyloglucosidase reaction mixture, which contained the original concentrations of free glucose and fructose, plus glucose and fructose liberated from starch and sucrose. Inclusion of sucrose standards in each set of samples subjected to amyloglucosidase treatment indicated that amyloglucosidase hydrolyzed sucrose as well as starch. Starch content of the samples was determined by subtracting the glucose content of the sample solution following invertase enzyme treatment from the total NSC content. All NSC, starch, sucrose, and glucose and fructose values for each tissue of each tree are averages of the two sampled branches collected in the field at each sampling date and are presented in units of percentage of dry weight (% dry weight).

Growth analyses

Two increment cores per tree were collected for growth analyses. These were air-dried, glued to wooden mounts with the transverse face upward and sanded with progressively finer

sandpaper until annual rings were distinguishable. We measured ring widths to a precision of 0.01 mm using a stereo microscope interfaced with a Velmex rotating measuring table and Measure J2X® software. We used the cross-dating program COFECHA (Holmes 1983, Grissino-Mayer 2001) to identify possible missing and false rings. The ring widths from each tree were averaged for each year and basal area increment (BAI) was calculated assuming circularity of consecutive growth increments. We used the average BAI from 2000 to 2011 for each tree to represent tree growth (mean BAI, cm^2).

Statistical analyses

To determine the effect of disease symptom severity on the relative priority of storage versus growth, we created an index by taking the ratio of the relative values of NSC to those of BAI for each tree (NSC/BAI; values were normalized with respect to their highest values). Because the NSC/BAI metric combines different units of measurement for NSC and BAI, we normalized the two measures to better demonstrate changes in the relative priorities of storage and growth as symptom severity varied among trees. All analyses exploring the relationship between disease explanatory variables (i.e., pseudothecia count and functional foliage mass) and the response variables of interest (i.e., BAI, foliage mass, total NSC, starch, sucrose, glucose and fructose, NSC/BAI) in the trunk, twigs and foliage were made using simple linear regression for all 15 trees, unless otherwise noted. Assumptions of simple linear regression were checked by plotting residuals of the response variable versus fitted values to assess the equality of variance and were also plotted within a normal probability plot to assess normality. Paired *t*-tests were performed to test for the differences in foliage mass, total NSC, starch, sucrose, and glucose and fructose from June to September for all 15 trees. Assumptions of the paired *t*-tests were checked by evaluating histograms of the distribution of the sample response variables.

Results

Disease severity assessment

The mean 1-year-old foliage dry mass per growth increment ranged from 0.05 to 0.66 g, and the pseudothecia count ranged from 5 to 36% stomata occluded in the 15 trees studied (Table 1). The maximum observed stomatal occlusion was comparable to the estimated threshold at which needle abscission would likely occur (Manter et al. 2000; Table 1). The mean mass of 1-year-old foliage (averaged across the three sampling dates) was ~0.26 g, whereas the mean growing season mass of 3-year-old foliage was only ~0.04 g (Figure 1). The mean difference in foliage mass between the two age classes was ~0.23 g (95% CI [0.16, 0.30]). There was no relationship between the functional foliage mass and the mean foliage mass per increment of new foliage (2012 cohort) at the end of the 2012 growing season (September sampling).

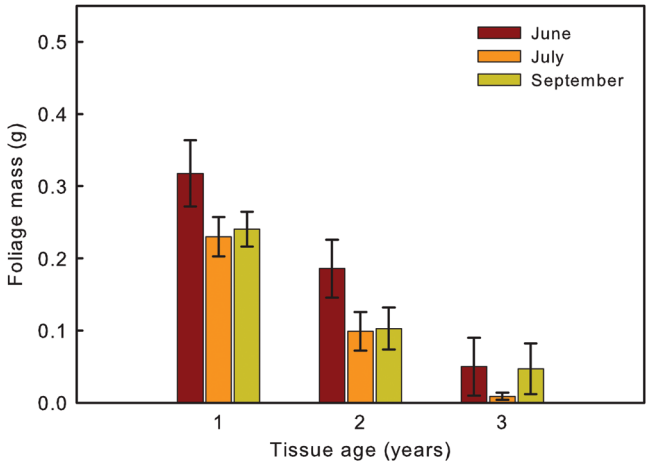

Figure 1. Mean foliage mass per branch growth increment for each sampled foliage tissue age at each sampling date (bars represent one standard error).

The 15 trees are ordered in Table 1 from the lowest to the highest BAI. There was a significant linear relationship between the pseudothecia count and both mean BAI ($R^2 = 0.58$, $P = 0.0009$) and mean 1-year-old foliage mass ($R^2 = 0.40$, $P = 0.01$), such that a 1% increase in pseudothecia abundance of 1-year-old foliage reflected a 0.58-cm^2 decrease in mean BAI (95% CI [0.29, 0.87]) and a 0.012-g decrease in mean foliage mass per growth increment (95% CI [0.003, 0.02]). There was a very strong relationship between the functional foliage mass and the mean BAI ($R^2 = 0.63$, $P = 0.0004$, Figure 2a). The rest of the analyses described below use functional foliage mass as a measure of disease severity for each tree.

NSC and growth analyses

There was a significant linear relationship between the functional foliage mass and the mean growing season (i.e., averaged over the three sampling dates) trunk NSC content ($R^2 = 0.35$, $P = 0.02$), and without the outlier (Tree 6), the relationship was substantially stronger ($R^2 = 0.54$, $P = 0.003$, Figure 2b). The trend in trunk NSC with functional foliage mass was similar for June and July, though the relationship was not significant in September (data not shown). Only two trees had average sapwood widths slightly less than the trunk sampling depth (i.e., 2 cm). We compared the trunk NSC concentrations of these two trees, as well as between other trees that had similar sapwood widths, and found no relationship between sapwood width and trunk NSC concentration (data not shown). The relationship between the functional foliage mass and the relative mean trunk NSC/BAI was also significant ($R^2 = 0.48$, $P = 0.004$, Figure 2c), indicating that with increasing disease symptom severity and therefore constraints on carbon supply,

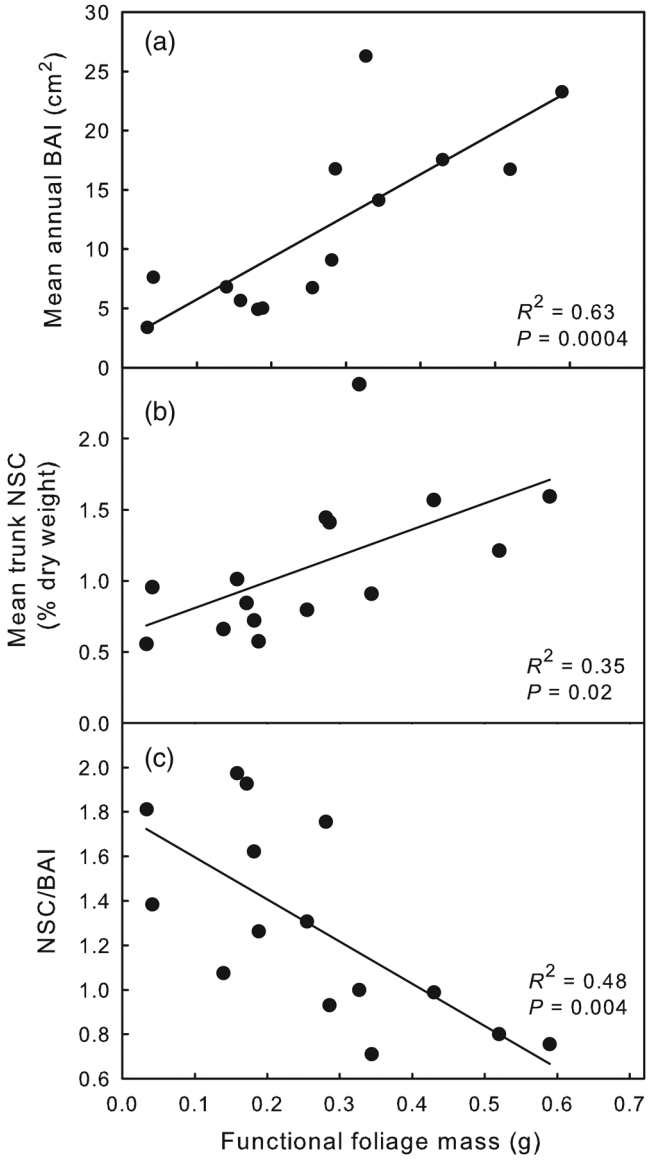

Figure 2. Mean annual 2000– 2011 BAI (a), mean trunk NSC content (b) and relative mean trunk NSC/BAI (c) versus functional foliage mass. Each point represents one tree. Simple linear regression analyses are shown. Relative NSC/BAI was calculated by taking the ratio of NSC to BAI after normalizing both measures with respect to their maximum values.

the relative reduction in basal area growth was greater than that of trunk NSC storage. The trend in relative mean trunk NSC/BAI with functional foliage mass was similar for each sampling date (data not shown).

The relationship between NSC concentration and tissue age for twigs and foliage did not differ with disease severity on any of the sampling dates (for data, see Tables S1, S2 and S3 available as Supplementary Data at *Tree Physiology* Online). For this reason, and because the functional foliage mass was only evaluated for prior year foliage, the following analyses with foliage and twigs only include 1-year-old tissues. The mean concentration of NSC was approximately four to five times higher in the crown (twigs and foliage) than in the trunk across trees (Table 2, Figure 3). There were no statistically significant relationships between the functional foliage mass and the mean growing season NSC content of twigs ($R^2 = 0.11$, $P = 0.23$) or foliage ($R^2 = 0.001$, $P = 0.91$, Figure 4a and b) or any individual sampling date (data not shown). However, there were strong positive relationships between the functional foliage mass and the ratio of mean trunk NSC to both twig NSC ($R^2 = 0.33$, $P = 0.02$) and foliage NSC ($R^2 = 0.32$, $P = 0.03$) (Figure 4c and d). These relationships were considerably stronger without the outlying Tree 6 ($R^2 \geq 0.48$, $P \leq 0.006$). The trend in trunk NSC to twig and foliage NSC, respectively, with functional foliage mass was similar for each sampling date (data not shown).

Starch was the largest component of NSC in the trunk, followed by glucose and fructose, and then sucrose (Table 2, Figure 3). In June, there was a significant linear relationship between functional foliage mass and trunk NSC content ($R^2 = 0.38$, $P = 0.02$), as well as with trunk starch content ($R^2 = 0.44$, $P = 0.007$). There were significant positive linear relationships between functional foliage mass and trunk sucrose content near the middle and end of the growing season in July ($R^2 = 0.47$, $P = 0.004$) and September ($R^2 = 0.38$, $P = 0.01$). There was no relationship between functional foliage mass and the mean growing season trunk glucose and fructose content ($R^2 = 0.04$, $P = 0.44$). In contrast to the patterns of NSC constituents observed in trunks, there did not appear to

Table 2. Mean concentrations (% dry weight) of total NSC, starch, sucrose, and glucose and fructose (Gluc/Fruc) of the trunk, and current-year twigs and foliage of the sampled trees from each sampling date.

	Trunk				Twigs				Foliage			
	NSC (%)	Starch (%)	Sucrose (%)	Gluc/ Fruc (%)	NSC (%)	Starch (%)	Sucrose (%)	Gluc/ Fruc (%)	NSC (%)	Starch (%)	Sucrose (%)	Gluc/ Fruc (%)
June	1.34 (0.16)	0.85 (0.13)	0.06 (0.02)	0.44 (0.05)	6.11 (0.38)	3.94 (0.35)	0.91 (0.08)	1.26 (0.11)	6.48 (0.53)	3.01 (0.43)	1.92 (0.13)	1.56 (0.10)
July	1.17 (0.13)	0.69 (0.10)	0.14 (0.02)	0.33 (0.03)	4.79 (0.34)	1.34 (0.19)	1.35 (0.12)	2.09 (0.21)	5.32 (0.30)	1.14 (0.17)	2.11 (0.09)	2.07 (0.11)
September	0.85 (0.11)	0.38 (0.07)	0.11 (0.02)	0.36 (0.04)	3.22 (0.34)	0.71 (0.19)	1.17 (0.12)	1.34 (0.11)	4.45 (0.26)	0.55 (0.10)	2.37 (0.14)	1.54 (0.11)

Parentheses contain one standard error from the mean.

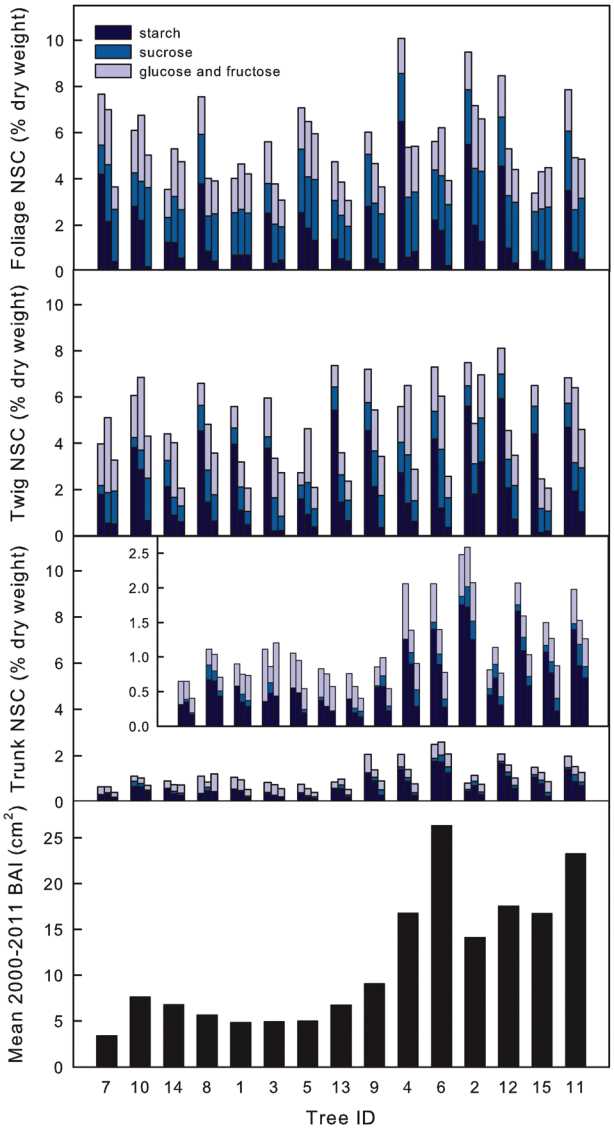

Figure 3. Mean foliage, twig and trunk NSC concentrations for current-year foliage and twigs, and trunk tissue, for each sampling date (ordered June, July and September for each tree), and mean 2000–2011 BAI for each sampled tree. Concentrations of NSC components (starch, sucrose, and glucose and fructose) are shown for each bar (see color legend). Trees are ordered by increasing the functional foliage mass. Inset in the trunk NSC panel enlarges the view of trunk NSC values.

be any relationship between NSC constituents in twigs and foliage and disease symptom severity at each sampling date (Table 2, Figure 3). There were no significant relationships between functional foliage mass and mean growing season starch content of twigs ($R^2 = 0.18$, $P = 0.12$) or foliage ($R^2 = 0.007$, $P = 0.77$), or between functional foliage mass and the mean growing season glucose and fructose content of twigs ($R^2 = 0.06$, $P = 0.38$) or foliage ($R^2 = 0.03$, $P = 0.54$). There were marginally significant relationships between the functional foliage mass and the mean growing season sucrose content of twigs ($R^2 = 0.23$, $P = 0.07$) and foliage ($R^2 = 0.20$, $P = 0.09$).

Non-structural carbohydrates fluctuated seasonally in all tissue types (Table 2, Figure 3). Seasonal fluctuation was not related to functional foliage mass, such that there were no statistically significant relationships between functional foliage mass and the percent decrease in mean NSC from June to September in the trunk ($R^2 = 0.03$, $P = 0.57$), twigs ($R^2 = 0.05$, $P = 0.40$) or foliage ($R^2 = 0.001$, $P = 0.92$). From June to September, mean trunk NSC content decreased by 0.49% dry weight (95% CI [0.26, 0.71]), starch content decreased by 0.47% dry weight (95% CI [0.26, 0.68]) and sucrose content increased by 0.05% dry weight (95% CI [0.00, 0.10]). There was no statistically significant change in mean trunk glucose and fructose over the growing season. Mean twig NSC content decreased by 2.89% dry weight from June to September (95% CI [2.05, 3.72]) and starch content decreased by 3.23% dry weight (95% CI [2.54, 3.93]). There was no statistically significant change in mean twig sucrose or glucose and fructose content over the growing season. Mean foliage NSC content decreased by 2.03% dry weight from June to September (95% CI [1.03, 3.03]), foliage starch content decreased by 2.46% dry weight (95% CI [1.58, 3.33]) and foliage sucrose content increased by 0.46% dry weight (95% CI [0.13, 0.79]). There was no statistically significant change in mean foliage glucose and fructose over the growing season.

Discussion

The high degree of disease severity at the site was evident in the reduction in mean growing season foliage mass by ~86% from the 1-year-old cohort to the 3-year-old cohort, when compared with healthier trees in the region, which have been reported to show a reduction in foliage mass of ~25% over the same cohort ages (Weiskittel et al. 2006). In addition, there was no evidence that trees with higher disease symptom severity produced more or less needle mass on individual shoot increments during the 2012 growing season. The relationships between disease severity (previous year functional foliage mass) and Douglas-fir growth and carbohydrate reserves observed in this study indicate that whereas the reduction in carbon assimilation caused by Swiss needle cast results in reduced annual growth and NSC in the trunk, there was no apparent relationship between disease symptom severity and NSC concentrations in twigs and foliage or new foliage growth. Retaining NSC in the crown appeared to have a greater priority than exporting the photosynthate for diameter growth in the trunk (Figures 2 and 4). Thus, the disease appeared to force trees to sacrifice stem growth and stem NSC storage to maintain crown growth under conditions of rapidly abscising foliage. Finally, we also found that carbohydrate reserves were depleted throughout the growing season to different extents in each tissue type (Table 2, Figure 3).

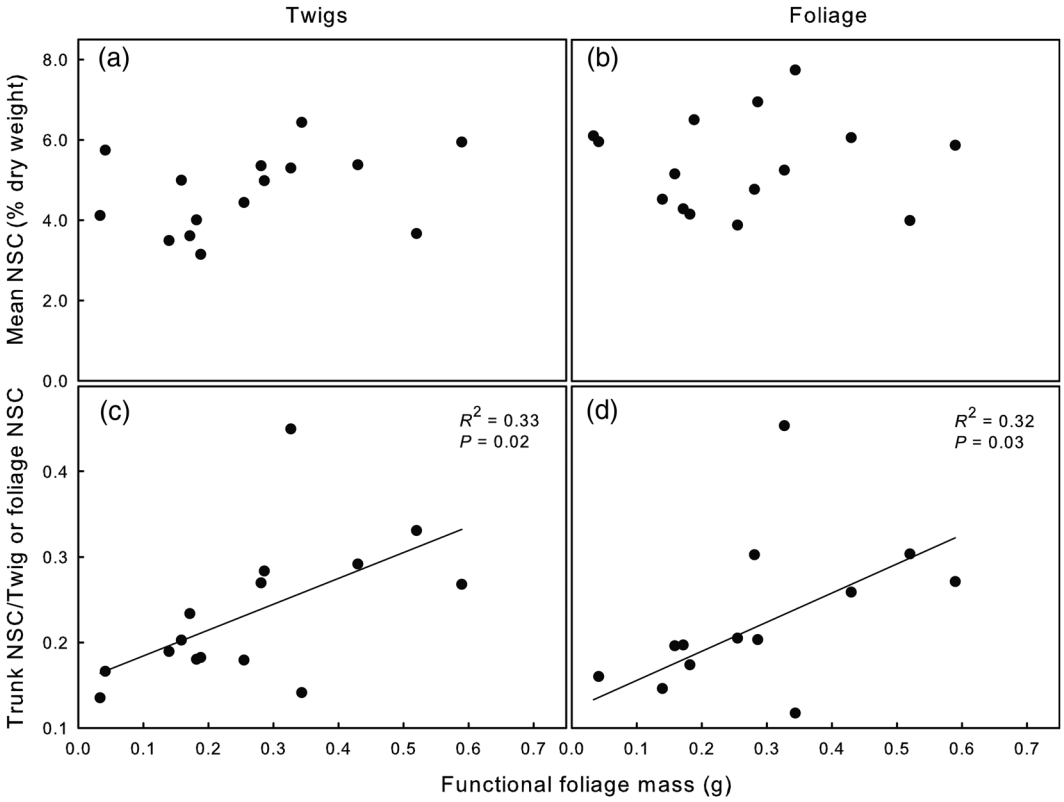

Figure 4. Mean twig (a) and foliage (b) NSC content and mean trunk NSC/twig NSC (c) and trunk NSC/foliage NSC (d) versus functional foliage mass. Each point represents one tree. Simple linear regression analyses are shown in (c) and (d).

The basis for seasonal trends in NSC of conifers is fairly well studied and understood. Starch concentrations are relatively high before bud break and are drawn upon over the growing season to aid in flushing and axial growth, while free sugar concentrations (i.e., sucrose, glucose and fructose) progressively increase and peak in autumn (Chung and Barnes 1980, Hansen and Beck 1990, 1994, Fischer and Höll 1991, Kibe and Masuzawa 1992, Oleksyn et al. 2000, Schaberg et al. 2000, Hoch et al. 2003, Bansal and Germino 2009). Starch is the main carbohydrate storage compound for conifers and is clearly a dynamic pool that accumulates over the winter and ensures that the tree will have adequate carbon reserves for producing a new cohort of needles during the following growing season (Webb 1981). Our results suggested that trunk radial growth was strongly dependent on current-year photosynthate rather than stored NSC. The total amount of NSC stored in the outer 2 cm of sapwood at the beginning of the growing season in June was estimated to be sufficient to supply only ~7% of the carbon required to generate a mean annual radial growth increment at the height where NSC samples were collected (data not shown). Interestingly, this percentage was nearly constant across the range of disease symptom severity in the 15 trees studied.

Although trunk and crown tissues in this study both exhibited the seasonal trend described above, they each behaved differently in response to limited carbon availability under relatively low water stress. There was a clear decrease in trunk NSC with increasing disease symptom severity, primarily due to a decrease in starch, which represented ~45–63% of total NSC over the growing season. In addition, there was a strong positive relationship between functional foliage mass and trunk sucrose at the end of the growing season. Thus, it appears that trunk storage (in the form of starch) was sacrificed with decreasing carbon availability, resulting in lower NSC values in more diseased trees. The higher trunk sucrose concentrations in healthier trees at the end of the growing season could be a consequence of healthier trees having more starch to mobilize at the end of the growing season for stem maintenance. The relative reduction in annual radial growth was greater than that of NSC concentrations with increasing disease-induced reduction in carbon assimilation, implying a priority of storage over growth in the trunk. Considering the lack of a relationship between disease symptom severity and trunk NSC in September, it is possible that all trees maintained a minimum threshold of NSC in the trunk, and trees with higher disease symptom severity reached the threshold earlier in the season due to the reduction in carbon assimilation associated with disease. The decrease in total NSC over the growing season was primarily attributable to the depletion of starch, which made up ~64 and 46% of total NSC in June for twigs and foliage,

respectively, and only ~22 and 12% of total NSC by September for twigs and foliage, respectively. In contrast to the trunk, there was no relationship between NSC and disease severity for twigs and foliage.

Taken together, there seemed to be a greater priority to retain NSC in the crown over exporting NSC to supply diameter growth in the trunk. Figure 4c and d demonstrates how the ratios of trunk NSC to twig and foliage NSC were lower for trees with higher disease symptom severity. Severely diseased trees appeared to be locked into a cycle of maintaining similar concentrations of NSC in twigs and foliage to those of less diseased trees to sustain the construction of new photosynthetic tissue and supporting branches that partially compensate for early needle abscission at the apparent expense of greater stem growth and increased mechanical support in the trunk. This could potentially explain why trees with Swiss needle cast can survive for decades under a chronic reduction in carbon supply. Thus, our results suggest that carbon storage is either partly active and/or a portion of carbohydrate reserves are sequestered, which has implications for our understanding of the role of NSC as a passively accumulated or actively managed pool. Non-structural carbohydrate concentration in a particular tissue does not necessarily indicate that a tree is healthy or has abundant access to carbon, or even that growth is not suffering. Furthermore, we have observed how various regions of a tree behave differently in response to a reduction in carbon supply.

An increase in the priority of carbon storage over other processes like growth during periods of limited carbon supply could have implications for other processes with a possible lower priority than storage. In the case of reduced carbon assimilation caused by Swiss needle cast, previous studies have provided evidence for changes in tree defense and interaction with biotic mortality agents, root NSC storage and mycorrhizal relationships. Kelsey and Manter (2004) found that trees with moderate-to-severe Swiss needle cast had a lower wound-induced oleoresin flow, as well as less ethanol and monoterpene production, compared with healthy Douglas-fir. The authors ascribed these results to reduced availability of photosynthate since carbohydrates are an important building block of defense compounds. Furthermore, the significant level of carbohydrates used by roots for growth, maintenance and mycorrhizal relationships, accounting for ~73% of net primary productivity in coniferous temperate forests (Grier et al. 1981, Fogel and Hunt 1983), should also be affected by reduced carbon supply. There is evidence that a reduction in carbon supply from the crown (e.g., from defoliation) can lead to depleted NSC reserves in roots of conifers (Webb and Karchesy 1977, Oleksyn et al. 2000). Although we currently do not know the effects of Swiss needle cast on Douglas-fir root carbohydrate reserves, our results implying that stem NSC levels are sacrificed to maintain high concentrations in the crown suggest that roots may also have reduced NSC. Lower root NSC concentrations could have significant implications for root growth, which could restrict soil exploration and the ability to obtain soil water and nutrients. Reduced NSC export might also limit root exudation, which plays a vital role in the cycling of soil organic matter (Millard et al. 2007) and attracting and establishing symbiotic relationships with mycorrhizae (e.g., Graham 1982), which have been shown to receive ~30% of total assimilate from the host tree (reviewed by Soderström 2002). Luoma and Eberhart (2006) observed that Douglas-fir stands with Swiss needle cast have a lower density and diversity of ectomycorrhizal fungi than typically found in healthy stands, suggesting that the reduction in photosynthate associated with the disease could be affecting these below-ground relationships.

Supplementary data

Supplementary data for this article are available at *Tree Physiology* Online.

Acknowledgments

The authors thank Alan Kanaskie and Erick Finnell for access to the site, and Alena Tofte, Valerie Sims and Horacio Paz for assistance in the field and laboratory.

Conflict of interest

None declared.

Funding

This research was supported in part by NSF grant DEB-073882 and a grant from the Swiss Needle Cast Cooperative.

References

Bansal S, Germino MJ (2009) Temporal variation of nonstructural carbohydrates in montane conifers: similarities and differences among developmental stages, species and environmental conditions. Tree Physiol 29:559–568.

Bustan A, Avni A, Lavee S, Zipori I, Yeselson Y, Schaffer AA, Riov J, Dag A (2011) Role of carbohydrate reserves in yield production of intensively cultivated oil olive (*Olea europaea* L.) trees. Tree Physiol 31:519–530.

Chapin FS III, Schulze ED, Mooney HA (1990) The ecology and economics of storage in plants. Annu Rev Ecol Syst 21:423–427.

Chung HH, Barnes RL (1980) Photosynthate allocation in *Pinus taeda*. II. Seasonal aspects of photosynthate allocation to different biochemical fractions in shoots. Can J For Res 10:338–347.

Fischer C, Höll W (1991) Food reserves of Scots pine (*Pinus sylvestris* L.). I. Season changes in the carbohydrate and fat reserves of pine needles. Trees 5:187–195.

Fogel R, Hunt G (1983) Contribution of mycorrhizae and soil fungi to nutrient cycling in a Douglas-fir ecosystem. Can J For Res 13:219–232.

Galvez DA, Landhäusser SM, Tyree MT (2011) Root carbon reserve dynamics in aspen seedlings: does simulated drought induce reserve limitation? Tree Physiol 31:250–257.

Graham JH (1982) Effect of citrus root exudates on germination of chlamydospores of the vesicular-arbuscular mycorrhizal fungus, *Glomus epigaeum*. Mycologia 74:831–835.

Grier CC, Vogt KA, Keyes MR, Edmonds RL (1981) Biomass distribution and above- and below-ground production in young and mature *Abies amabilis* zone ecosystems of the Washington Cascades. Can J For Res 11:155–167.

Grissino-Mayer HD (2001) Evaluating crossdating accuracy: a manual and tutorial for the computer program COFECHA. Tree Ring Res 57:205–221.

Hansen J, Beck E (1990) The fate and path of assimilation products in the stem of 8-year-old Scots pine (*Pinus sylvestris* L.) trees. Trees 4:16–21.

Hansen J, Beck E (1994) Seasonal changes in the utilization and turnover of assimilation products in 8-year-old Scots pine (*Pinus sylvestris* L.) trees. Trees 8:172–182.

Hoch G, Körner C (2009) Growth and carbon relations of tree line forming conifers at constant vs. variable low temperatures. J Ecol 97:57–66.

Hoch G, Popp M, Körner C (2002) Altitudinal increase of mobile carbon pools in *Pinus cembra* suggests sink limitation of growth at the Swiss treeline. Oikos 98:361–374.

Hoch G, Richter A, Körner C (2003) Non-structural carbon compounds in temperate forest trees. Plant Cell Environ 26:1067–1081.

Holmes RL (1983) Computer assisted quality control in tree-ring dating and measurement. Tree Ring Bull 43:69–78.

Johnson DM, McCulloh KA, Woodruff DR, Meinzer FC (2012) Hydraulic safety margins and embolism reversal in stems and leaves: why are conifers and angiosperms so different? Plant Sci 195:48–53.

Johnson GM, Gartner BL, Maguire D, Kanaskie A (2003) Influence of Bravo fungicide applications on wood density and moisture content of Swiss needle cast affected Douglas-fir trees. For Ecol Manag 186:339–348.

Johnson GM, Grotta AT, Gartner BL, Downes G (2005) Impact of the foliar pathogen Swiss needle cast on wood quality of Douglas-fir. Can J For Res 35:331–339.

Kelsey RG, Manter DK (2004) Effect of Swiss needle cast on Douglas-fir stem ethanol and monoterpene concentrations, oleoresin flow, and host selection by the Douglas-fir beetle. For Ecol Manag 190:241–253.

Kibe T, Masuzawa T (1992) Seasonal changes in the amount of carbohydrates and photosynthetic activity of *Pinus pumila* Regel on alpine in central Japan. Proc NIPR Symp Polar Biol 5:118–124.

Körner C (2003). Carbon limitation in trees. J Ecol 91:4–17.

Latta G, Adams D, Shaw DC (2009) Mapping western Oregon Douglas-fir foliage retention with a simultaneous autoregressive model. In: Shaw DC, Woolley T (eds) Swiss Needle Cast Cooperative Annual Report 2009. Oregon State University, Corvallis, OR, pp 37–51. http://sncc.forestry.oregonstate.edu/annual-reports.

Luoma DL, Eberhart JL (2006) Are differences in the ectomycorrhizal community correlated with Swiss needle cast severity? In: Shaw DC (ed.) Swiss Needle Cast Cooperative Annual Report 2006. Oregon State University, Corvallis, OR, pp 60–64. http://sncc.forestry.oregonstate.edu/annual-reports.

Maguire DA, Kanaskie A, Voelker W, Johnson R, Johnson G (2002) Growth of young Douglas-fir plantations across a gradient in Swiss needle cast severity. West J Appl For 17:86–95.

Maguire DA, Mainwaring DB, Kanaskie A (2011) Ten-year growth and mortality in young Douglas-fir stands experiencing a range in Swiss needle cast severity. Can J For Res 41:2064–2076.

Manter DK, Bond BJ, Kavanagh KL, Rosso PH, Filip GM (2000) Pseudothecia of Swiss needle cast fungus, *Phaeocryptopus gaeumannii*, physically block stomata of Douglas-fir, reducing CO_2 assimilation. New Phytol 148:481–491.

Manter DK, Winton LM, Filip GM, Stone JK (2003) Assessment of Swiss needle cast disease: temporal and spatial investigations of fungal colonization and symptom severity. J Phytopathol 151:344–351.

Manter DK, Reeser PW, Stone JK (2005) A climate-based model for predicting geographic variation in Swiss needle cast severity in the Oregon coast range. Phytopathology 95:1256–1265.

McDowell NG (2011) Mechanisms linking drought, hydraulics, carbon metabolism, and vegetation mortality. Plant Physiol 155:1051–1059.

Millard P, Sommerkorn M, Grelet GA (2007) Environmental change and carbon limitation in trees: a biochemical, ecophysiological and ecosystem appraisal. New Phytol 175:11–28.

Muller B, Pantin F, Génard M, Turc O, Freixes S, Piques M, Gibon Y (2011) Water deficits uncouple growth from photosynthesis, increase C content, and modify the relationship between C and growth in sink organs. J Exp Bot 62:1715–1729.

Nikinmaa E, Hölttä T, Hari P, Kolari P, Mäkelä A, Sevanto S, Vesala T (2013) Assimilate transport in phloem sets conditions for leaf gas exchange. Plant Cell Environ 36:655–669.

Oleksyn J, Zytkowiak R, Karolewski P, Reich PB, Tjoelker MG (2000) Genetic and environmental control of seasonal carbohydrate dynamics in trees of diverse *Pinus sylvestris* populations. Tree Physiol 20:837–847.

Quick WP, Chaves MM, Wendler R et al. (1992) The effect of water stress on photosynthetic carbon metabolism in four species grown under field conditions. Plant Cell Environ 15:25–35.

Rosso PH, Hansen EM (2003) Predicting Swiss needle cast disease distribution and severity in young Douglas-fir plantations in coastal Oregon. Phytopathology 93:790–798.

Runyon J, Waring RH, Goward SN, Welles JM (1994) Environmental limits on net primary production and light-use efficiency across the Oregon transect. Ecol Appl 4:226–237.

Ryan MG (2011) Tree responses to drought. Tree Physiol 31:237–239.

Sala A, Piper F, Hoch G (2010) Physiological mechanisms of drought-induced tree mortality are far from being resolved. New Phytol 186:274–281.

Sala A, Woodruff DR, Meinzer FC (2012) Carbon dynamics in trees: feast or famine? Tree Physiol 32:764–775.

Schaberg PG, Snyder MC, Shane JB, Donnelly JR (2000) Seasonal patterns of carbohydrate reserves in red spruce seedlings. Tree Physiol 20:549–555.

Silpi U, Lacointe A, Kasempsap P et al. (2007) Carbohydrate reserves as a competing sink: evidence from tapping rubber trees. Tree Physiol 27:881–889.

Soderstrom B (2002) Challenges for mycorrhizal research into the new millennium. Plant Soil 244:1–7.

Srichuwong S, Jane JL (2007) Physicochemical properties of starch affected by molecular composition and structures: a review. Food Sci Biotechnol 16:663–674.

Stone JK, Coop LB, Manter DK (2008) Predicting effects of climate change on Swiss needle cast disease severity in Pacific Northwest forests. Can J Plant Pathol 30:169–176.

Webb WL (1981) Relation of starch content to conifer mortality and growth loss after defoliation by the Douglas-fir tussock moth. For Sci 27:224–232.

Webb WL, Karchesy JJ (1977) Starch content of Douglas-fir defoliated by the tussock moth. Can J For Res 7:186–188.

Weiskittel AR, Maguire DA, Garber SM, Kanaskie A (2006) Influence of Swiss needle cast on foliage age-class structure and vertical foliage distribution in Douglas-fir plantations in north coastal Oregon. Can J For Res 36:1497–1508.

Wiley E, Helliker B (2012) A re-evaluation of carbon storage in trees lends greater support to carbon limitation to growth. New Phytol 195:285–289.

Woodruff DR, Meinzer FC (2011*a*) Water stress, shoot growth and storage of non-structural carbohydrates along a tree height gradient in a tall conifer. Plant Cell Environ 34:1920–1930.

Woodruff DR, Meinzer FC (2011*b*) Size-dependent changes in biophysical control of tree growth: the role of turgor. In: Meinzer FC, Lachenbruch B, Dawson TE (eds) Size- and age-related changes in tree structure and function. Oxford University Press, Oxford, pp 363–384.

Würth MKR, Pelaez-Riedl S, Wright SJ, Körner C (2005) Non-structural carbohydrate pools in a tropical forest. Oecologia 143:11–24.

Zhao J, Mainwaring DB, Maguire DA, Kanaskie A (2011) Regional and annual trends in Douglas-fir foliage retention: correlations and climatic variables. For Ecol Manag 262:1872–1886.

Tree Physiology Advance Access published March 11, 2014

Tree Physiology 00, 1–3
doi:10.1093/treephys/tpu010

Commentary

Carbon storage in trees: pathogens have their say

Jordi Martínez-Vilalta[1,2,3]

[1]CREAF, Cerdanyola del Vallès 08193, Barcelona, Spain; [2]Univ. Autònoma Barcelona, Cerdanyola del Vallès 08193, Barcelona, Spain; [3]Corresponding author (jordi.martinez.vilalta@uab.es)

Received January 28, 2014; accepted February 3, 2014; handling Editor Danielle Way

The study of the role and dynamics of nonstructural carbohydrates (NSCs) in woody plants, and particularly in trees, has received renewed attention in the recent past (Sala et al. 2012, Dietze et al. 2014). There are several reasons for this increased interest but it seems clear that an important event was the publication of the McDowell et al. (2008) paper on the mechanism of drought-induced mortality in trees, in which the authors put forward the carbon-starvation hypothesis. According to this hypothesis, stomatal closure to prevent hydraulic failure under drought causes photosynthetic carbon uptake to diminish and, eventually, the plant may deplete its carbon reserves and starve as a result of continued metabolic demand for carbohydrates. This idea was not new (e.g., Waring 1987, Martínez-Vilalta et al. 2002, Bréda et al. 2006), but McDowell et al. (2008) presented it in a coherent and wider hydraulic framework, which made it compelling and influential. The carbon-starvation hypothesis implies that the amount and dynamics of carbohydrate storage in trees provide useful information on their drought responses. And off we went, many of us, to measure NSC concentrations in our field- and greenhouse-based studies of drought-induced tree mortality.

The carbon-starvation hypothesis was controversial from the beginning (McDowell and Sevanto 2010, Sala et al. 2010) and, although direct links between low NSC content and drought-induced tree mortality have been found in some cases (e.g., Galiano et al. 2011, Galvez et al. 2013), its overall importance in the tree-mortality process remains to be established. What is clear, however, is that these discussions have opened new perspectives into the study of plant responses to drought (McDowell 2011, Ryan 2011) and other stress factors, and, most importantly, they have bolstered the cross-communication between fields that had been rather disconnected in the recent past, including plant hydraulics, plant carbon economy and plant pathology. In addition, the renewed interest in the dynamics of NSCs has reopened an old debate on carbon allocation in plants and, in particular, on the role of carbon supply in limiting tree growth (Wiley and Helliker 2012, Fatichi et al. 2014, Palacio et al. 2014).

The classical view of the role of NSCs and their dynamics is based on a source–sink model and holds that carbon storage in plants is the result of the supply of newly assimilated carbon being higher than the overall demand at the sink tissues, including growth, respiration, defence and export (Kozlowski 1992). Although this view is consistent with different carbon allocation paradigms, it has frequently been taken to imply a passive storage, in which NSC builds up only when all the other demands have been satisfied. Under this paradigm, the fact that trees tend to have substantial amounts of NSC even under stressful conditions has been interpreted as implying that carbon availability does not limit tree growth (Körner 2003). However, NSCs may play a key role in maintaining hydraulic and osmotic functions and thus may not represent a simple overflow acting as a repository pool for future uses (McDowell 2011, Sala et al. 2012), in which case allocation to storage may be highly regulated (i.e., not passive) and may compete with growth at least under certain conditions (Chapin et al. 1990, Sala et al. 2012). From this perspective, the relatively high NSC levels in trees are not necessarily evidence of excess carbon and are compatible with carbon limiting, or co-limiting, tree growth (Wiley and Helliker 2012). This dispute is not trivial, as it has key implications on how we understand plant carbon economy and the way we model ecosystem carbon flows (Richardson et al. 2013, Dietze et al. 2014).

In this issue, Saffell et al. (2014) use a novel approach to study the relative priority of storage versus growth, taking advantage of the effects of Swiss needle cast (SNC, not to be

confused with NSC) on Douglas-fir (*Pseudotsuga menziesii* (Mirb.) Franco). This disease is caused by an ascomycete (*Phaeocryptopus gäumannii* (Rohde) Petrak) that colonizes Douglas-fir foliage and causes stomatal blockage and, ultimately, leaf abscission. Interestingly, SNC occurs in wet environments, providing a natural experiment that is not complicated by the effects of drought stress. In agreement with previous studies, Saffell et al. (2014) find much lower radial growth in SNC-diseased trees with less functional leaf mass, presumably due to lower overall carbon uptake. However, the novelty of this study is the concurrent measurement of NSC dynamics and growth on infected trees. Their results show that NSC concentrations are unrelated to functional leaf mass (in twigs and foliage) or only decline slightly compared with growth (in the main trunk). This result is interpreted to imply that infected Douglas-fir maintains NSC levels, particularly in the crown, at the expense of stem growth, with important implications for the current debate between passive and active carbohydrate storage in trees.

The results by Saffell et al. (2014) are intriguing, but they also raise questions. An important one has to do with metrics. How should we measure the relative priority of storage versus growth? Ideally we should be able to monitor the carbon balance of whole, mature trees and all its components at relevant time scales. Unfortunately, this is a daunting task (see Dietze et al. 2014) and alternative measures of allocation priority are needed. Saffell et al. (2014) use the ratio of NSC concentration to basal area increment. This is an appealing measure mostly for practical reasons, as it combines the two most common ways of quantifying tree carbon storage and growth. However, it is only part of the story. Nonstructural carbohydrate concentration measures a (relative) content, whereas growth is a flux. A better index of relative priority would compare growth concurrently with the rest of the fluxes in and out the NSC compartment (or at least the changes in NSC content) (Ryan 2011), all expressed in the same or comparable units (Figure 1). Unfortunately, this is again challenging and brings us to yet another problem in plant carbon economy research. While it is reasonably easy to measure growth at the whole-tree level, even retrospectively using growth rings, estimating the total NSC content of an entire tree is exceedingly difficult and has only been done in very few studies (see Dietze et al. 2014). Nonstructural carbohydrate concentration varies among organs and tissues and a whole-tree assessment requires many measurements, as well as a precise quantification of the total biomass in each organ/tissue. And even that would not be enough, as repeated measurements would be required to assess changes in NSC.

Another exciting aspect in Saffell et al. (2014) has to do with the role of pathogens. Fungal pathogens can establish very rich and diverse trophic interactions with trees, in which they may affect their carbon balance indirectly, as stressed in the

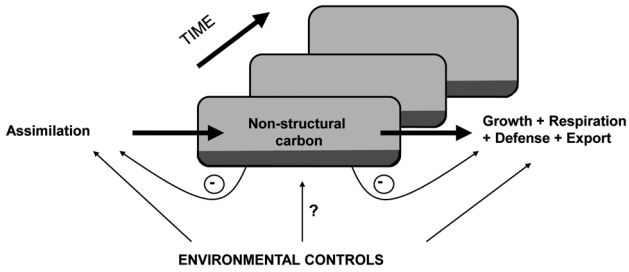

Figure 1. A possible view of nonstructural carbon (including NSC) as a pool resulting from the balance between carbon sources (assimilation) and sinks. Changes in this balance over time determine variation in the size of the pool. The dark grey area corresponds to nonstructural carbon serving immediate functions in osmotic regulation and vascular transport. The arrows with encircled minus signs indicate feedback and feedforward mechanisms by which sink and source activity is regulated. Environmental controls on source and sink activity illustrate the co-limitation between assimilation and other processes such as growth, which provides a middle ground between the extreme views of a purely carbon-limited growth and a 'growth-controlled' photosynthesis.

Saffell et al. work, but also directly. *Phaeocryptopus gäumannii*, the fungal pathogen that causes SNC, is a biotroph, and as such it is able to obtain carbon directly from living leaf cells (Deacon 1997). This direct consumption, together with any carbon-expensive defence mechanisms or other hormonal responses that may be triggered, will have implications for the carbon balance of the affected leaves and elsewhere in the plant. Accounting for these effects is probably essential if we are to understand whole-tree carbon dynamics and its response to biotic and abiotic stress, as these two sources of stress appear to be intimately linked to each other (Desprez-Loustau et al. 2006, Jactel et al. 2011, Gaylord et al. 2013).

Clearly, elucidating the role of NSCs in trees will require additional research. We need to address the complexity of plant carbon economy and this can only be done if all the relevant disciplines come together into a common research framework and agenda. Saffell et al.'s (2014) study provides an example of a fruitful approach. Trophic (i.e., carbon-based) interactions between pathogens and trees are ubiquitous and it seems clear that a complete understanding of tree carbon dynamics will not be achieved until these interactions are explicitly accounted for. To find a common ground in disputes such as the role of carbon in limiting tree growth, we need to recognize the central importance of time scales in any discussion about carbon allocation (Dietze et al. 2014), and we need to be aware that data interpretation might be complicated by issues of definition. After all, what is storage? Chapin et al. (1990) define storage as resources that build up in the plant and can be mobilized in the future to support biosynthesis for growth or other plant functions. This definition highlights the role of storage as a pool/repository for future uses. But if NSCs have immediate functions in plant metabolism (osmotic regulation, maintaining vascular integrity; Sala et al. 2012), should we

see them simply as storage? Do we need to view growth and NSC formation as competing flows or could we see NSCs simply as a pool from which different but interacting uses are possible (cf. Figure 1)? What is that we measure when we quantify NSC concentrations? I suspect that these important conceptual (and related technical) aspects will need to be resolved before current disputes are settled and a common view on plant carbon allocation emerges.

Conflict of interest

None declared.

Funding

Financial support was obtained from the Spanish Ministry of Economy and Competitiveness (competitive grant CGL2010-16373).

References

Bréda N, Huc R, Granier A, Dreyer E (2006) Temperate forest trees and stands under severe drought: a review of ecophysiological responses, adaptation processes and long-term consequences. Ann For Sci 63:625–644.

Chapin FS III, Schulze ED, Mooney HA (1990) The ecology and economics of storage in plants. Annu Rev Ecol Syst 21:423–447.

Deacon JW (1997) Modern mycology. 3rd edn. Blackwell, Oxford.

Desprez-Loustau ML, Marccais B, Nageleisen LM, Piou D, Vannini A (2006) Interactive effects of drought and pathogens in forest trees. Ann For Sci 63:597–612.

Dietze MC, Sala A, Carbone MS, Czimczik CI, Mantooth JA, Richardson AD, Vargas R (2014) Nonstructural carbon in woody plants. Annu Rev Plant Biol, in press. doi:10.1146/annurev-arplant-050213-040054

Fatichi S, Leuzinger S, Körner C (2014) Moving beyond photosynthesis: from carbon source to sink-driven vegetation modeling. New Phytol 201:1086–1095.

Galiano L, Martínez-Vilalta J, Lloret F (2011) Carbon reserves and canopy defoliation determine the recovery of Scots pine 4 yr after a drought episode. New Phytol 190:750–759.

Galvez DA, Landhäusser SM, Tyree MT (2013) Low root reserve accumulation during drought may lead to winter mortality in poplar seedlings. New Phytol 198:139–148.

Gaylord ML, Kolb TE, Pockman WT, Plaut JA, Yepez EA, Macalady AK, Pangle RE, McDowell NG (2013) Drought predisposes piñon–juniper woodlands to insect attacks and mortality. New Phytol 198: 567–578.

Jactel H, Petit J, Desprez-Loustau ML, Delzon S, Piou D, Battisti A, Koricheva J (2011) Drought effects on damage by forest insects and pathogens: a meta-analysis. Glob Change Biol 18:267–276.

Körner C (2003) Carbon limitation in trees. J Ecol 91:4–17.

Kozlowski TT (1992) Carbohydrate sources and sinks in woody plants. Bot Rev 58:107–222.

Martínez-Vilalta J, Piñol J, Beven K (2002) A hydraulic model to predict drought-induced mortality in woody plants: an application to climate change in the Mediterranean. Ecol Model 155:127–147.

McDowell NG (2011) Mechanisms linking drought, hydraulics, carbon metabolism, and vegetation mortality. Plant Physiol 155:1051–1059.

McDowell NG, Sevanto S (2010) The mechanisms of carbon starvation: how, when, or does it even occur at all? New Phytol 186:264–266.

McDowell N, Pockman WT, Allen CD et al. (2008) Mechanisms of plant survival and mortality during drought: why do some plants survive while others succumb to drought? New Phytol 178:719–739.

Palacio S, Hoch G, Sala A, Körner C, Millard P (2014) Does carbon storage limit tree growth? New Phytol 201:1096–1100.

Richardson AD, Carbone MS, Keenan TF, Czimczik CI, Hollinger DY, Murakami P, Schaberg PG, Xu X (2013) Seasonal dynamics and age of stemwood nonstructural carbohydrates in temperate forest trees. New Phytol 197:850–861.

Ryan MG (2011) Tree responses to drought. Tree Physiol 31:237–239.

Saffell BJ, Meinzer FC, Woodruff DR, Shaw DC, Voelker SL, Lachenbruch B, Falk K (2014) Seasonal carbohydrate dynamics and growth in Douglas-fir trees experiencing chronic, fungal-mediated reduction in functional leaf area. Tree Physiol, in press. doi:10.1093/treephys/tpu002.

Sala A, Piper F, Hoch G (2010) Physiological mechanisms of drought-induced tree mortality are far from being resolved. New Phytol 186:274–281.

Sala A, Woodruff DR, Meinzer FC (2012) Carbon dynamics in trees: feast or famine? Tree Physiol 32:764–775.

Waring RH (1987) Characteristics of trees predisposed to die. Bioscience 37:569–577.

Wiley E, Helliker B (2012) A re-evaluation of carbon storage in trees lends greater support for carbon limitation to growth. New Phytol 195:285–289.

Appendix

Field Protocols

FIELD EQUIPMENT CHECKLIST

Hard hats
Field vests
Safety goggles
Compass
PVC
Rebar
Pens, pencils, sharpies
Data sheets
Clipboard
GPS
Laser
Extra AA and AAA batteries
Loppers
Handsaw
Chainsaw
Chainsaw toolbox
Firebox
Fire extinguisher
Hammers
Pulaski
5 gallons of water (Weyerhauser)
Al nails
Tree tags
Aluminum writeable tags
Zip ties
Stapler
Flagging (Pink, orange, orange/black striped)
Logger tapes
Extra nails for logger tapes
Garbage bags
Paint (orange, blue)

Foliage sampling:

Ziploc bags (1-gallon and sandwich size)
Sharpies
Clippers/pruners
Paint (blue)

Climbing gear

Soil sampling:

Push probe
4 – 2 gallon buckets
Block of wood (10x10)
Field knife
1-gallon Ziploc freezer bags
Ziploc sandwich bags
Trowel
Tape measure

General stand parameters:
Candidate stands fall into three general targets. 1) 10-30 year old Douglas-fir plantations that haven't been treated (no thinning or fertilization) in past 5 years; 2) Stand is composed of at least 80% Douglas-fir basal area (flexibility on this should be applied due to hemlock fecundity, particularly in coastal areas where intense SNC pressure needs representation within the plot network); and 3) Stand density of Douglas-fir ranges between 300 and 400 trees per acre.

Plot location:
Using a list of potential stands provided by landowners, assess plantation suitability and select plot location based on the targets described above. Using a Google-Earth aerial photo or a satellite image, pre-determine potential areas of the stand that meet the criteria. Often, these areas do not meet the criteria on the ground, therefore it is important to select multiple locations, ideally 3 or more. Once in the stand, walk these potential areas for a visual determination. Roughly pace out a 30m area to check if all criteria are met sufficiently. Ideally, plot orientation is along the cardinal directions or aligned with the stands' slope. Once a plot location has been determined, choose and mark the plot starting point/corner, determine the distance and azimuth to the nearest/most convenient road, and clearly flag the trail with orange/black stripped flagging. On the road, choose a visible reference tree, and mark it with three orange paint stripes. Record GPS coordinates.

Plot establishment:
To lay out a square 1/5 acre plot, place a 5-foot PVC pipe over a two-foot length of rebar that has been hammered into the soil at the plot start corner. Flag the top of the PVC with two pink flags and on an attached writable aluminum tag, note the plot number and orientation of the corner. Record GPS coordinates. With a compass and a measuring tape attached to the PVC corner, establish the remaining 3 corners, each 28.45 meters apart (horizontal distance). If necessary, remove lower dead limbs and heavy brush to get an accurate distance and azimuth. Flag each side of the plot with pink flagging. Mark each PVC corner using the same method as the start corner. Record GPS coordinates for all corners.

Buffer establishment:
All measurement plots require a 10m buffer. Establish buffer zone by pulling a measuring tape 14.1m at a 45 degree angle from the plot edge azimuths. Mark buffer corners with PVC pipes and double orange flagging. Some land owners (e.g. Stimson) require the buffer perimeter to be delineated. If required, delineate with orange flagging.
Before leaving the stand, sketch the location of the plot on the data sheet.

Tree tagging:
Following the establishment and marking of plot boundaries, give all trees (meeting the below criteria) within the plot a numbered tag. Divide plot into 4 corridors, approximately 7 meters wide, dividing corridors with an orange/black flagging. Starting at a corner, following corridors, tag all trees facing the same direction and record data.

1) Record all information listed in the header of the data form entitled **2013 (2014 or 2015) Research and Monitoring Plot Network:** include plot, date, crew, and data provided on the sheet. Use common name abbreviations for tree species. **See appendix 1.**

2) All Douglas-fir trees with DBH ≥ 3 cm should be nailed with a stamped aluminum tag at breast height (1.3 m from ground on uphill side of tree). If trees are too small to be tagged by nail at breast height, attach a tag using a plastic ladder tie and a staple at breast height. If too small to be stapled, attach looped ladder tie to a branch near breast height (1.3 m from ground on uphill side of tree). If at breast height there is a stem abnormality (such as a branch whorl, fork, canker, bulge, etc.) hammer the nail at the nearest spot of a uniform stem diameter either above or below breast height.

3) All other tree species with DBH ≥ 5 cm should also be tagged with a nail. (see above). Use the species codes provided; if unsure of a particular hardwood species, code it as OH (other hardwood.)

4) Measure each tagged tree for DBH to the nearest 0.1 cm, being sure that the bottom of the D-tape is immediately above the nail holding the tree tag (or, alternatively, immediately above where the plastic tie is connected to the tree.

5) Measure and record total height (nearest 0.01 m) and height to lowest live branch (height of the lowest live branch of contiguous live crown; nearest 0.01 m) on 40 Douglas-fir trees as follows: the ten largest Douglas-fir by DBH, the four smallest Douglas-fir by DBH, and twenty six Douglas-fir distributed evenly across the diameter range. Avoid trees with damaged tops, i.e. broken, multiple, or dead top. Paint each height tree with an orange paint at breast height. Paint ten largest Douglas-fir by DBH with blue paint (above breast height/orange paint).

6) If any Douglas-fir tree has some type of top damage, record this in the Notes column, using one of the tree designated codes (BT: broken top; DT: dead top; MT: multiple top).

Appendix 1

Tree Species Codes

DF	Douglas-fir
WH	Western hemlock
SS	Sitka Spruce
NF	Noble fir
GF	Grand Fir
RC	Western redcedar
RA	Red alder
BM	Bigleaf maple
CB	Cascara buckthorn
MA	Madrone
BC	Bitter cherry
GC	Chinkapin
OH	Other hardwood

Foliage Sampling

In the first spring (April-June) after plot establishment: revisit newly established plots and choose the 10 largest trees (by dbh) that are undamaged (no broken tops, root rot, stem decay, bear damage, etc.). These 10 largest trees will be assessed for foliage retention, and needles will be sampled for pseudothecial occlusion and foliar nutrition.

Sample Tree Selection

The following steps can be done ahead of time:

1. Using the tree data collected the previous dormant season, select the 10 largest trees by dbh (choose 15, in case some are newly damaged).

2. Divide the live crown (HT-HLC) into thirds (hereafter referred to as the upper, mid, and lower-third), and record the midpoint of each crown third on the datasheet which will be used in the field.

3. Prepare data sheets and label sample collection bags.

In the field, access and collect three lateral branches from the south side of the 10 sample trees, one branch each from the lower, mid, and upper crown third. Do not sample damaged branches. These branches should be as close as practical to the mid-point of each crown third. Record the height of the whorls from which the samples are collected—this is best accomplished by taping the distance from the crown base to the base of the sample branch.

Given the size of the trees within the plot network and the need for at least two needle cohorts, for the upper live crown, collect a two-year-old lateral from a three-year-old branch (i.e. the third whorl). Record height of each branch collected.

For the mid- and lower- crown thirds, collect the largest four- year- old secondary lateral on the southernmost primary branch in the approximate middle of each crown third. Because the fifth whorl (from the top) has been a standard sampling location for many SNC studies, if this whorl is in an appropriate sampling location, use it. Record the whorl # of the mid-crown sampling position.

For all collected branches, estimate foliage retention in the field and then bag the sample branches for transport to the laboratory for disease severity assessment. See below Foliage collection.

Foliage Retention (FR) Estimate

Examine sampled secondary lateral branches from each crown third and estimate the average number of annual needle compliments present (Figure 1). Estimate the proportion of attached needles present within each cohort of the primary axis of the secondary lateral. Estimate FR values for each cohort on the following scale from 1 to 10:

0 = no live foliage remaining in cohort
1 = 1 – 10% of live foliage remaining in cohort
2 = 11 – 20% of live foliage remaining in cohort
3 = 21 – 30% of live foliage remaining in cohort
4 = 31 – 40% of live foliage remaining in cohort
5 = 41 – 50% of live foliage remaining in cohort
6 = 51 – 60% of live foliage remaining in cohort
7 = 61 – 70% of live foliage remaining in cohort
8 = 71 – 80% of live foliage remaining in cohort
9 = 81 – 90% of live foliage remaining in cohort
10 = 91 – 100% of live foliage remaining in cohort

Foliage Collection

For each of the pseudothecial occlusion, crown third branches, clip one-year needles and place in appropriate bags. Repeat process with two-year needles.

For the foliar nutrition samples, collect 3 branch tips from mid-crown with 1- and 2-year old needles.

Labeling Bags

Labeling of sample bags should be completed ahead of time. For each tree sampled, we will have six small (sandwich or quart-size) Ziplocs bags, one Whirl-pak, and one 1-gallon Ziploc bag to collectively store the smaller bags. Collect the following samples and record on bags:

Pseudothecial occlusion

For the one-year and two-year needles from upper branch, label 2 bags: plot, tree ID, upper, year 1 (or 2). For example: N151/232/U/1.

For the one-year and two-year needles from mid branch, label 2 bags: plot, tree ID, mid, year 1 (or 2). For example: N151/232/M/2.

For the one-year and two-year needles from lower branch, label 2 bags: plot, tree ID, lower, year 1 (or 2). For example: N151/232/L/1.

Foliar nutrition

The seventh sample from each tree is for the chemical analysis of foliage. Label one whirl-pak bag as follows: JH Soil, plot, tree ID, and date.

On the large, 1-gallon bag write: plot, tree ID, date, crew. For example: N151/232/3-21-14/EB&PH.

Molecular Ecology Sampling Protocol

1. In the lab, pre-label one 1-gallon Ziplock bag and 7 quart-sized Ziplock bags. Place the quart-sized Ziplocks into the one-gallon bag.

i. Gallon bag:

1. Stone, plot, date, crew initials.

ii. 3 quart-sized bags:

1. Low, plot, tree, date.
2. Mid, plot, tree, date.
3. Upper, plot, tree, date.

iii. 4 quart-sized bags:

1. Plot, tree, date. In the field note the age of the whorl, from which each branch is collected (e.g. whorl 5).

2. Select 5 out of the 10 largest by diameter trees per site.
3. Sample ONE TREE extensively:

a. Collect 5 secondary branches with 2 and 3 year old needles from this tree (1 lower, 2 middle, and 2 upper crown, if possible).

b. Place branchlets from lower, mid, upper into 3 labeled perforated (punch a small hole with a pencil) Ziploc bags.

4. For the remaining four trees, sample ONE secondary branch from the mid-crown whorl.
5. Place branches in pre-labeled, perforated Ziploc bag.
6. Place in cooler on ice or ice packs. Foliage only needs to be kept cool enough to prevent mold growth (~ 50-60 F).
7. Place in cold-room within 48 hrs after collection.

Field Soil Sampling

Materials:

1 Push probe

1 Compass

4 2- gallon buckets

Mark the first bucket with ”0-10”, second with “10-20”, and third with “20-30” with garishly colored tape to avoid mixing them up in the field.

Many pin flags (for marking sample locations – optional)

1 O-horizon sampling template

Block of wood cut to a known dimension (10x10 cm)

1 Field knife (steak knives work well)

2 1 quart to 1 gallon zip-loc freezer bags (the most durable bag)

3 500ml whirl-pak bags

1 trowel

1 metric tape measure

Sample Bag labeling:

Item	Label
Project name:	SNC
Date:	the date
Plot #	follow the SNCC plot labeling system
Soil depth sampled:	We’ll have 4-5 possible labels here: O horizon (moss and litter), 0-10cm, 10-20cm, and 20-30cm
Initials of samplers:	Initials of whoever is out collecting samples
Other info:	Depths of O-horizon

1. Sample points

1-1. Soils will be collected from 5 different locations within each 1/5-acre plot.

1-2. The first location will be approximately at plot center.

1-3. The next 4 locations will be 4.5 m in towards the plot center from the 4 plot corners. This is approximately 2/3 the distance from the plot center. To speed up sampling in the field approximate distances and azimuths are OK. If resampling will take place, we don’t want to resample in the same locations due to disturbance.

2. O-horizon sampling at plot center.

2-1. Label 1-2 zip-loc bags (see above).

2-2. Place the O-horizon cutting template at the plot center. Cut around the template using your field knife.

2-3. Collect all the material and place in the bucket labeled “O”. Include any moss in the sample, but try to avoid any live plants. Be careful not to collect mineral soil. You may have to shake some soil off of the moss you will uproot in this process.

2-4. Once all the moss and litter material is collected down to the mineral soil. Record the depths of the O-horizon on all 4 sides of sample location to nearest 5mm. Write these values on the O-horizon sample bags, as well as in a notebook.

3. Mineral soil sample collection.

3-1. While at plot center push your 30cm long push probe into the ground in the square devoid of O-horizon material. Push the probe so that 30cm has been inserted into the ground. Gently rotate about 45-90 degrees and pull the probe from the soil. If there’s an obstruction (rocks, roots, etc.) resample at a nearby location after scrapping away the O-horizon.

3-2. Measuring from the bottom of the soil profile in the push probe, cut the soil at 10cm (this will be the 20-30 sample) and 20cm (this will be the 10-20cm sample). The 0-10cm sample will be less than 10cm, this is OK since this depth/horizon tends to compact the most during sampling.

3-3. Hold the probe over the bucket labeled 0-10 and carefully scoop out the 0-10cm sample. Repeat this procedure for 10-20 and 20-30cm samples. A lab spatula works well for this.

3-3 NOTE. For some areas it may be easier to collect the soil by pushing the probe into the ground 10 cm, extracting and placing the material into the appropriate bucket (for the 0-10cm sample). In the same probe hole push the probe to 20 cm (since 0-10 has been sampled you should just have the 10-20cm sample). Repeat for the 20-30cm sample.

3-4. Repeat for the other 4 locations in the plot. Since we did not collect an O-horizon sample at these locations you will need to scrape away this material with your hand. All depths collected from this plot will go into their respective buckets. At the end of this procedure you should have 3 buckets with soil collected from the 0-10, 10-20, and 20-30cm depths from 5 locations.

3-5. Use a trowel to mix the soil in each bucket. Scoop the mixed soil material into the appropriately labeled bag.

3-6. Store soils in an area out of direct sun-light. A cooler is the best idea, but not necessary if samples are kept in the shade and temps remain below about 60 degrees F.

3-7. Place soils in a refrigerator (RH 280) as soon as returning from the field. If it isn’t possible to return to campus in the evening then store samples in the hotel fridge or in a cooler with blue ice (not water based ice due to problems liquid water and contamination of samples).

Laboratory Protocols

Pseudothecia Counting Protocol

Tools and Equipment

- Data sheets
- 3x5 white index cards
- Dissecting microscope or DinoLight
- Ruler (mm)
- Double-sided tape
- Fine point pen (blue or black)
- Mechanical (tally) counter
- Random number table

Needle Storage and Preparation

1. Needles should be stored in a freezer (RH 280) until mounted on index cards, and when not used store needle samples in freezer to avoid desiccation.
2. Following steps a-c for needle selection, use double-sided tape to affix individual needles to 3x5 index cards vertically with the stomata facing up (fig. 1). The following steps are to be performed for both needle age classes (1 and 2-year old needles)
   a. Attach label sticker and fill in plot, tree, treatment, and needle age information in pen or fine-tip marker.
   b. Randomly select 50 needles from bag. Attach needles to the card flat, with the undersides of needles facing upward and the tips oriented in the same direction (shown in Fig. 1). Avoid touching the underside of the needle as much as possible to minimize damage to the stomatal surface. If possible, use forceps to grab needles at the petiole (stem).
   c. Store prepared and labeled cards in a plastic bag in freezer until they are ready for counting.

Fig. 1

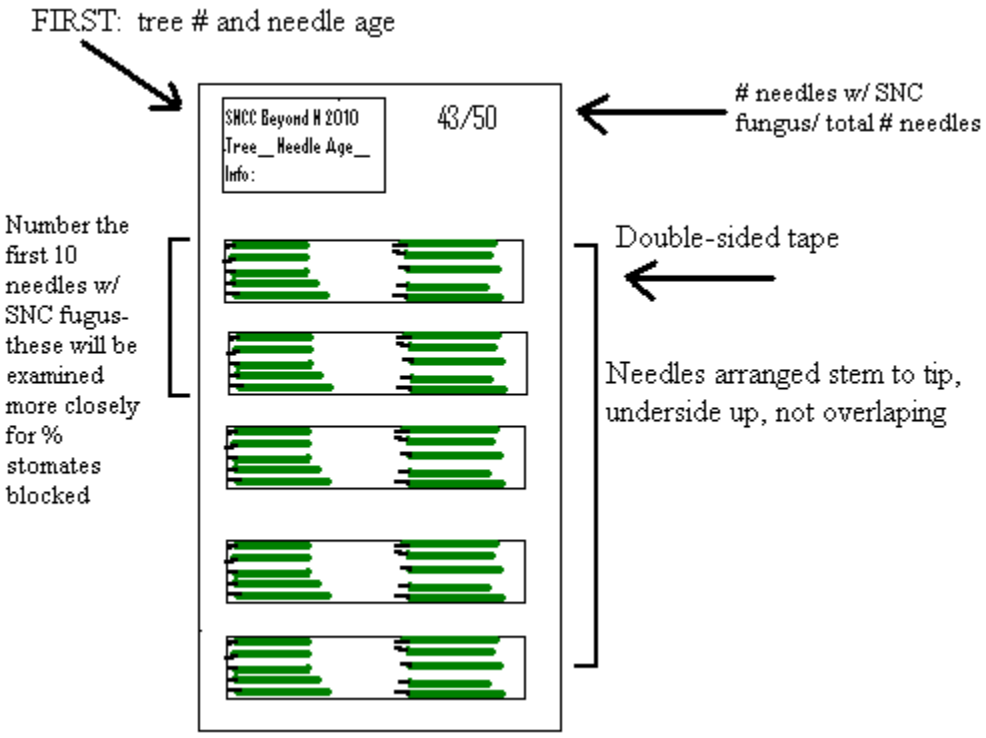
FIRST: tree # and needle age
SNCC Beyond N 2010
Tree__ Needle Age__
Info:
43/50
needles w/ SNC fungus/ total # needles
Number the first 10 needles w/ SNC fugus- these will be examined more closely for % stomates blocked
Double-sided tape
Needles arranged stem to tip, underside up, not overlaping

Evaluating Infection Incidence & Percent of Occluded (blocked) Stomates

1. Use blue or black ink fine-tip ballpoint pen for recording data on datasheets.
2. When recording information on datasheets, fill in your name, date, plot, tree number, treatment, and needle age information, and initial next to each row of data that you record.
3. Distinguish pseudothecia of Phaeocryptopus gaeumanii from other fungal species/contaminants on needles. If other fungal species are present, record this information in the notes column on the datasheet. See attached appendix for SNC and other foliar fungi ID.

Infection Incidence (percentage of needles with Phaeocryptopus)

1. Count the number of needles mounted on the card. If fewer than 50, note this on the datasheet in the incidence column. When you process a notecard for incidence, initial the notecard.
2. Using a dissecting microscope, scan each needle on the card to look for pseudothecia.
3. Use a tally counter to keep track of the number of needles with the fungus present.
4. Record the number of needles with pseudothecia/ total number of needles (i.e. 44/50) on the top right corner of the card (see diagram).
5. Number the first ten needles with pseudothecia.This is the subsample of needles that will be used to estimate the percent of blocked stomata.

Designating counting points

6. Three designated points per needle will be used to count pseudothecia.
7. Using the methods described in the following section (Selecting Random Points on Needles), we will randomly select 3 locations on each needle at which we will evaluate the percent of stomates blocked. Select and mark these points after evaluating infection incidence so that they are ready to be processed at the digital microscope.
8. IMPORTANT: We will record the length of the first five (5) needles on which the SNC-fungus is present, and record these lengths (in mm) at the base of the notecard. This way, the needle length, number of pseudothecia with SNC-fungus present and the tree and needle age information can all be recorded at the same time when needle cards are processed at the digital microscope.

For example, at the bottom of the notecard, you might record:

NL: 28, 25, 33, 29, 28, or needle length: 28, 25, 33, 29, 28

If there is not room at the bottom of the card, find another place on the card (front or back) to record these lengths.

Selecting Random Points on Needles

1. The first ten needles on which pseudothecia were present have been numbered from 1 to 10. These needles will be use to estimate the % of blocked stomata.

2. For each needle to be evaluated, counts will be conducted on three separate sections of the needle: the base (B), middle (M) and tip (T). Measure the needle with a ruler (mm), careful not to damage adjacent needles.

3. Based on the total length, use the Needle Length Table to determine the bounds of each needle section. Then, using the Random Number Table, move left to right until you reach 1- or 2-digit numbers that are within the bounds of each needle section (these marks must be at least 3mm apart to ensure space to count 100 stomata). In each needle section, make a fine mark in pencil or pen next to the needle corresponding to the length that you selected on the Random Number Table. See Figure 2 below. If a portion of the leaf tissue is obviously dead at your intended starting point, use the Random Number Table to select a new starting point. Non-Phaeocryptopus fungi are common on dead leaf tissue.

4. For the remainder of each work session, continue through the random number table without repeating the numbers that you have already scanned through- this will ensure truly random number selection.

Fig. 2

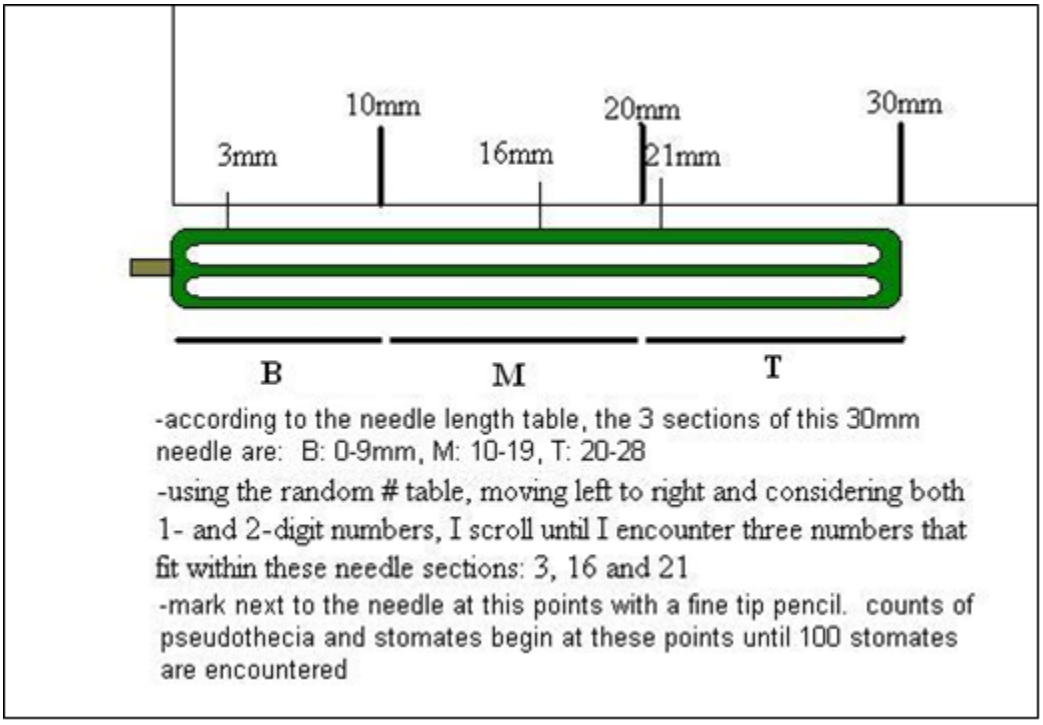

Counting Pseudothecia

1. At each randomly selected point within each section (B, M, T), begin counting the number of stomata plugged with pseudothecia. Very large irregularly shaped black structures tend to be fungi other than P. gaeumanii. Check appendix: SNC and other fungal spp ID.
2. Count stomata vertically from base towards tip until you reach 50, then move to the other side of the midrib and count 50 beginning again at the pencil line (Fig. 3).
3. Every stomate encountered that has a pseudothecium present is recorded on the tally counter. When all 100 stomata have been observed, record the number and reset the tally counter. As in the example below, if 20 out of 100 stomata contain pseudothecia, record 20 on the datasheet.
4. If you encounter non-Phaeocryptopus fungi blocking stomates, simply skip those stomata (i.e. count visible around the non-Phaeocryptopus fruiting bodies/discoloration).

Fig. 3.

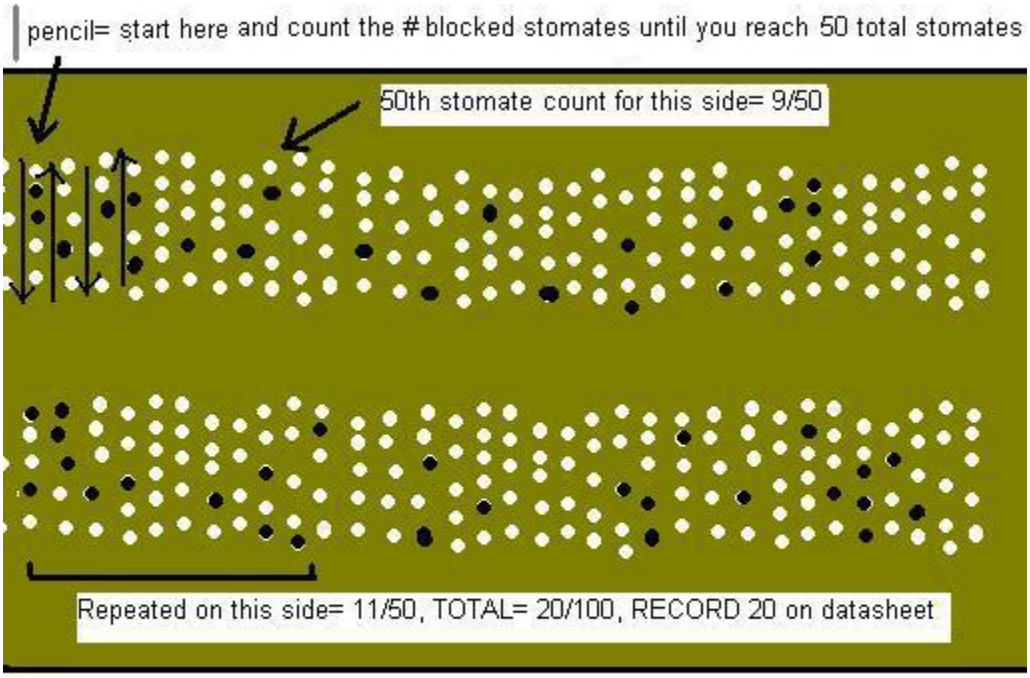

- Do not count pseudothecia under a regular desk lamp, or any lamp that puts off a considerable amount of heat. Needles will become desiccated and will be unusable.
- Whenever not counting pseudothecia on a current index card, place the index card that you are working on in a plastic bag in the freezer or a cooler until you resume work.
- Completed index cards should be stored with a blank index card covering needles, inside a plastic bag in the freezer.

Dino-Lite Digital Microscope Guidelines

The microscopes have been set to a position that should allow you to easily magnify needles by ~215 times without having to significantly adjust the coarse or fine focus. With the current set-

up, the view of the needle that will appear on the screen corresponds to the orientation of the needle as it is mounted on the index card.

When viewing needles, you should always be able to see the entire width of the needle, and the magnification should remain set at 210-230. The height of the microscope will be just millimeters above the needle samples, so take care not to push the microscope against the needles as you adjust the microscope height.

Please do not change the height of the microscope radically. If you are having difficulty focusing the microscope by very gently turning the knob on the right side of the microscope stand and the magnification knob on the microscope itself, ask someone else in the lab to assist you.

1. The Dino-Lite microscopes should only be used to evaluate the proportion of stomates blocked with pseudothecia.
a. Examination of the number of needles on which the SNC fungus is present should take place beforehand using a dissecting microscope. When this is done, the first ten needles on which the fungus is present should be numbered from 1 to 10 adjacent to the stem of each needle. The number of needles with fungus will be written on the top-right corner of the card.
b. Before beginning work at the digital microscope, each of the 10 needles that will be evaluated more closely should be measured, and three random points within the basal, middle and tip sections of the needle should be selected (according to guidelines) and marked using a pen or fine pencil.

2. To begin, plug the microscope into a USB connection on the computer, and the Dino-Lite program will automatically open and the microscope light will turn on (if this doesn't work, try another USB port). If the microscope is already plugged into the USB port, simply double-click on the Dino-Lite shortcut on the desktop. If you close the program or unplug the USB cable, the microscope will turn off. Do not leave the microscope on when it is not in use.

3. For each needle, first locate the needle number adjacent to the stem of the needle. This will ensure that you are examining the correct needle. Gently move the needle card to the left until you reach the pencil mark in the basal needle section. Adjust the microscope to bring the needle into focus. The brightness of the image can also be adjusted by placing the mouse arrow in the gray area below the image, which will bring up an adjustable light exposure scale. To take a picture, press any key or click the mouse once. If needles are not laying flat on the card, it may not be possible to focus the top and bottom rows of stomates simultaneously, and you may need to focus on one part of the needle at a time. It is not necessary to take multiple photos of one needle section- capture the best image you can.

4. Accurate and complete recording of file names is important and should be done as follows:

a. Each time that you work at the digital microscope, you should begin by creating a temporary folder on the desktop and name the folder with your name and the date (e.g. GRitok.04.04.14). At the end of the work period, this entire folder and its contents can be copied to the external hard drive, or the T-drive/Groups/SNCC/Pseudothecia photos (MA and KF only).

b. Right-click on the thumbnail of your most recent image in the panel on the left part of the screen and select "Save As". A Picture Size box will pop up and you should press enter or click "ok" to accept the default size.

c. You will save pictures to the temporary folder that you have created on the desktop. Click on the arrow next to "Save In" and select the appropriate drive under "Desktop".

d. The file name must include all identifying information for that image:

i. Plot ID

ii. Tree Number

iii. Branch Position (L, M, U)

iv. Needle Age (1 or 2)

v. Needle Number (1-10)

vi. Needle Section (B, M, T)

vii. Your initials

viii. Example: for plot N152, tree 100, mid third branch, needle age 2, needle number 5, basal needle section, and image captured by Beavis Butthead, the file would be coded: SNC.N152.100.M.2.5.B.BB

5. The number of stomates blocked with pseudothecia out of 100 stomates must be evaluated according to the established methods, and recorded in the appropriate row and column on the datasheet. Repeat these steps for the other needle sections and for all 10 preselected needles on the card.

6. As we begin this project, we will record images at three locations on every needle for 5 needles per card. We may reduce the number of images saved if this process proves to be too time-consuming. Accurately recording the number of stomates blocked with pseudothecia per needle section is a higher priority than capturing and saving images.

SNCC NEEDLE LENGTH TABLE

Needle Length (mm)	B (base)	M (middle)	T (tip)
10	0 - 3	4 - 5	6 - 8
11	0 - 3	4 - 6	7 - 9
12	0 - 3	4 - 7	8 - 10
13	0 - 4	5 - 7	8 - 11
14	0 - 4	5 - 8	9 - 12
15	0 - 4	5 - 9	10 - 13
16	0 - 5	6 - 9	10 - 14
17	0 - 5	6 - 10	11 - 15
18	0 - 5	6 - 11	12 - 16
19	0 - 6	7 - 11	12 - 17
20	0 - 6	7 - 12	13 - 18
21	0 - 6	7 - 13	14 - 19
22	0 - 7	8 - 13	14 - 20
23	0 - 7	8 - 14	15 - 21
24	0 - 7	8 - 15	16 - 22
25	0 - 8	9 - 15	16 - 23
26	0 - 8	9 - 16	17 - 24
27	0 - 8	9 - 17	18 - 25
28	0 - 9	10 - 17	18 - 26
29	0 - 9	10 - 18	19 - 27
30	0 - 9	10 - 19	20 - 28
31	0 - 10	11 - 19	20 - 29
32	0 - 10	11 - 20	21 - 30
33	0 - 10	11 - 21	22 - 31
34	0 - 11	12 - 21	22 - 32
35	0 - 11	12 - 22	23 - 33
36	0 - 11	12 - 23	24 - 34
37	0 - 12	13 - 23	24 - 35
38	0 - 12	13 - 24	25 - 36
39	0 - 12	13 - 25	26 - 37
40	0 - 13	14 - 25	26 - 38
41	0 - 13	14 - 26	27 - 39
42	0 - 13	14 - 27	28 - 40
43	0 - 14	15 - 27	28 - 41
44	0 - 14	15 - 28	29 - 42
45	0 - 14	15 - 29	30 - 43

Foliar sample processing for chemical analysis

1. Foliar samples from a mid-crown branch from the south side of the tree will be sampled and analyzed for elemental composition.
2. Approximately 1 g of material will be collected (200-250 needles). Age class 1, from 3 branch tips.
3. Place these needles in a small whirl-pak and freeze them until we have time to dry them.
4. Dry needle samples at 40 degrees C in a convection oven (inside a paper lunch sack), or using a freeze dryer (if available) for 72 hours.
5. Once dry, seal the sample bag and store samples in a desiccator until the mass of 10 needles can be weighed.

Soil storage and processing

1. Store soils in a refrigerator until they can be dried, 2-4 weeks.
2. Set oven to 40 degrees C.
3. Dump samples into a paper bag. Place sample bag inside paper sack.
4. Place samples with paper sack open in oven for 2-3 days. 2 days for dry-moist soils and 3 days for moist-wet soils.
5. Once dry, place samples back into sample bag, seal, and store in a durable container (cardboard, large Tupperware, etc)

List of Refereed Publications

Disease Distribution, Severity and Epidemiology

Hansen, E. M., Stone, J. K., Capitano, B. R., Rosso, P., Sutton, W., Winton, L., Kanaskie, A., M. G. McWilliams. 2000. Incidence and impact of Swiss needle cast in forest plantations of Douglas-fir in coastal Oregon. Plant Disease. 84: 773-779.

Manter, D. K., Reeser, P. W., and J. K. Stone. 2005. A climate-based model for predicting geographic variation in Swiss needle cast severity in the Oregon coast range. Phytopathology. 95: 1256-1265.

Rosso, P. H. and E. M. Hansen. 2003. Predicting Swiss needle cast disease distribution and severity in young Douglas-fir plantations in coastal Oregon. Phytopathology. 93: 790-798.

Shaw, D.C., Wooley, T., Kanaskie, A. 2014. Vertical foliage retention in Douglas-fir across environmental gradient of the western Oregon coast range influenced by Swiss needle cast. Northwest Science. 88(1):23-32.

Stone, J. K., Hood, I. A., Watt, M. S. and J. L. Kerrigan. 2007. Distribution of Swiss needle cast in New Zealand in relation to winter temperature. Australasian Plant Pathology. 36: 445-454.

Stone, J. K., Capitano, B. R. and J. L. Kerrigan. 2008. The histopathology of *Phaeocryptopus gaeumannii* on Douglas-fir needles. Mycologia. 100: 431-444.

Stone, J. K., Coop, L. B. and D. K. Manter. 2008. Predicting the effects of climate change on Swiss needle cast disease severity in Pacific Northwest forests. Canadian Journal of Plant Pathology. 30: 169-176.

Watt, M. S., Stone, J. K., Hood, I. A. and D. J. Palmer. 2010. Predicting the severity of Swiss needle cast on Douglas-fir under current and future climate in New Zealand. Forest Ecology and Management (*in press*).

Forest Protection Issues

Kelsey, R. G. and D. K. Manter. 2004. Effect of Swiss needle cast on Douglas-fir stem ethanol and monoterpene concentrations, oleoresin flow, and host selection by the Douglas-fir beetle. Forest Ecology and Management. 190: 241-253.

Shaw, D. C., Filip, G. M., Kanaskie, A., Maguire, D. A. and W. Littke. 2011. Managing an epidemic of Swiss needle cast in the Douglas-fir region of Oregon: The Swiss Needle Cast Cooperative. Journal of Forestry (*in press*).

Genetic Resistance/Tolerance in Douglas-fir

Kastner, W., Dutton, S. and D. Roche. 2001. Effects of Swiss needle cast on three Douglas-fir seed sources on a low-elevation site in the northern Oregon Coast Range: Results after five growing seasons. Western Journal of Applied Forestry. 16 (1): 31-34.

Jayawickrama, K.J.S., D. Shaw, and T.Z. Ye. 2012. Genetic Selection in Coastal Douglas-fir for tolerance to Swiss Needle Cast Disease. Proceedings of the fourth international workshop on the genetics of host-parasite interactions in forestry: Disease and insect resistance in forest trees. Gen. Tech. Rep. PSW-GTR-240. Albany, CA: Pacific Southwest Research Station, Forest Service, U.S. Department of Agriculture. 372 p.

Johnson, G. R. 2002. Genetic variation in tolerance of Douglas-fir to Swiss needle cast as assessed by symptom expression. Silvae Genetica. 51: 80-86.

Temel, F., Johnson, G. R. and J. K. Stone. 2004. The relationship between Swiss needle cast symptom severity and level of *Phaeocryptopus gaeumannii* colonization in coastal Douglas-fir (*Pseudotsuga menziesii var. menziesii*). Forest Pathology. 34: 383-394.

Temel, F., Johnson, G. R. and W. T. Adams. 2005. Early genetic testing of coastal Douglas-fir for Swiss needle cast tolerance. Canadian Journal of Forest Research. 35: 521-529.

Genetics of *Phaeocryptopus gaeumannii*

Winton, L. M., Hansen, E. M. and J. K. Stone. 2006. Population structure suggests reproductively isolated lineages of *Phaeocryptopus gaeumannii*. Mycologia. 98 (5): 781-791.

Winton. L. M., Stone, J. K. and E. M. Hansen. 2007. The systematic position of *Phaeocryptopus gaeumannnii*. Mycologia. 99: 240-252.

Mensuration and growth effects

Maguire D. A., Kanaskie, A., Voelker, W., Johnson, R. and G. Johnson. 2002. Growth of young Douglas-fir plantations across a gradient in Swiss needle cast severity. Western Journal of Applied Forestry. 17: 86-95.

Maguire, D. A. and A. Kanaskie. 2002. The ratio of live crown length to sapwood area as a measure of crown sparseness. Forest Science. 48: 93-100.

Maguire, D. A., Mainwaring, D. B. and Kanaskie A. 2011. Ten-year growth and mortality in young Douglas-fir stands experiencing a range in Swiss needle cast severity. Can. J. For. Res. 41: 2064-2076.

Weiskittel, A. R., Garber, S. M., Johnson, G. P., Maguire, D. A. and R.A. Monserud. 2007. Annualized diameter and height growth equations for Pacific Northwest plantation-grown

Douglas-fir, western hemlock, and red alder. Forest Ecology and Management. 250: 266-278.

Weiskittel, A. R., Maguire, D. A., Garber, S. M. and A. Kanaskie. 2006. Influence of Swiss needle cast on foliage age class structure and vertical distribution in Douglas-fir plantations of north coastal Oregon. Canadian Journal of Forest Research. 36: 1497-1508.

Weiskittel, A. R., Maguire, D. A. and R. A. Monserud. 2007. Modeling crown structural responses to competing vegetation control, thinning, fertilization, and Swiss needle cast in coastal Douglas-fir of the Pacific Northwest, USA. Forest Ecology and Management. 245: 96-109.

Weiskittel, A. R., Maguire, D. A. and R. A. Monserud. 2007. Response of branch growth and mortality to silvicultural treatments in coastal Douglas-fir plantations: Implications for predicting tree growth. Forest Ecology and Management. 251: 182-194.

Weiskittel, A. R. and D. A. Maguire. 2007. Response of Douglas-fir leaf area index and litterfall dynamics to Swiss needle cast in north coastal Oregon, USA. Annals of Forest Science. 64: 121-132.

Weiskittel, A. R. and D. A. Maguire. 2006. Branch surface area and its vertical distribution in coastal Douglas-fir. Trees. 20: 657-667.

Weiskittel, A. R., Temesgen, H., Wilson, D. S. and D. A. Maguire. 2008. Sources of within and between-stand variability in specific leaf area of three ecologically distinct conifer species. Annals of Forest Science. 65: 103-112.

Zhao, J., Maguire, D. A., Mainwaring, D. B., Kanaskie, A. 2012. Climatic influences on needle cohort survival mediated by Swiss needle cast in coastal Douglas-fir. Trees 26: 1361-1371

Zhao, J., Mainwaring, D. B., Maguire, D. A., Kanaskie, A. 2011. Regional and annual trends in Douglas-fir foliage retention: Correlations with climatic variables. For. Ecol. And Management 262: 1872-1886

Zhao, J., Maguire, D. A., Mainwaring, D. B., Wehage, J., Kanaskie, A. 2014. Thinning Mixed Species Stands of Douglas-Fir and Western Hemlcok in the Presence of Swiss Needle Cast: Guidelines Based on Relative Basal Area Growth of Individual Trees. For. Sci. 60 (1): 191-199.

Nutrition and soil interactions

El-Hajj, Z., Kavanagh, K., Rose, C., and Z. Kanaan-Atallah. 2004. Nitrogen and carbon dynamics of a foliar biotrophic fungal parasite in fertilized Douglas-fir. New Phytologist. 163: 139-147.

Luoma, D.l., Eberhart, J.L. 2014. Relationship betwee Swiss needle cast and ectomycorrhizal fungus diversity. Mycologia. 106 (4):666-675.

Mulvey, R.L., Shaw, D.C., Maguire, D.A. 2013. Fertilization impacts on Swiss needle cast disease severity in Western Oregon. Forest Ecology and Management 287: 147-158.

Perakis, S. S., Maguire, D. A., Bullen, T. D., Cromack, K., Waring, R. H. and J. R. Boyle. 2005. Coupled nitrogen and calcium cycles in forests of the Oregon Coast Range. Ecosystems. 8: 1-12.

Waring, R. H., Boyle, J., Cromack, K. Jr., Maguire, D. and A. Kanaskie. 2000. Researchers offer new insights into Swiss needle cast. Western Forester. 45 (6): 10-11.

Pathology and physiological host effects

Black, B. A., Shaw, D. C. and J. K. Stone. 2010. Impacts of Swiss needle cast on overstory Douglas-fir forests of western Oregon Coast Range. Forest Ecology and Management. 259: 1673-1680.

Lee, H.E., Beedlow, P.A., Waschamnn, R.S., Burdick, C.A., Shaw, D.C. 2013. Tree-ring analysis of the fungal disease Swiss needle cast in western Oregon coastal forests. Can Journal of For. 43(8):677-690.

Manter, D. K., Bond, B. J., Kavanagh, K. L., Rosso, P. H. and G. M. Filip. 2000. Pseudothecia of Swiss needle cast fungus, *Phaeocryptopus gaeumannii*, physically block stomata of Douglas-fir, reducing CO_2 assimilation. New Phytologist. 148 (3): 481-491.

Manter, D. K. 2002. Energy dissipation and photoinhibition in Douglas-fir needles with a fungal-mediated reduction in photosynthetic rates. Phytopathology. 150: 674-679.

Manter, D. K., Bond, B. J., Kavanagh, K. L., Stone, J. K. and G. M. Filip. 2003. Modeling the impacts of the foliar pathogen, *Phaeocryptopus gaeumannii*, on Douglas-fir physiology: net canopy carbon assimilation, needle abscission and growth. Ecological Modeling. 164: 211-226.

Manter, D. K. and Kavanagh, K. L. 2003. Stomatal regulation in Douglas-fir following a fungal-mediated chronic reduction in leaf area. Trees. 17: 485-491.

Manter, D. K., Kelsey, R. G., and J. K. Stone. 2001. Quantification of *Phaeocryptopus gaeumannii* colonization in Douglas-fir needles by ergosterol analysis. Forest Pathology. 31: 229-240.

Manter, D. K., Winton, L. M., Filip, G. M. and J. K. Stone. 2003. Assessment of Swiss needle cast disease: temporal and spatial investigations of fungal colonization and symptom severity. Phytopathology. 151: 344-351.

Saffell, B.J., Meinzer, R.C., Voelker, S.L., Shaw, D.C., Brooks, R.J., Lachenbruch, B, McKay, J. 2014. Tree-ring stable isotopes record the impact of a foliar fungal pathogen on CO_2 assimilation and growth in Douglas-fir. Plant, Cell & Environment. doi: 10.1111/pce.12256

Saffell, B.J., Meinzer, R.C., Woodruff, D.R., Voelker, S.L., Shaw, D.C., Brooks, R.J., Lachenbruch, B. 2014. Seasonal carbohydrate dynamics and growth in Douglas-fir trees experiencing chronic, fungal-mediated reduction in functional leaf area. Tree physiology. 00: 1-11.

Winton, L. M., Manter, D. K., Stone, J. K. and E. M. Hansen. 2003. Comparison of biochemical, molecular and visual methods to quantify *Phaeocryptopus gaeumannii* in Douglas-fir foliage. Phytopathology. 93: 121-126.

Winton, L. M., Stone, J. K., Watrud, L. S. and E. M. Hansen. 2002. Simultaneous one-tube quantification of host and pathogen DNA with real-time polymerase chain reaction. Phytopathology. 92: 112-116.

Winton, L. M., Stone, J. K. and E. M. Hansen. 2007. Polymorphic microsatellite markers for the Douglas-fir pathogen *Phaeocryptopus gaeumannii*, causal agent of Swiss needle cast disease. Molecular Ecology. 7: 1125-1128.

Silviculture and Control

Filip, G., Kanaskie, A., Kavanagh, K., Johnson, G., Johnson, R. and D. Maguire. 2000. Research Contribution 30, Forest Research Laboratory, College of Forestry, Oregon State University, Corvallis, Oregon.

Mainwaring, D. B., Maguire, D. A., Kanaskie, A. and J. Brandt. 2005. Growth responses to commercial thinning in Douglas-fir stands with varying intensity of Swiss needle cast. Canadian Journal of Forest Research. 35: 2394-2402.

Stone, J. K., Reeser, P. W. and A. Kanaskie. 2007. Fungicidal suppression of Swiss needle cast and pathogen reinvasion in a 20-year-old Douglas-fir stand. Western Journal of Applied Forestry. 22: 248-252.

Wood Quality

Johnson, G. R., Gartner, B. L., Maguire, D. and A. Kanaskie. 2003. Influence of Bravo fungicide applications on wood density and moisture content of Swiss needle cast affected Douglas-fir trees. Forest Ecology and Management. 186: 339-348.

Grotta, A. T., Leichti, R. J., Gartner, B. L. and G. R. Johnson. 2004. Effect of growth ring orientation and placement of earlywood and latewood on MOE and MOR of very-small clear Douglas-fir beams. Wood and Fiber Science. 37: 207-212.

Johnson, G. R., Grotta, A. T., Gartner, B. L. and G. Downes. 2005. Impact of the foliar pathogen Swiss needle cast on wood quality of Douglas-fir. Canadian Journal of Forest Research. 35: 331-339